

Wilson loops, instantons and quantum mechanics

Dissertation
zur
Erlangung des Doktorgrades (Dr. rer. nat.)
der
Mathematisch-Naturwissenschaftlichen Fakultät
der
Rheinischen Friedrich-Wilhelms-Universität Bonn

von
Marc Schiereck
aus
Herford

Bonn 2014

Dieser Forschungsbericht wurde als Dissertation von der
Mathematisch-Naturwissenschaftlichen Fakultät der Universität Bonn angenommen und ist
auf dem Hochschulschriftenserver der ULB Bonn
http://hss.ulb.uni-bonn.de/diss_online elektronisch publiziert.

1. Gutachter: Prof. Dr. Albrecht Klemm
2. Gutachter: PD Dr. Stefan Förste

Tag der Promotion: 23.5.2014
Erscheinungsjahr: 2014

Abstract

In this thesis we will examine two different problems. The first is the computation of vacuum expectation values of Wilson loop operators in ABJM theory, the other problem is finding the instanton series of the refined topological string on certain local Calabi–Yau geometries in the Nekrasov–Shatashvili limit.

Based on the description of ABJM theory as a matrix model, it is possible to find a description of it in terms of an ideal Fermi gas with a non-trivial one-particle Hamiltonian. The vacuum-expectation-values of Wilson loop operators in ABJM theory correspond to averages of operators in the statistical-mechanical problem. Using the WKB expansion, it is possible to extract the full $1/N$ expansion of the vevs, up to exponentially small contributions, for arbitrary Chern–Simons coupling. We will compute these vevs for the $1/6$ and $1/2$ BPS Wilson loops at any winding number. These can be written in terms of the Airy function. The expressions we found reproduce the low genus results previously obtained in the 't Hooft expansion.

In another problem we use mirror symmetry, quantum geometry and modularity properties of elliptic curves to calculate the refined free energies, given in terms of an instanton sum, in the Nekrasov–Shatashvili limit on non-compact toric Calabi–Yau manifolds, based on del Pezzo surfaces. Quantum geometry here is to be understood as a quantum deformed version of rigid special geometry, which has its origin in the quantum mechanical behavior of branes in the topological string B-model. We will argue that in the Seiberg–Witten picture only the Coulomb parameters lead to quantum corrections, while the mass parameters remain uncorrected. In certain cases we will also compute the expansion of the free energies at the orbifold point and the conifold locus. We will compute the quantum corrections order by order on \hbar by deriving second order differential operators, which act on the classical periods.

Danksagungen

Mein besonderer Dank gilt Prof. Dr. Albrecht Klemm, der es mir ermöglichte, auf diesem interessanten Gebiet arbeiten zu können. Weiterhin bedanke ich mich bei Dr. Min-xin Huang, Prof. Dr. Marcos Mariño, Dr. Masoud Soroush und Jonas Reuter für die Zusammenarbeit bei meinen Veröffentlichungen. PD Dr. Stefan Förste danke ich für die Übernahme der Zweitkorrektur.

Während meiner Zeit als Doktorand habe ich mit Dr. Hans Jockers, Dr. Denis Klevers, Dr. Daniel Lopes, Dr. Jan Manschot, Dr. Marco Rauch, Dr. Thomas Wotschke, Navaneeth Gaddam, Jie Gu, Maximilian Poretschkin, Jose Miguel Zapata Rolon und Thorsten Schimannek viele anregende und erhellende Diskussionen gehabt. Vielen Dank dafür.

Nicht zuletzt bedanke ich mich bei meiner Familie und meinen Freunden für die Unterstützung.

Contents

1	Introduction	1
1.1	Fermi gas	4
1.2	Quantum Geometry	5
1.3	Structure	6
2	Preliminaries	9
2.1	Matrix Models	9
2.1.1	Definitions	9
2.1.2	Perturbative solutions of matrix models	11
2.1.2.1	Spectral curves	12
2.1.3	The topological recursion of Eynard and Orantin	14
2.1.3.1	local $\mathbb{P}^1 \times \mathbb{P}^1$	16
2.2	ABJM theory	19
2.3	Localization	20
2.3.1	ABJM as a Matrix model	25
2.3.2	The geometry of ABJM theory	28
2.3.3	Wilson loops in the geometric description	33
3	ABJM Wilson loops in the Fermi gas approach	37
3.1	Introduction	37
3.2	The Fermi gas approach	38
3.2.1	Quantum mechanics in phase space	38
3.2.2	Quantum Statistical Mechanics in phase space	39
3.2.3	Large N expansion from the grand canonical ensemble	43
3.2.4	Quantum corrections	43
3.2.4.1	Wigner–Kirkwood expansion	44
3.2.4.2	Sommerfeld expansion	45
3.2.5	Fermi Gas for Chern Simons Matter theories	46
3.2.5.1	The Fermi Surface	49
3.2.5.2	Derivation of the $N^{3/2}$ behaviour of ABJM theory	52
3.3	Wilson loops in the Fermi gas approach	53
3.3.1	Incorporating Wilson loops	53
3.3.2	Quantum Hamiltonian and Wigner–Kirkwood corrections	54
3.3.3	Integrating over the Fermi surface	61
3.3.4	Genus expansion	65

4	Quantum Geometry of del Pezzo surfaces in the Nekrasov–Shatashvili limit	71
4.1	Introduction	71
4.2	Geometric setup	73
4.2.1	Branes and Riemann surfaces	73
4.2.1.1	Mirror symmetry for non-compact Calabi-Yau spaces	74
4.3	The refinement	75
4.3.1	The Nekrasov-Shatashvili limit	76
4.3.2	Schrödinger equation from the β -ensemble	77
4.3.3	Special geometry	79
4.3.4	Quantum special geometry	81
4.3.5	Genus 1-curves	84
4.3.5.1	Elliptic curve mirrors and closed modular expressions	84
4.3.5.2	Special geometry	86
4.3.5.3	Quantum Geometry	87
4.4	Examples	88
4.4.1	The resolved Conifold	88
4.4.2	local \mathbb{F}_0	89
4.4.2.1	Difference equation	90
4.4.2.2	Operator approach	92
4.4.2.3	Orbifold point	93
4.4.3	$\mathcal{O}(-3) \rightarrow \mathbb{P}^2$	97
4.4.3.1	Orbifold point	98
4.4.3.2	Conifold point	99
4.4.4	local \mathbb{F}_1	100
4.4.4.1	Operator approach	101
4.4.4.2	Difference equation	101
4.4.5	$\mathcal{O}(-K_{\mathbb{F}_2}) \rightarrow \mathbb{F}_2$	103
4.4.6	$\mathcal{O}(-K_{\mathcal{B}_2}) \rightarrow \mathcal{B}_2$	106
4.4.7	local $\mathcal{B}_1(\mathbb{F}_2)$	108
4.4.8	A mass deformation of the local E_8 del Pezzo	111
4.5	Relation to the Fermi Gas	113
5	Conclusions and Outlook	117
5.1	Fermi gas	117
5.2	Quantum Geometry of del Pezzo surfaces in the Nekrasov–Shatashvili limit	119
A	Matrix Models	121
A.1	Schwinger Dyson	121
A.1.1	Correlators of the β -ensemble	122
B	Fermi Gas	123
B.1	1/6 BPS Wilson loops at arbitrary winding number	123
B.2	Results at $g = 3$ and $g = 4$	124
C	Quantum Geometry	127
C.1	Eisenstein series	127

C.2	local \mathbb{F}_0	127
C.2.1	Orbifold point	128
C.3	$\mathcal{O}(-3) \rightarrow \mathbb{P}^2$	129
C.3.1	Orbifold point	130
C.3.2	Conifold point	130
C.4	local \mathbb{F}_1	131
C.5	local \mathbb{F}_2	132
Bibliography		135
List of Figures		145
List of Tables		147
Acronyms		149

Introduction

Instantons in gauge theories are of long standing interest to physicists. One well known example was given by Belavin, Polyakov, Schwartz and Tyupkin in [1], where the authors analyzed the solutions of the pure Yang–Mills Lagrangian. This is relevant for the correct definition of QCD, because it is a solution to the $U(1)$ –problem [2], which describes the apparent existence of an $U(1)$ symmetry in QCD that is not realized in the real world. The relevant solutions are called *instantons* [3], which are topologically non–trivial stationary points of the Yang–Mills action. They give nonperturbative contributions to the functional integral, which means they are not visible in the perturbative expansion in the coupling. The result described above shows us, that it is necessary to consider the nonperturbative structure of a quantum field theory in order to properly analyze it.

This problem is generally very difficult, but the introduction of supersymmetry restricts the structure of gauge theories in a manner so that their exploration is often possible in an exact way. Especially $\mathcal{N} = 2$ supersymmetric gauge theories in four dimensions attracted a lot of interest, because they exhibit non–perturbative effects, while it is possible to find exact results due to the work of Seiberg and Witten [4, 5]. At first their work was only about $SU(2)$ theories, but it was extended to different gauge groups and those of higher rank since then. The information about the instanton sum is encoded in an elliptic curve \mathcal{C} which we call *Seiberg–Witten curve*, and a meromorphic differential λ , defined on this curve. More precisely, the *prepotential* of such a gauge theory is encoded in the tuple (\mathcal{C}, λ) . Later the relation to topological string theory was studied. The Seiberg–Witten curve also appears in the topological string theory as a mirror geometry in the B–model [6, 7]. It is possible to construct a topological string theory on certain local Calabi–Yau manifolds, which, when taking a suitable limit, correspond to Seiberg–Witten theories. The genus zero amplitudes of the topological B–model amplitudes on this local Calabi–Yau manifold is captured by the Seiberg–Witten curve. Furthermore the topological B–model on local Calabi–Yau threefolds is dual to matrix models [8, 9] in the large N limit. In this approach the spectral curve corresponds to the curve \mathcal{C} and the differential λ encodes the filling fractions and the one point function.

One way to obtain the instanton sum is a localization computation on the moduli space of instantons, invented by Nekrasov [10]. He proposed the Ω –background, which introduced the two deformation parameters ϵ_1 and ϵ_2 in order to regularize the moduli space of instantons in $\mathcal{N} = 2$ supersymmetric gauge theories. The work of [11, 12] anticipated a geometrical interpretation of this in terms of a refined counting of Bogomol’nyi–Prasad–Sommerfield (BPS)

states corresponding to D0–D2 branes in the large volume limit of rigid $\mathcal{N} = 2$ theories in four dimensions. The multiplicities $N_{j_L, j_R}^\beta \in \mathbb{N}$ of the refined BPS states lift the degeneracy of the j_R spin–multiplets that is present in the corresponding BPS index $n_g^\beta \in \mathbb{Z}$ of the topological string, which corresponds to the specialization $ig_s = \epsilon_1 = -\epsilon_2$. A mathematical definition of the refinement of cohomology of the moduli space of the BPS configurations was recently given [13] starting with the moduli space of Pandharipande–Thomas invariants.

The free energies $F = \log(Z)$ of the topological string at large radius in terms of the BPS numbers N_{j_L, j_R}^β are obtained by a Schwinger-Loop calculation [14, 15] and read

$$F^{hol}(\epsilon_1, \epsilon_2, t) = \sum_{\substack{j_L, j_R=0 \\ k=1}}^{\infty} \sum_{\beta \in H_2(M, \mathbb{Z})} (-1)^{2(j_L + j_R)} \frac{N_{j_L, j_R}^\beta}{k} \frac{\sum_{m_L=-j_L}^{j_L} q_L^{km_L}}{2 \sinh\left(\frac{k\epsilon_1}{2}\right)} \frac{\sum_{m_R=-j_R}^{j_R} q_R^{km_R}}{2 \sinh\left(\frac{k\epsilon_2}{2}\right)} e^{-k\beta \cdot t}, \quad (1.0.1)$$

where

$$q_L = \exp\left(\frac{1}{2}(\epsilon_1 - \epsilon_2)\right) \quad \text{and} \quad q_R = \exp\left(\frac{1}{2}(\epsilon_1 + \epsilon_2)\right). \quad (1.0.2)$$

This expression admits an expansion in ϵ_1, ϵ_2 in the following way

$$F(\epsilon_1, \epsilon_2, t) = \log(Z) = \sum_{n, g=0}^{\infty} (\epsilon_1 + \epsilon_2)^{2n} (\epsilon_1 \epsilon_2)^{g-1} F^{(n, g)}(t). \quad (1.0.3)$$

This defines the refinement of the free energies as a two parameter deformation of the unrefined topological string. The usual genus expansion of the unrefined string is just encoded in $F^{0, g}$, which we obtain by setting $\epsilon_1 = -\epsilon_2$.

Techniques to compute this instanton series already exist. Starting with the mathematical definition one can now do a direct localization calculation [13]. Alternatively one can use the refined topological vertex [14], or the holomorphic anomaly equation, which was generalized for the use in the refined case in [15, 16, 17].

Another point of view was introduced in [18], where the topological B–model on manifolds which are the mirror of local Calabi–Yau threefolds were analyzed. This geometry is described by

$$e^{u+v} = H(e^x, e^p; z_I), \quad (1.0.4)$$

where $u, v, x, p \in \mathbb{C}$ and z_I are complex structure moduli. The equation $H(e^x, e^p; z_I) = 0$ defines a Riemann surface Σ . By considering branes, touching Σ in only one point, the Riemann surface itself can be identified with the moduli space of the branes. In this case the coordinates x and p become noncommutative

$$[x, p] = ig_s, \quad (1.0.5)$$

which suggests that H can be interpreted as the Hamiltonian describing the brane. The conjecture is that the open amplitudes corresponding to these branes are encoded into a quantum mechanical problem. One result of the refinement is, that we do not only find branes in the coupling g_s , but two kinds of branes corresponding to ϵ_1 and ϵ_2 , respectively. In the Nekrasov–Shatashvili limit one of these branes decouples, depending on which parameter we send to zero. This was used in [19] to show that the *Nekrasov–Shatashvili* limit $\epsilon_1 = 0$ [20] provides an even simpler quantization description of special geometry in which the rôle of \hbar is now played by ϵ_1 (or equivalently ϵ_2) and the rôle of the configuration space is played by the moduli space of a

brane, which is identified with the B–model curve itself.

There exist various different string theories, namely type I, type IIA, type IIB and heterotic string theories, which are connected by a set of dualities [21]. A theory unifying all these string theories was proposed in [22]. It is called *M–theory*. M–theory is an eleven–dimensional theory having so called M2– and M5–branes as its fundamental objects. Its low energy–limit is given by eleven–dimensional supergravity. There is strong evidence that M–theory reproduces the different string theories in various compactification limits. For string theory the effective action of its degrees of freedoms, e. g. branes, are known. In case of M–theory this structure is not as clear yet. One interesting question about the structure of the M–theory membranes is – analogous to a stack of D–branes: What is the world–volume theory of a stack of coincident M–branes? Here we want to concentrate on the analysis of the case of M2–branes. The worldvolume theory is known to have $\mathcal{N} \geq 6$ superconformal invariance. Such theories were constructed in [23], leading to the Bagger–Lambert–Gustavsson (BLG) model. Finally in [24] Aharony–Bergman–Jafferis–Maldacena (ABJM) theory was found. This is an $\mathcal{N} = 6$ supersymmetric Chern Simons matter (CSM) theory in three dimensions with gauge group $U(N) \times U(N)$ and integer coupling $(k, -k)$. This theory is consistent with the worldvolume theory of a stack of N M2–branes put on the orbifold $\mathbb{R}^8/\mathbb{Z}_k$.

A powerful conjecture which had a huge impact was made in [25], which related type IIB string theory on a background $AdS_5 \times S^5$ to a $\mathcal{N} = 4$ supersymmetric Yang–Mills (SYM) theory in $d = 4$. This is a famous example for dualities in string theory and was extensively studied since it was first proposed. This conjecture is called the *AdS/CFT conjecture* and is an implementation of the *holographic principle* [26, 27], as the physics of the $(d + 1)$ –dimensional bulk theory is encoded in the d dimensional boundary gauge theory. The $\mathcal{N} = 4$ SYM theory with gauge group $U(N)$ is the low energy limit of a stack of N D3–branes in type IIB string theory.

This duality is also a weak–strong coupling duality in the sense, that the weakly coupled field theory is dual to strongly coupled string theory and vice versa. We can see, for example, the $\mathcal{N} = 4$ SYM–theory as a nonperturbative definition of type IIB string theory on the background $AdS_5 \times S^5$.

In the case of ABJM theory this dual is M–theory on $AdS_4 \times S^7/\mathbb{Z}_k$, hence AdS/CFT allows us to give a nonperturbative definition of M–theory on this geometry in terms of a CFT without gravity. In order for this duality to hold we send N to infinity while keeping k finite. For weakly coupled ABJM theory this becomes $AdS_4 \times \mathbb{CP}^3$, where k controls the size of the M–theory circle. For more general cases the AdS–dual is given by $AdS_4 \times X$, where X is a seven dimensional Tri–Sasaki Einstein space [28, 29, 30]. In this case the field theory duals are $\mathcal{N} \geq 3$ superconformal $U(N)^p$ Chern–Simons theories with bifundamental matter. They have quartic superpotentials and the Chern–Simons levels k_1, k_2, \dots, k_p sum up to zero.

Lately localization techniques were extended [31], showing that Wilson loops in $\mathcal{N} = 4$ and $\mathcal{N} = 2$ SYM theories in four dimensions localize to matrix integrals with an operator insertion. In [32] these techniques were extended for the use in CSM theories in three dimensions. Based on these results, localization formulas for the 1/2 and 1/6 BPS Wilson loop in ABJM theory were derived and analyzed [33, 34]. The matrix models we find here are much more complicated than the matrix models found for the SYM theories in four dimensions. Still, it is possible to compute it to every order in $1/N$ [35, 36] in a recursive way. This is achieved by using the holomorphic anomaly equations of topological string theory [37] as adapted to matrix models and local geometries in for example [38, 39, 40].

Based on this matrix model description ABJM theory was related to topological string theory

on local $\mathbb{P}^1 \times \mathbb{P}^1$ [41] and was subsequently further analyzed in [36]. One notable property of M2-branes is that their degrees of freedom scale with $N^{3/2}$ [42]. This behavior was also derived from the field theory side via localization in [36]. The relation of the matrix model description to topological strings and the holomorphic anomaly equation was used [43] to resum the 't Hooft expansion of ABJM theory, which yielded an expression in terms of the Airy function.

Natural observables in Chern Simons theories are the partition function and Wilson loops. In terms of matrix models these were studied before in [44, 45, 46, 47]. The information of their vacuum expectation values (vevs) is encoded in period integrals on the spectral curve of the matrix model. In [41, 36] this connection was used to solve ABJM theory using its matrix model description. The vevs of the 1/6 and 1/2 BPS Wilson loops can be written in terms of contour integrals on the spectral curve of the ABJM matrix model.

1.1 Fermi gas

In case of more than three supercharges the partition function of these matrix models can be rewritten as a partition function of a non-interacting one-dimensional Fermi gas of N particles [48]. This is a systematic approach for solving $\mathcal{N} \geq 3$ CSM theories in the M-theory expansion. In the Fermi gas the coupling of the Chern–Simons theory k becomes the Planck constant \hbar and the M-theory expansion corresponds to the thermodynamic limit of the quantum gas in the grand canonical ensemble. This is a statistical physics problem which we solved successfully by already well understood and established techniques. By neglecting exponentially small corrections the partition function of the gas could be computed to all orders in $1/N$ via the Wentzel–Kramers–Brillouin (WKB) expansion. Once again the $N^{3/2}$ -behavior was derived and it can be interpreted as the scaling for a Fermi gas with a linear dispersion relation and a linear confining potential [48]. If one disregards worldsheet instantons, the partition function is given by

$$Z_{\text{ABJM}} = C^{-1/3} e^{A(k)} \text{Ai} \left[C^{-1/3} \left(N - \frac{k}{24} - \frac{1}{3k} \right) \right], \quad (1.1.1)$$

where we again see that it can be written in terms of the Airy-function.

Here we are extending this approach to also include Wilson loops. We already introduced two types of Wilson loops for ABJM theory. They were analyzed in terms of matrix models before in [41, 36] and here we compute the vevs of these Wilson loop operators using the Fermi gas approach. In order to compare the results obtained in this manner to results in M-theory, we extract the large N expansion of correlators corresponding to the Wilson loops. In the statistical mechanical formulation these are averages of n -body operators. Since we are dealing with a non-interacting gas, the computation of these can be reduced to a quantum-mechanical one-body problem. This can basically be done in a semiclassical expansion, but in this case the determination of the expectation value demands that we resum an infinite number of quantum corrections. This resummation leads to a very simple form. Namely, similar to the partition function we can write the result up to exponentially suppressed terms in terms of Airy functions. This was already shown for the free energy, but this structure even holds for Wilson loop operators. In case of the 1/2 BPS Wilson loop operator in the fundamental representation

this has the simple form

$$\langle W_{\square}^{1/2} \rangle = \frac{1}{4} \operatorname{csc} \left(\frac{2\pi}{k} \right) \frac{\operatorname{Ai} \left[C^{-1/3} \left(N - \frac{k}{24} - \frac{7}{3k} \right) \right]}{\operatorname{Ai} \left[C^{-1/3} \left(N - \frac{k}{24} - \frac{1}{3k} \right) \right]}. \quad (1.1.2)$$

Another important aspect of this computation is that the semiclassical expansion of the Fermi gas corresponds to an expansion of the CSM theory in the strongly coupled regime, where we can make actual contact with the AdS dual. This is generally a very hard problem because the perturbative region of one theory is the strongly coupled region of its dual theory.

While we were able to completely resum the large N expansion, lower order perturbative results computed via the Eynard–Orantin recursion directly from the matrix model, already existed and are in perfect agreement with our results. Even though results already exist for the strongly coupled regime, our formalism to compute expectation values is very efficient.

1.2 Quantum Geometry

In chapter 4 we will use a conjecture made in [19] about the computation of the free energy of the refined topological string in the *Nekrasov–Shatashvili* limit. The authors take the structure discovered in [18] about the behavior of branes in the topological B–model and extend it to the refined case. Using this method we are able to apply a quantum deformed version of special geometry [49, 50] in order to compute the instanton series (1.0.1) on local Calabi–Yau manifolds, given by a del Pezzo surface as a base, in the Nekrasov–Shatashvili–limit. This limit is given by setting ϵ_1 or ϵ_2 to zero and picks exactly the terms $F^{(n,0)}$ with $n \geq 0$ in the expansion (1.0.3).

For the topological string A–model on these manifolds there exist a dual geometry, described by a Riemann surface in the topological string B–model. One can generally show that branes ending on one point of this Riemann surface, act like quantum mechanical objects [18]. Moving branes around cycles of the geometry leads to monodromies, which can be used to extract the closed amplitudes. But generally a problem exists, namely we have no control over the higher order corrections in g_s to the Hamiltonian. This means taking the defining equation of the Riemann surface as the Hamiltonian is only correct to leading order in the WKB expansion. This problem disappears if we are taking the Nekrasov–Shatashvili limit, giving us a way to use the fact that branes ending on Riemann surfaces is a basic quantum mechanical problem, to compute the instanton series of the closed amplitudes [19]. Now we can write down a time independent Schrödinger equation, based on the defining equation of the Riemann surface. This Schrödinger equations is solved by wavefunctions of the ϵ_i branes that did not decouple in the Nekrasov–Shatashvili limit.

We consider two different ways of solving this Schrödinger equation. The first is the WKB expansion, which yields a perturbative expansion in the Planck constant \hbar , while being exact in the complex structure moduli. The alternative is to set up a difference equation, which can be solved perturbatively in the moduli, while being exact in \hbar . In both cases we extract a meromorphic differential and the periods of this differential obey the usual special geometry relations between.

Finding the right contours and parameterizations of the curve to obtain the periods is not an easy task, therefore we introduce differential operators of order two in the moduli, which result in higher order contributions to the periods when applied to the classical part of the period. We find the classical part of the periods by the standard method of solving the Picard–

Fuchs equations related to the geometry we consider. This approach is also useful for going to different points in the moduli space, because in this picture everything is exact in the moduli. We will make use of this to compute the Nekrasov–Shatashvili limit of topological string theory on geometries with del Pezzos as a base. For the local \mathbb{P}^2 and local \mathbb{F}_0 we also derive the closed amplitudes at different points in the moduli space.

1.3 Structure

We start with giving a general introduction to some concepts necessary in order to understand the techniques used in chapter 2. These include an introduction to matrix models in section 2.1 together with methods to solve them to all orders of N in the 't Hooft expansion. In section 2.2 we briefly introduce ABJM theory, its field content and the relation to the AdS/CFT conjecture. Afterwards, in section 2.3 we show, how it is possible to rewrite the partition function of ABJM theory and certain Wilson loop operators to a matrix model.

In section 3 we use the Fermi gas approach to compute the vevs of the 1/2 and 1/6 Wilson loop operators in ABJM theory.

Then, in section 4 we first introduce the necessary concepts needed to work with the quantum geometry of branes ending on a Riemann surface and use this to compute the instanton series of a selection of local geometries with a del Pezzo–surface as a base.

In section 5 we conclude the Fermi gas computations as well as the quantum geometry computations and give an outlook about possible future work on these topics.

Publications

Parts of this thesis have been published in scientific journals and on the preprint server arxiv.org.

A. Klemm, M. Marino, M. Schiereck and M. Soroush , “*ABJM Wilson loops in the Fermi gas approach*”, *Z. Naturforsch.* 68a, 178–209 (2013), [arXiv:1207.0611 [hep-th]].

M. -x. Huang, A. Klemm, J. Reuter and M. Schiereck , “*Quantum geometry of del Pezzo surfaces in the Nekrasov–Shatashvili limit*”, [arXiv:1401.4723 [hep-th]].

Preliminaries

2.1 Matrix Models

In this section we will give an introduction to matrix models, which will mainly follow the references [51, 52]. First we will define what we mean by a matrix model and give some general definitions for important quantities. In the next step we will present some means of solving matrix models in different ways. A basic case is the computation of correlators in the Gaussian matrix model. In the next step we will introduce the saddle point method, leading to a geometric solution of matrix models, in order to find the leading order contribution in the $1/N$ expansion of general hermitian matrix models. Finally we extend the geometric method via a topological recursion of Eynard and Orantin [53, 54].

2.1.1 Definitions

The partition function of an hermitian matrix model is given by

$$Z = \frac{1}{\text{vol}(U(N))} \int dM e^{-\frac{1}{g_s} V(M)}, \quad (2.1.1)$$

where we V is a polynomial of degree $n + 1$ given by

$$\frac{1}{g_s} V(M) = \frac{1}{2g_s} \text{Tr} M^2 + \frac{1}{g_s} \sum_{p=3}^{n+1} \frac{g_p}{p} \text{Tr} M^p, \quad (2.1.2)$$

where g_s and g_p are coupling constants. This polynomial has the gauge symmetry

$$M \rightarrow U M U^\dagger, \quad (2.1.3)$$

where U is an $U(N)$ matrix. This is the reason for the volume factor in the partition function (2.1.1). The differential dM is the Haar measure of the gauge group.

Matrix models basically are quantum gauge theories in zero dimensions, where we have (2.1.2) as an action and the matrix M is the field.

The simplest example of such a matrix model is the *Gaussian matrix model* where the poly-

nomial is just given by

$$\frac{1}{g_s} V(M) = \frac{1}{2g_s} \text{Tr} M^2. \quad (2.1.4)$$

We also define *normalized expectation values* by

$$\langle f(M) \rangle = \frac{\int dM f(M) e^{-\frac{1}{g_s} V(M)}}{\int dM e^{-\frac{1}{g_s} V(M)}}. \quad (2.1.5)$$

This is useful in particular because it enables us to make power series expansion of correlators for matrix models of general actions (2.1.2) in terms of correlators $\langle f(M) \rangle_G$ of the Gaussian matrix model, which can be solved exactly. The correlators in the representation basis are

$$\langle \text{Tr}_R M \rangle_G = c(R) \dim R \quad (2.1.6)$$

for even $|R|$, where R denotes a representation. Here

$$c(R) = (-1)^{\frac{A(A-1)}{2}} \frac{\prod_{f \text{ odd}} f!! \prod_{f' \text{ even}} (f' - 1)!!}{\prod_{f \text{ odd}, f' \text{ even}} (f - f')}, \quad (2.1.7)$$

where $A = l(R)/2$, with even $l(R)$ to have a non-vanishing result.

If we now expand the partition function (2.1.1) with general potential (2.1.2) in terms of the Gaussian matrix model, we obtain a perturbative expansion in the couplings g_s and g_p , which can be interpreted in terms of Feynman diagrams. The perturbative expansion of the free energy

$$F = \log Z \quad (2.1.8)$$

will only receive contributions from connected vacuum bubbles. This is a quantum field theory of a field in the adjoint representation, therefore we are able to express this expansion in terms of 't Hooft's double line notation [55]. But the perturbative expansion of these matrix models does not only depend on the couplings g_s and g_p , but also on the rank N of the gauge group. The Feynman diagrams are good at keeping track of powers in the coupling constants, but are lacking in keeping track of powers of N . But there is a way to organize the perturbative expansion in a meaningful way in terms of N . If we split the diagrams in the correct way, we obtain *fatgraphs* which we can associate with Riemann surfaces with holes, where each closed loop represents the boundary of a hole. This surface has a genus g which is related to the diagram by the relation

$$2g - 2 = E - V - h, \quad (2.1.9)$$

where E counts the number of propagators or edges, V counts the number of vertices and h the number of closed loops. Using this knowledge, we can write the factor associated with a fatgraph like

$$g_s^{2g-2} t^h \prod_p g_p^{V_p}, \quad (2.1.10)$$

where the *'t Hooft parameter*

$$t = N g_s \quad (2.1.11)$$

was introduced. We will call the fatgraphs with $g = 0$ *planar* and the ones with $g > 0$ *nonplanar*, for which examples are depicted in figure 2.1. In the end we find that the free energy admits

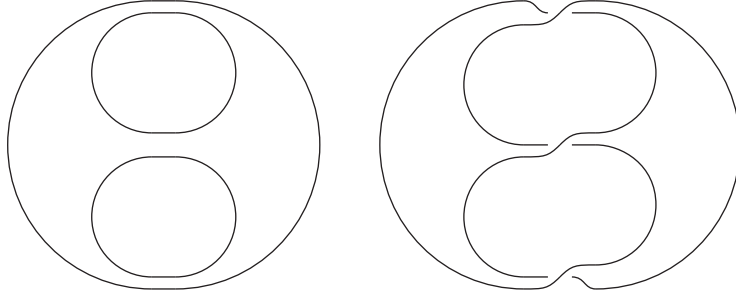


Figure 2.1: This figure depicts two cubic vertices. On the left-hand side a genus zero diagram is depicted, while the diagram shown on the right-hand side is of genus one.

an expansion in g_s and t as

$$F = \sum_{g=0}^{\infty} \sum_{h=1}^{\infty} F_{g,h} g_s^{2g-2} t^h, \quad (2.1.12)$$

where we define

$$F_g(t) = \sum_{h=1}^{\infty} F_{g,h} t^h \quad (2.1.13)$$

so that we can finally write down the *genus expansion*

$$F = \sum_{g=0}^{\infty} F_g(t) g_s^{2g-2}. \quad (2.1.14)$$

This model has the gauge symmetry (2.1.3), which is the transformation of a matrix M by a unitary matrix. This can be used to gauge fix the matrices M in the integral like

$$M \rightarrow U M U^\dagger = D, \quad (2.1.15)$$

where $D = \text{diag}(\lambda_1, \dots, \lambda_N)$. Using this as our choice of gauge and applying the Faddeev–Popov techniques in order to compute the gauge-fixed integral, we are able to write the partition function (2.1.1) in terms of eigenvalues of the hermitian matrices

$$Z = \frac{1}{N!} \int \frac{d\lambda^N}{(2\pi)^N} \Delta^2(\lambda) e^{-\frac{2}{g_s} \sum_{i=1}^N V(\lambda_i)}, \quad (2.1.16)$$

where

$$\Delta(\lambda) = \prod_{i < j} (\lambda_i - \lambda_j) \quad (2.1.17)$$

is the *Vandermonde determinant*.

2.1.2 Perturbative solutions of matrix models

There exist various ways of solving matrix models. The Gaussian matrix model has been solved in [44, 51] by means of e.g. orthogonal polynomials. Here we will introduce another possibility presented in e.g. [56].

If we insert a total derivative into (2.1.16) like in

$$\sum_k \int d\lambda^N \frac{\partial}{\partial \lambda_k} \left(\lambda^{p+1} \prod_{i \neq j} (\lambda_i - \lambda_j) \exp \left(-\frac{1}{2g_s} \sum_i V(\lambda_i) \right) \right) = 0, \quad (2.1.18)$$

we are able to derive a recursive relation for the correlation functions of this matrix model.

First we notice that

$$\langle \text{Tr } \mathbf{1} \rangle = N \quad (2.1.19)$$

and then we deduce from (2.1.18), the recursion relation

$$\sum_{j=0}^p \langle \text{Tr } M^j \text{Tr } M^{p-j} \rangle = \frac{1}{2g_s} \text{Tr}(M^{p+1} V'(M)), \quad (2.1.20)$$

which, for the Gaussian matrix model, just becomes

$$\sum_{j=0}^p \langle \text{Tr } M^j \text{Tr } M^{p-j} \rangle = \frac{1}{g_s} \text{Tr}(M^{p+2}). \quad (2.1.21)$$

This result can be used to compute all correlators with a single trace. We present a generalized formula in appendix A.1.

2.1.2.1 Spectral curves

The description (2.1.16) leads to a method of obtaining the genus zero free energy F_0 by solving a Riemann-Hilbert problem [57]. This method is based on the saddle point analysis of the matrix integral and will be extended in section 2.1.3 to a procedure which allows us to compute also higher order corrections of the free energy F_g .

In the next step we write the partition function like

$$Z = \frac{1}{N!} \int \frac{d\lambda^N}{(2\pi)^N} e^{N^2 S_{\text{eff}}(\lambda)}, \quad (2.1.22)$$

where we defined the effective action

$$S_{\text{eff}} = -\frac{1}{tN} \sum_{i=1}^N V(\lambda_i) + \frac{2}{N^2} \sum_{i < j} \log |\lambda_i - \lambda_j|. \quad (2.1.23)$$

This effective action is of order $\mathcal{O}(1)$, because the sums over the eigenvalues are roughly of order N . This means for $N \rightarrow \infty$ the integral will be dominated by a saddle-point configuration that extremizes the effective action. Variation of (2.1.23) with respect to the eigenvalue λ_i gives the equation

$$\frac{1}{2t} V'(\lambda_i) = \frac{1}{N} \sum_{j \neq i} \frac{1}{\lambda_i - \lambda_j}, \quad i = 1, \dots, N. \quad (2.1.24)$$

Let us define the eigenvalue distribution for finite N as

$$\rho(\lambda) = \frac{1}{N} \sum_{i=1}^N \delta(\lambda - \lambda_i), \quad (2.1.25)$$

where the λ_i are such that they solve the saddle point equation (2.1.24). We expect ρ to become a continuous function in the large N limit, so that we can describe the sums over eigenvalues in terms of continuum quantities by replacing

$$\frac{1}{N} \sum_{i=1}^N f(\lambda_i) \rightarrow \int_{\mathcal{C}} f(\lambda) \rho(\lambda) d\lambda, \quad (2.1.26)$$

where ρ is normalized like

$$\int_{\mathcal{C}} \rho(\lambda) d\lambda = 1, \quad (2.1.27)$$

and the path \mathcal{C} surrounds cuts introduced by the condensation of eigenvalues. In this expression ρ can be considered an *eigenvalue density*.

Using this eigenvalue density, in the planar limit we can write correlators of the matrix model as

$$\frac{1}{N} \langle \text{Tr} M^\ell \rangle = \int_{\mathcal{C}} d\lambda \lambda^\ell \rho(\lambda). \quad (2.1.28)$$

In order to find this eigenvalue density we introduce an auxiliary function we call the *resolvent*. It is defined as the generating function of the correlators (2.1.28)

$$\omega(p) = \frac{1}{N} \langle \text{Tr} \frac{1}{p - M} \rangle. \quad (2.1.29)$$

which can be seen by rewriting this expression formally as a geometric series

$$\omega(p) = \frac{1}{N} \sum_{k=0}^{\infty} \langle \text{Tr} M^k \rangle p^{-k-1}. \quad (2.1.30)$$

The resolvent admits an expansion of the form

$$\omega(p) = \sum_{g=0}^{\infty} g_s^{2g} \omega_g(p) \quad (2.1.31)$$

as this is the generating functional of connected correlators. Using (2.1.28), the resolvent at genus zero just becomes

$$\omega_0(p) = \sum_{k=0}^{\infty} p^{-k-1} \int d\lambda \rho(\lambda) \lambda^k = \int d\lambda \frac{\rho(\lambda)}{p - \lambda}. \quad (2.1.32)$$

From this, we can extract the eigenvalue density

$$\rho(\lambda) = -\frac{1}{2\pi i} (\omega_0(\lambda + i\epsilon) - \omega_0(\lambda - i\epsilon)), \quad (2.1.33)$$

which means that, if we know the resolvent at genus zero, we can use it to find the eigenvalue density.

The solutions of the matrix model can be encoded in the equation

$$y(p) = V'(p) - 2t\omega_0(p), \quad (2.1.34)$$

which leads to

$$y^2 = V'(p)^2 - R(p), \quad (2.1.35)$$

where

$$R(p) = 4t \int d\lambda \rho(\lambda) \frac{V'(p) - V'(\lambda)}{p - \lambda}. \quad (2.1.36)$$

This defines the *classical spectral curve* of the matrix model.

2.1.3 The topological recursion of Eynard and Orantin

A simple loop equation has the form

$$\oint_{\mathcal{C}} \frac{d\omega}{2\pi i} \frac{V'(\omega)}{p - \omega} W(\omega) = (W(p))^2 + \frac{1}{N^2} W(p, p). \quad (2.1.37)$$

In the large- N limit we can expand this equation in g_s and write, by extracting the expressions order by order,

$$(\hat{K} - 2W_0(p))W_g(p) = W_{g-1}(p, p) + \sum_{k=1}^{g-1} W_k(p)W_{g-k}(p), \quad (2.1.38)$$

where we defined the operator

$$\hat{K}f(p) = \oint_{\mathcal{C}} \frac{d\omega}{2\pi i} \frac{V'(\omega)}{p - \omega} f(\omega). \quad (2.1.39)$$

We see that the one-point function $W_g(p)$, when acted upon by the operator on the l. h. s. in (2.1.38), can be written in terms of two-point and one-point functions of lower genus. If we could invert the operator, we would have a recursive prescription for finding higher genus corrections to the resolvent. We can make use of the meromorphic forms on the Riemann surface defined by the spectral curve and invert operators of the form

$$(\hat{K} - 2W_0(p))f(p) = \phi(p). \quad (2.1.40)$$

This inversion is given [53, 58, 59] in terms of contour integrals around the cuts as

$$f(p) = \oint_{\mathcal{C}} \left(\frac{dS(p, q)}{y(q)} \phi(q) \right) = \sum_{i=1}^{2s} \text{Res}_{q=x_i} \left(\frac{dS(p, q)}{y(q)} \phi(q) \right), \quad (2.1.41)$$

where dS are unique meromorphic differentials which only have two simple poles in q , located at $q = p$ and $q = \bar{p}$ with the conditions

$$dS(q, p) \underset{q \rightarrow p}{\sim} \frac{dq}{q - p} + \text{finite}, \quad (2.1.42a)$$

$$dS(q, p) \underset{q \rightarrow \bar{p}}{\sim} \frac{dq}{q - p} + \text{finite} \quad (2.1.42b)$$

and the condition that the integral w.r.t. q over the A cycles vanishes

$$\oint_{q \in A_j} dS(q, p) = 0 \quad j = 1, \dots, s-1. \quad (2.1.43)$$

By using the loop insertion operator [60]

$$\frac{d}{dV}(p) = - \sum_{k=1}^{\infty} \frac{k}{p^{k+1}} \frac{\partial}{\partial g_k} \quad (2.1.44)$$

we are able to generally write a recursive equation for the many-point functions of genus g [53, 54]

$$W_{h+1}^{(g)}(p, p_1, \dots, p_h) = \text{Res}_{q=q_i} \frac{dE_q(p)}{\Phi(q) - \Phi(\bar{q})} \left(W_{h+2}^{(g-1)}(q, \bar{q}, p_1, \dots, p_h) \right) \quad (2.1.45)$$

$$\sum_{l=0}^g \sum_{J \subset H}^l W_{|J|+1}^{(g-l)}(q, p_J) W_{|H|-|J|+1}^{(l)}(\bar{q}, p_{H \setminus J}) . \quad (2.1.46)$$

In the following text we want to compute Wilson loop operators in the matrix model description, which only require one-point resolvents $W_g(p)$. However, in order to go to higher genus, we need contributions coming from many-point resolvents. For $g = 2$ this involves contributions with up to three legs.

In the next step, we introduce the so called *kernel differentials* [61, 53] which are an important tool in solving the recursion

$$\chi_i^{(n)} = \text{Res}_{q=x_i} \left(\frac{dS(p, q)}{\tilde{y}(q)} \frac{1}{(q-x_i)^n} \right) . \quad (2.1.47)$$

Using these kernel differentials we are able to systematically write down expressions formed by multiplying an expression $f(q, p_i, x_i)$ by $\frac{dS(p, q)}{y(q)}$ and taking the sum of the residua at $q = x_i$. Let us denote the operator that applies this by $\Theta(p, q)$, and define

$$\Theta(p, q)f(q, p_i, x_i) = \sum_i \text{Res}_{q=x_i} \left(\frac{dS(p, q)}{\tilde{y}(q)} f(q, p_i, x_i) \right) . \quad (2.1.48)$$

To start the recursion we do not only need the resolvent $\mu_0(x)$ at genus zero, but also another initial condition, namely the *annulus amplitude*

$$W_0(p, q) = -\frac{1}{2(p-q)^2} + \frac{\sigma(p)}{2(p-q)^2 \sqrt{\sigma(p)} \sqrt{\sigma(q)}} - \frac{\sigma'(p)}{4(p-q) \sqrt{\sigma(p)} \sqrt{\sigma(q)}} + \frac{A(p, q)}{\sqrt{\sigma(p)} \sqrt{\sigma(q)}} , \quad (2.1.49)$$

which is related to the *Bergman kernel* by

$$B(p, q) = \left(W_0(p, q) + \frac{1}{(p-q)^2} \right) dpdq . \quad (2.1.50)$$

We are considering an elliptic curve and in this case $A(p, q)$ as well as the kernel differentials

are given in terms of elliptic integrals:

$$A(p, q) = (p - x_1)(p - x_2) + (p - x_3)(p - x_4) + (x_1 - x_2)(x_4 - x_2)G(k), \quad (2.1.51)$$

where

$$k^2 = \frac{(x_1 - x_2)(x_3 - x_4)}{(x_1 - x_3)(x_2 - x_4)} \quad (2.1.52)$$

is the elliptic modulus and

$$G(k) = \frac{E(k)}{K(k)} \quad (2.1.53)$$

is the ratio between the two complete elliptic integrals

$$E(k) = \int_0^{\frac{\pi}{2}} \sqrt{1 - k^2 \sin^2 \theta} d\theta, \quad K(k) = \int_0^{\frac{\pi}{2}} \frac{d\theta}{\sqrt{1 - k^2 \sin^2 \theta}}. \quad (2.1.54)$$

2.1.3.1 local $\mathbb{P}^1 \times \mathbb{P}^1$

As explained in [62] the ordering of the branch points here follows the one appropriate for local $\mathbb{P}^1 \times \mathbb{P}^1$, which is obtained from the one in [61] by the exchange

$$x_2 \leftrightarrow x_4. \quad (2.1.55)$$

The kernel differentials appear in this formalism by expanding

$$\frac{dS(p, q)}{\tilde{y}(q)} = \frac{1}{M(q)\sqrt{\sigma(p)}} \left(\frac{1}{p - q} + \mathcal{N}^{(1)}(q) \right) dp \quad (2.1.56)$$

with an adjacent function $f(q, p, x_i)$ around the branch points. We introduce the function

$$\mathcal{N}^{(1)}(q) = \mathcal{K}C^{(1)}(q) = \frac{\pi\sqrt{(x_1 - x_3)(x_2 - x_4)}}{2K(k)} C^{(1)}(q), \quad (2.1.57)$$

which is a normalization of the \mathcal{C} (or equivalently the \mathcal{A}) cycle integral

$$C^{(1)}(q) = \int_{\mathcal{C}} \frac{1}{2\pi i} \frac{dx}{(q - x)\sqrt{\sigma}}, \quad (2.1.58)$$

so that the property (2.1.43) holds. Note that, if q approaches the branch points of the cuts defining the \mathcal{C} cycle, this integral has to be regularized,

$$C^{(1)}(x_i) = \begin{cases} \frac{1}{2\pi i} \int_{\mathcal{C}} \frac{dx}{(q-x)\sqrt{\sigma}} \Big|_{q=x_i} & \text{if } x_i \text{ is not a branch point defining } \mathcal{C} \\ \frac{1}{2\pi i} \int_{\mathcal{C}} \frac{dx}{(q-x)\sqrt{\sigma}} - \frac{1}{\sqrt{\sigma(q)}} \Big|_{q=x_i} & \text{if } x_i \text{ is a branch point defining } \mathcal{C}. \end{cases} \quad (2.1.59)$$

This definition of the regularization ensures that one can move the contour from the $x_1 - x_2$ cut to the $x_3 - x_4$ cut without getting a contribution from the poles. As a consequence the so defined integrals $C(x_i)$ obey a symmetry under certain permutations of the branch points. We

can evaluate e. g. the manifestly regular integral¹

$$\alpha_4 = \mathcal{N}^{(1)}(x_4) = \frac{1}{x_4 - x_3} \left[\frac{(x_3 - x_1)}{(x_1 - x_4)} G(k) + 1 \right] \quad (2.1.60)$$

and obtain from the symmetrization the evaluation at the other branch points

$$\mathcal{N}^{(1)}(x_1) = \mathcal{N}^{(1)}(x_4) \Big|_{\substack{x_1 \leftrightarrow x_4 \\ x_2 \leftrightarrow x_3}}, \quad \mathcal{N}^{(1)}(x_2) = \mathcal{N}^{(1)}(x_4) \Big|_{\substack{x_1 \leftrightarrow x_3 \\ x_2 \leftrightarrow x_4}}, \quad \mathcal{N}^{(1)}(x_3) = \mathcal{N}^{(1)}(x_4) \Big|_{\substack{x_1 \leftrightarrow x_2 \\ x_3 \leftrightarrow x_4}}. \quad (2.1.61)$$

Higher kernel differentials are therefore given by

$$\chi_i^{(n)} = \frac{1}{(n-1)!} \frac{1}{\sqrt{\sigma(q)}} \frac{d^{n-1}}{dq^{n-1}} \left[\frac{1}{M(q)} \left(\frac{1}{p-q} + \mathcal{N}^{(l)}(q) \right) \right]_{q=x_i}. \quad (2.1.62)$$

Here $\mathcal{N}^{(l)}(q) = \mathcal{K}C^{(l)}(q)$, and since the normalization factor \mathcal{K} is independent of q , the only nontrivial task is to calculate the derivatives

$$C^{(n)}(q) = \frac{d^{n-1}}{dq^{n-1}} C^{(1)}(q). \quad (2.1.63)$$

There are various ways to do this. One fast way is to compute

$$C^{(n)}(q) = \frac{(-1)^{n-1} (n-1)!}{2\pi i} \int_{\mathcal{C}} \frac{dx}{(q-x)^n \sqrt{\sigma}}. \quad (2.1.64)$$

These integrals have poles at finite points and are very similar to the ones with poles at infinity. By similar formulas they can be expressed by linear expressions in $K(k)$ and $E(K)$ with rational coefficients in the moduli. In particular the normalized integrals $\mathcal{N}^{(n)}(q)$ depend only on the ratio of elliptic functions $G(k)$ defined in (2.1.53). To get expressions which are valid at all branch points one calculates first $\mathcal{N}^{(n)}(x_4)$, which is regular, and then uses (2.1.61) to get $\mathcal{N}^{(n)}(x_i)$. These derivatives have symmetric expressions in terms of the branch points and the α_i . The first two derivatives are

$$\begin{aligned} \mathcal{N}^{(2)}(x_i) &= \frac{1}{3} \sum_{j \neq i} \frac{\alpha_j - \alpha_i}{x_j - x_i}, \\ \mathcal{N}^{(3)}(x_i) &= \frac{2}{15} \left[\frac{1}{\prod_{j \neq i} (x_j - x_i)} + \sum_{j \neq i} \left(\frac{7\alpha_j - \alpha_i}{(x_j - x_i)^2} + 3 \sum_{j \neq k} \frac{1}{(x_j - x_i)^2 (x_k - x_i)} \right) \right]. \end{aligned} \quad (2.1.65)$$

Eventually one needs integrals over meromorphic forms with mixed poles

$$\omega_{n,k} = \frac{x^n}{(x-p)^k \sqrt{\sigma(x)}} dx, \quad (2.1.66)$$

which are obtained from the obvious relations

$$\omega_{n,k} = \omega_{n-1,k-1} + p\omega_{n-1,k}. \quad (2.1.67)$$

¹ Here we make contact with the shorthand notation α_i introduced in [61].

The genus one differential is then determined by evaluating

$$W_1(p) = \Theta(p, q)W_0(q, q) \quad (2.1.68)$$

using (2.1.49,2.1.47), as well as the explicit formulas for the kernel differentials for elliptic curves. It was first calculated explicitly in [61]. One can order $W_1(p)$ according to its poles at the branch points

$$W_1(p) = \frac{4}{\sqrt{\sigma(p)}} \sum_{i=1}^4 \left(\frac{A_i}{(p-x_i)^2} + \frac{B_i}{p-x_i} + C_i \right), \quad (2.1.69)$$

where

$$\begin{aligned} A_i &= \frac{1}{16} \frac{1}{M(x_i)}, & B_i &= -\frac{1}{16} \frac{M'(x_i)}{M^2(x_i)} + \frac{1}{8M(x_i)} \left(2\alpha_i - \sum_{j \neq i} \frac{1}{x_i - x_j} \right), \\ C_i &= -\frac{1}{48} \frac{1}{M(x_i)} \sum_{j \neq i} \frac{\alpha_i - \alpha_j}{x_j - x_i} - \frac{1}{16} \frac{M'(x_i)}{M^2(x_i)} \alpha_i + \frac{\alpha_i}{8M(x_i)} \left(2\alpha_i - \sum_{j \neq i} \frac{1}{x_i - x_j} \right). \end{aligned} \quad (2.1.70)$$

To obtain the form

$$W_2(p) = \Theta(p, q) (W_1(q, q) + W_1(q)W_1(q)) \quad (2.1.71)$$

one needs $W_1(p, p_1)$ from

$$W_1(p, p_1) = \Theta(p, q) (W_0(q, q, p_1) + 2W_1(q)W_0(q, p_1)) \quad (2.1.72)$$

and $W_0(p, p_1, p_2)$ from

$$W_1(p, p_1, p_2) = 2\Theta(p, q)W_0(q, p_1)W_0(q, p_2). \quad (2.1.73)$$

By repeated application of the recursion, one expresses any amplitude through a calculation of repeated residues of products of the annulus amplitude. The function $W_2(p)$ can be for example written like

$$\begin{aligned} W_2(p) &= 2\Theta(p, q)\Theta(q, q_1)\Theta(q_1, q_2)W_0(q_2, q)W_0(q_2, q_1) + \\ & 2\Theta(p, q)\Theta(q, q_1)\Theta(q_1, q_2)W_0(q_1, q)W_0(q_2, q_2) + \\ & \Theta(p, q)\Theta(q, q_1)\Theta(q, q_2)W_0(q_1, q_1)W_0(q_2, q_2). \end{aligned} \quad (2.1.74)$$

It is easy to derive that for amplitude with genus g and h holes all terms will be of the general form

$$W_{g,h} \sim \Theta^{2g-2+h} W_{0,2}^{g+h-1}. \quad (2.1.75)$$

However the number of terms grows exponentially with g and h . A few examples for the number of contributions counted with multiplicity is given in the table below.

Since $W \sim G$, and each Θ increases the power of G by one, we get for the leading power $W_{g,h} \sim G^{3g+2h-3}$. More precisely, the $W_{g,h}$ are meromorphic differentials with the following pole structure

$$W_{g,h}(p_1, \dots, p_h) = \frac{1}{\prod_l^h \sqrt{\sigma(p_l)}} \left(\sum_{j=0}^{3g-2+h} \sum_{k=1}^h \sum_{i=1}^4 \frac{A_{i,k}^{(j)}}{(p_k - x_i)^{3g-2+h-j}} \right), \quad (2.1.76)$$

h	g	0	1	2	3	4	5
1		disk	1	5	60	1105	27120
2		1	4	50	960	24310	
3		2	32	700	19200		
4		12	384	12600			

Table 2.1: Number of terms involved in the recursive definition of $W_{g,h}$.

where

$$A_{i,k}^{(j)} = \sum_{p=0}^j G^p a_{i,k}^{(p)}(x_i) \quad (2.1.77)$$

are polynomials in the ratio of the complete elliptic integrals. For $W_g(p)$, $g = 2, 3$ we found a explicit expressions for general moment functions. To write down all $A_{i,k}^{(j)}$ takes however several pages. We display the coefficient of the leading pole

$$A_{i,1}^{(0)} = \frac{105}{2^7 M(x_i)^3 \prod_{k \neq i} (x_i - x_k)} . \quad (2.1.78)$$

and $a_1^{(3g-2+h)} := \sum_i a_{i,1}^{(3g-2+h)}$ multiplying the highest power of G^{3g-2+h} in $W_{g,h}(p)$. For $h = 1$ we find

$$a_1^{(3g-2+1)} = c_{g,1} \left(\sum_{i=1}^4 \frac{1}{M(x_i) \prod_{j \neq i} (x_i - x_j)^2} \right)^{2g-1} [(x_1 - x_3)(x_2 - x_4)]^{3g-1}, \quad (2.1.79)$$

where $c_{2,1} = -\frac{5}{16}$, $c_{3,1} = \frac{7}{8}$. The other expressions are available on request.

All the results above are valid for any spectral curve of genus one. The calculation of the higher genus functions $W_g(p)$ is obviously quite involved.

2.2 ABJM theory

By considering the different dualities connecting the various string theories, Witten conjectured the existence of a theory, unifying all these into one [22]. We know its low energy limit, namely eleven dimensional supergravity, which was defined in [63], from which one can deduce that the fundamental objects of M–theory are membranes.

The construction of the low–energy field theory of a stack of M2–branes has been a long-standing problem. To achieve this it has been found, that one needs to explore conformal Chern–Simons theories in three dimensions [64]. But it turned out that they do not possess enough supersymmetry. Usually CSM theories in three dimensions only have $\mathcal{N} = 2$ or $\mathcal{N} = 3$ supersymmetry. This is not enough to describe the low–energy field theory of such a stack of M2–branes. A theory with more supersymmetry, namely $\mathcal{N} = 8$, has been constructed later on [65, 66, 67, 23], which was conjectured to correspond to a certain setup of M2–branes.

Additionally there needs to exist a sensible interpretation in the context of AdS/CFT. All the problems mentioned here were solved in [24] where a $\mathcal{N} = 6$ Chern–Simons matter theory in three dimensions has been constructed, which fulfills the necessary conditions. It is a quiver

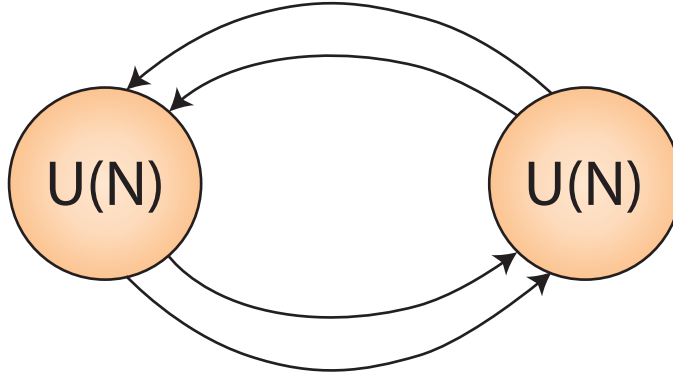


Figure 2.2: A gauge quiver describing the field content of ABJM theory.

gauge theory with two nodes, i.e. it has the gauge group $U(N) \times U(N)$, with bifundamental matter. The relevant quiver diagram can be found in figure 2.2. In this diagram is encoded that the field content is given by four complex scalar fields and four complex fermions transforming in the (\bar{N}, N) and (N, \bar{N}) -representation of $U(N) \times U(N)$. The gauge fields have a Chern–Simons action with opposite integer levels k and $-k$ for the two gauge groups. A specific scalar potential is chosen in a way such that supersymmetry is enhanced to $\mathcal{N} = 6$ in the general case or even $\mathcal{N} = 8$ for $k = 1, 2$. With $\mathcal{N} = 6$ this theory has a total of 12 real supercharges. This theory is weakly coupled for large k ($k \gg N$).

It is possible to set up a brane construction in type IIA string theory which has ABJM as its low energy limit. This setup can be lifted to M–theory on the orbifold $\mathbb{C}^4/\mathbb{Z}_k$. The AdS dual of ABJM is M–theory on

$$\text{AdS}_4 \times S^7/\mathbb{Z}_k, \quad (2.2.1)$$

where k is given by the coupling constant k of the CSM theory. In the limit $N \gg k^5$ this geometry is weakly curved and the theory is described by type IIA string theory on $\text{AdS}_4 \times \mathbb{CP}^3$.

2.3 Localization

A very useful property appearing in supersymmetric gauge theories is called *localization*. This property makes it possible to reduce the full path integral, defining the theory, to lower-dimensional integrals. In the case we are considering the path-integral of CSM theories in three dimensions will reduce to common integrals, meaning we will effectively reduce the problem to a zero dimensional QFT, like e.g. a matrix model. Let us look a simple example presented in [68] and explain the basics of localization following this reference.

Let us consider a very simple example with one bosonic field X and two fermionic fields ψ_1 and ψ_2 . We consider the partition function defined by the path integral

$$Z = \int e^{-S(X, \psi_1, \psi_2)} dX d\psi_1 d\psi_2, \quad (2.3.1)$$

where the action is given by

$$S(X, \psi_1, \psi_2) = \frac{1}{2}(\partial h)^2 - \partial^2 h \psi_1 \psi_2, \quad (2.3.2)$$

with $\partial h = \partial_X h(X)$. Consider the transformations

$$\delta X = \epsilon^1 \psi_1 + \epsilon^2 \psi_2, \quad (2.3.3a)$$

$$\delta \psi_1 = \epsilon^2 \partial h, \quad (2.3.3b)$$

$$\delta \psi_2 = -\epsilon^2 \partial h, \quad (2.3.3c)$$

where ϵ^i and ψ_i are Grassmann odd variables. These transformations leave the action invariant and exchange bosons and fermions, i. e. these define a supersymmetry.

If we assume $\partial h \neq 0$ for all X the partition function (2.3.1) just vanishes. This can be shown by applying the transformation

$$\hat{X} = X - \frac{\psi_1 \psi_2}{\partial h(X)}, \quad (2.3.4a)$$

$$\hat{\psi}_1 = \alpha(X) \psi_1, \quad (2.3.4b)$$

$$\hat{\psi}_2 = \psi_1 + \psi_2, \quad (2.3.4c)$$

where $\alpha(X)$ is an arbitrary function. The action is invariant under the transformation

$$(X, \psi_1, \psi_2) \rightarrow (\hat{X}, 0, \hat{\psi}_2). \quad (2.3.5)$$

Therefore we can write

$$S(X, \psi_1, \psi_2) = S(\hat{X}, 0, \hat{\psi}_2) \quad (2.3.6)$$

and have effectively eliminated one fermionic field. Using this in the Grassmanian integration and noting that the remaining term is a total derivative, we can show that $Z = 0$.

In the next step, we will extend this to the case where ∂h vanishes for some X . For such h the change of variables (2.3.3) is singular. Let us therefore integrate over the set where $\partial h = 0$ is deleted. If $\partial h = 0$ we also have $\delta \psi_i = 0$ in (2.3.3). At these point we cannot trade the supersymmetry–transformation variable with one of the fermionic fields. Hence the points where ∂h are fixed points of the symmetry (2.3.3) and the computation localizes to the vicinity of the set of fixed points. Or in other words, the path–integral is localized at loci where the r.h.s. of the fermionic transformation in (2.3.3) under supersymmetry vanishes. This principle holds for any QFT with supersymmetry.

Let us analyze our simple setup at the critical points now. In order to do that, let us assume h is a polynomial of order n with isolated critical points. Then it has at most $n - 1$ critical points. Near a critical point X_c we write h as

$$h(X) = h(X_c) + \frac{\alpha_c}{2} (X - X_c)^2 + \dots. \quad (2.3.7)$$

We saw before that the partition function localizes at the critical points and we only have to consider infinitesimal small regions around them. As a result we only have to keep the leading order terms in the action, expanded around the critical point, corresponding to some infinitesimal neighborhood. Finally, the partition function (2.3.1) becomes, with a suitable normalization,

$$\sum_{X_c} \int \frac{dX d\psi^1 d\psi^2}{\sqrt{2\pi}} e^{-\frac{1}{2}(X-X_c)^2 + \alpha_c \psi^1 \psi^2} = \sum_{X_c} \frac{\alpha_c}{|\alpha_c|} = \sum_{X_c} \frac{h''(X_c)}{|h''(X_c)|}, \quad (2.3.8)$$

so that we can write

$$Z = \sum_{x_0: \partial h|_{x_0}=0} \frac{\partial^2 h(X)}{|\partial^2 h(X)|}. \quad (2.3.9)$$

More generally, if we have a quantum field theory with a symmetry, then the correlation functions of quantities that are variations of other fields under the symmetry vanish. Let us, for example, consider $f = \delta g$, where δg is the variation of g under a symmetry. Then we can write

$$\langle f \rangle = \int f e^{-S} = \int \delta g e^{-S} = \int \delta(g e^{-S}) = 0, \quad (2.3.10)$$

if we can discard boundary terms. This principle applies to bosonic symmetries as well as fermionic symmetries. Let us consider

$$g = \partial \rho(X) \psi_1, \quad (2.3.11)$$

which yields, when we apply the symmetry–transformation (2.3.3) where we set $\epsilon^1 = \epsilon^2 = \epsilon$,

$$f = \delta_\epsilon g = \epsilon(\partial_\rho \partial h - \partial^2 \rho \psi_1 \psi_2). \quad (2.3.12)$$

As we know, the expression $\langle f \rangle$ vanishes, thus we have

$$\langle \partial_\rho \partial h - \partial^2 \rho \psi_1 \psi_2 \rangle = 0. \quad (2.3.13)$$

Let us now transform the action (2.3.2) by applying $h \mapsto h + \rho$ to it. The variation of the action is

$$\delta_\rho S = \partial_\rho \partial h - \partial^2 \rho \psi_1 \psi_2 \quad (2.3.14)$$

and by looking at (2.3.13) we see, that the vev of this expression vanishes. Hence the partition function is invariant under this transformation

$$\langle \delta_\rho S \rangle = 0. \quad (2.3.15)$$

This can also be used to compute the partition function. Let us rescale $h \rightarrow \lambda h$ with $\lambda \gg 1$. In this case the action S is very large, while $\exp(-S)$ is very small, except for points nearby the critical points of h . Using this method the problem reduces to the computations presented earlier in this section.

Supersymmetry enables us to define nilpotent operators Q , meaning $Q^2 = 0$, which is a property that can be used to localize the path integral to zero–loci of the supersymmetric transformations along the lines described before.

An important result was derived in [31] where the vevs of certain Wilson loops in $\mathcal{N} = 4$ and $\mathcal{N} = 2$ SYM theories in four dimensions were localized to simple matrix integrals. The results extracted from these matrix models were in agreement with the AdS/CFT correspondence.

New techniques in localization were presented in [32] which made it possible to localize the partition functions and expectation values of Wilson loops of $\mathcal{N} \geq 3$ CSM theories to matrix integrals. ABJM theory is such a CSM theory and can therefore be localized by applying this formalism.

Let us show this procedure for the gauge sector of a CSM theory. A general CSM theory without matter can be described by an $\mathcal{N} = 2$ multiplet which consists of the gauge field A_μ , two real auxiliary scalars σ and D , auxiliary fermion λ which is a two–component complex spinor.

The Lie algebra of the gauge group G is denoted by \mathfrak{g} . All of the above fields are valued in this Lie algebra \mathfrak{g} . The kinetic term we will be using is a supersymmetric Chern–Simons term, which in flat Euclidean space is given by

$$S = \int d^3x \operatorname{Tr} \left(\operatorname{Ad}A + \frac{2i}{3}A^3 - \lambda^\dagger\lambda + 2D\sigma \right), \quad (2.3.16)$$

where Tr denotes some inner product on \mathfrak{g} .

We actually do not consider flat Euclidean space but transfer the above action, which is conformally invariant, to the unit three-sphere S^3 . Therefore we have to include the measure factor \sqrt{g} and have to change the supersymmetry transformations in a way that they are covariant with respect to both, the gauge field and the metric on S^3 .

The transformations of the fields, which leave the action on the S^3 invariant are given by

$$\delta A_\mu = \frac{i}{2}(\eta^\dagger\gamma_\mu\lambda - \lambda^\dagger\gamma_\mu\epsilon) \quad (2.3.17a)$$

$$\delta\sigma = -\frac{1}{2}(\eta^\dagger\lambda + \lambda^\dagger\epsilon) \quad (2.3.17b)$$

$$\begin{aligned} \delta D &= \frac{i}{2}(\eta^\dagger\gamma^\mu(D_\mu\lambda) - (D_\mu\lambda^\dagger)\gamma^\mu\epsilon) \\ &\quad - \frac{i}{2}(\eta^\dagger[\lambda, \sigma] - [\lambda^\dagger, \sigma]\epsilon) + \frac{i}{6}(\nabla_\mu\eta^\dagger\gamma^\mu\lambda - \lambda^\dagger\gamma^\mu\nabla_\mu\epsilon) \end{aligned} \quad (2.3.17c)$$

$$\delta\lambda = -\frac{1}{2}\gamma^{\mu\nu}F_{\mu\nu}\epsilon - D\epsilon + i\gamma^\mu D_\mu\sigma\epsilon + \frac{2i}{3}\sigma\gamma^\mu\nabla_\mu\epsilon \quad (2.3.17d)$$

$$\delta\lambda^\dagger = \frac{1}{2}\eta^\dagger\gamma^{\mu\nu}F_{\mu\nu} - D\eta^\dagger + i\eta^\dagger\gamma^\mu D_\mu\sigma - \frac{2i}{3}\sigma\nabla_\mu\eta^\dagger\gamma^\mu, \quad (2.3.17e)$$

where ϵ and η are two-component complex spinors, which are independent as we are in euclidean space. The γ_μ here are the Pauli matrices which we use to define

$$\gamma_{\mu\nu} = \frac{1}{2}[\gamma_\mu, \gamma_\nu]. \quad (2.3.18)$$

The expression

$$D_\mu = \partial_\mu + i[A_\mu, \cdot] \quad (2.3.19)$$

is the gauge covariant derivative. If we only consider the gauge part, ϵ and η can be arbitrary. However, if we add matter it is necessary to take ϵ and η to be Killing spinors.

By means of the fermionic symmetry δ we can construct the term

$$t\delta V = t\delta \operatorname{Tr}' \left((\delta\lambda)^\dagger\lambda \right), \quad (2.3.20)$$

where Tr' is some positive definite inner product on the Lie algebra. The bosonic part of this term is positive definite. The reason for adding this term is that for any δ -invariant observable this does not change the expectation value, as we saw in (2.3.10). Hence by sending $t \rightarrow \infty$ we do not change the partition function and also do not change the vevs of for example supersymmetric Wilson loops.

We find the localization conditions

$$\frac{1}{2}\epsilon_{\mu\nu\rho}F^{\nu\rho} = D_\mu\sigma \quad (2.3.21a)$$

$$D = -\sigma. \quad (2.3.21b)$$

We also see that $F_{\mu\nu} = 0$, meaning the solution consists of flat connections of the gauge field on S^3 . The only flat connection on S^3 is $A_\mu = 0$, leaving us with the relation $D_\mu\sigma = \partial_\mu\sigma = 0$, so that $\sigma = \sigma_0 = \text{const.}$ from which follows that $D = -\sigma_0$ is also constant. All other fields are vanishing.

The localization locus only consists of configuration where σ and D are constant, hence the path integral localizes to

$$Z = \int d\sigma_0 e^{S_{\text{cl}}[\sigma_0]} Z_{1\text{-loop}}^g[\sigma_0], \quad (2.3.22)$$

which is the saddle point approximation for $t \rightarrow \infty$. The classical part of the action reduces to just

$$S_{\text{cl}}[\sigma_0] = -4i\pi^2 \text{Tr}(\sigma_0^2), \quad (2.3.23)$$

leaving us with the factor $Z_{1\text{-loop}}^g$ coming from the quadratic fluctuations. Everything else will be suppressed.

Now we will explicitly introduce the zero modes of σ and D , by setting

$$\sigma \rightarrow \sigma_0 + \frac{1}{\sqrt{t}}\sigma', \quad (2.3.24a)$$

$$D \rightarrow -\sigma_0 + \frac{1}{\sqrt{t}}D', \quad (2.3.24b)$$

$$A_\mu, \lambda, c \rightarrow \frac{1}{\sqrt{t}}A_\mu, \lambda, c, \quad (2.3.24c)$$

where c is the ghost field we have to introduce to gauge fix the action. The factor t in front of the fields has been introduced in order to eliminate an overall factor in the action. All the fields except σ and D do not have zero modes.

If we take t large and drop the quadratic terms, we are left, after some calculations, with

$$S = \int \sqrt{g}d^3x \sum_\alpha \left(B^\mu{}_\alpha (-\nabla^2 + \alpha(\sigma_0)^2) B_{\mu\alpha} + \lambda_\alpha^\dagger \left(i\nabla + i\alpha(\sigma_0) - \frac{1}{2} \right) \lambda_\alpha \right), \quad (2.3.25)$$

where B_μ is defined by splitting the gauge field A_μ in divergenceless and pure divergence part

$$A_\mu = \partial_\mu\phi + B_\mu. \quad (2.3.26)$$

Now we decompose B_μ as

$$B_\mu = \sum_\alpha B_\mu{}^\alpha X_\alpha + h_\mu, \quad (2.3.27)$$

where X_α are representatives of the root spaces of G , α runs over the roots of G and h_μ is the component of B_μ along the Cartan.

Knowing the eigenvalues [69] of the vector laplacian acting on divergenceless vector fields we

find the determinant of the bosonic part

$$\det(\text{bosons}) = \prod_{\alpha} \prod_{l=1}^{\infty} ((l+1)^2 + \alpha(\sigma_0)^2)^{2l(l+2)} \quad (2.3.28)$$

and analogously for the fermions

$$\det(\text{fermions}) = \prod_{\alpha} \prod_{l=1}^{\infty} ((l + i\alpha(\sigma_0))(-l - 1 + i\alpha(\sigma_0)))^{l(l+1)}. \quad (2.3.29)$$

Using these expressions one can show that the one-loop contribution is just given by

$$Z_{1\text{-loop}}^g[\sigma_0] = \prod_{\alpha} \left(\frac{\sinh(\pi\alpha(\sigma_0))}{\pi\alpha(\sigma_0)} \right), \quad (2.3.30)$$

where α runs over the roots of G . Now we can plug this result into (2.3.22).

This is the story for the gauge sector. When adding matter we can follow a similar approach to localize the path integral, but let us state here only the results without going into detail about the computation.

For convenience we introduce the notation

$$\det_R f(a) = \prod_{\rho} f(\rho(a)), \quad (2.3.31)$$

where R is some representation and the product runs over the weights of R . Considering a CSM theory with gauge group G and chiral multiplets in a representation $R \oplus R^*$, we are able to write the partition function as

$$Z = \frac{1}{|\mathcal{W}|} \int da \exp(-4i\pi^2 \text{Tr}(a^2)) \frac{\det_{\text{Ad}}(2 \sinh(\pi a))}{\det_R(2 \cosh(\pi a))}, \quad (2.3.32)$$

where $|\mathcal{W}|$ denotes the order of the Weyl group of G and Tr is an invariant inner product on \mathfrak{g} . A standard Wilson loop operator in a theory is defined by

$$W = \frac{1}{\dim S} \text{Tr}_S \left(\mathcal{P} \exp \left(\oint d\tau (iA_{\mu} \dot{x}^{\mu} + \sigma |\dot{x}|) \right) \right). \quad (2.3.33)$$

Here $x^{\mu}(\tau)$ is the closed world-line of the Wilson loop and \mathcal{P} denotes the path-ordering operator.

The vev of this Wilson loop operator is just given by a simple insertion into the partition function

$$\langle W \rangle = \frac{1}{Z|\mathcal{W}|\dim S} \int da \exp(-4i\pi^2 \text{Tr}(a^2)) \text{Tr}(e^{2\pi a}) \frac{\det_{\text{Ad}}(2 \sinh(\pi a))}{\det_R(2 \cosh(\pi a))} \quad (2.3.34)$$

with an additional normalization.

2.3.1 ABJM as a Matrix model

As stated in section 2.2, the matter content of ABJM theory consists of two chiral multiplets in the bifundamental (N, \bar{N}) representation and two chiral multiplets in the dual (\bar{N}, N) representation.

If we set a to

$$a = \text{diag}(\lambda_1, \dots, \lambda_N, \hat{\lambda}_1, \dots, \hat{\lambda}_N) \quad (2.3.35)$$

we can write the roots as

$$\rho_{i,j}^{(N,\bar{N})}(a) = \lambda_i - \hat{\lambda}_j, \quad (2.3.36a)$$

$$\rho_{i,j}^{(\bar{N},N)}(a) = -\lambda_i + \hat{\lambda}_j \quad (2.3.36b)$$

and the inner product we use is

$$\text{Tr} = \frac{k}{4\pi} (\text{tr} - \hat{\text{tr}}), \quad (2.3.37)$$

where tr and $\hat{\text{tr}}$ are traces in the fundamental representation of the two $U(N)$ factors and k is an integer. Plugging this into (2.3.32) yields

$$Z_{\text{ABJM}}(N) = \frac{1}{N!^2} \int \frac{d^N \mu}{(2\pi)^N} \frac{d^N \nu}{(2\pi)^N} \frac{\prod_{i<j} \left[2 \sinh \left(\frac{\mu_i - \mu_j}{2} \right) \right]^2 \left[2 \sinh \left(\frac{\nu_i - \nu_j}{2} \right) \right]^2}{\prod_{i,j} \left[2 \cosh \left(\frac{\mu_i - \nu_j}{2} \right) \right]^2} e^{-\frac{1}{2g_s} (\sum_i \mu_i^2 - \sum_i \nu_i^2)}, \quad (2.3.38)$$

where the coupling g_s is related to the Chern–Simons coupling k of ABJM theory as

$$g_s = \frac{2\pi i}{k}, \quad (2.3.39)$$

which can be interpreted as an hermitian two-matrix model where the Vandermonde determinant is replaced like $\prod_{i<j} (\lambda_i - \lambda_j) = \prod_{i<j} \sinh(\lambda_i - \lambda_j)$, so that we have a sinh-deformed Vandermonde determinant.

A BPS Wilson loop has been analyzed in [70, 34] which is explicitly given by

$$W_R^{1/6} = \text{Tr}_R \mathcal{P} \exp \oint \left(i A_\mu \dot{x}^\mu + \frac{2\pi}{k} M_I^J C_I \bar{C}^J |\dot{x}| \right) ds. \quad (2.3.40)$$

Here X^A denote the four scalar fields of the theory and X_A denotes their adjoints. M_A^B is a constant hermitian matrix and it can be chosen to be $\text{diag}(1, 1, -1, -1)$, which makes this operator 1/6 BPS.

From the localization approach we know that the normalized vev of the 1/6 BPS Wilson loop is given by inserting

$$\sum_i e^{2\pi \lambda_i} = \text{Tr} e^{2\pi \lambda}. \quad (2.3.41)$$

Therefore we have

$$\langle W_R \rangle = \frac{1}{\dim R(U(N_1))} \langle \text{Tr}_R(e^{\mu_i}) \rangle_{\text{ABJM}} \quad (2.3.42)$$

and analogously for the second gauge group

$$\langle \hat{W}_R \rangle = \frac{1}{\dim R(U(N_2))} \langle \text{Tr}_R(e^{\nu_i}) \rangle_{\text{ABJM}}. \quad (2.3.43)$$

One can obtain (2.3.43) from (2.3.42) by exchanging $N_1 \leftrightarrow N_2$ and sending the coupling constant from g_s to $-g_s$. From now on we will focus, without loss of generality, on the Wilson loop associated to the first node, and we will also assume that $k > 0$ in the first node.

These Wilson loops break the symmetry between the gauge groups. But in [33] an operator has been derived (see also [71]), which handles the gauge groups in a more symmetric way. There the quiver gauge group $U(N_1) \times U(N_2)$ has been promoted to the super group $U(N_1|N_2)$ due to the supergroup structure, that these Wilson loop possess. We denote the representations of these supergroups by \mathcal{R} . The operator localizes to the matrix model correlator

$$\langle W_{\mathcal{R}} \rangle = \left\langle \text{Str} \begin{pmatrix} e^{\mu_i} & 0 \\ 0 & -e^{-\nu_j} \end{pmatrix} \right\rangle_{\text{ABJM}} \quad (2.3.44)$$

in the ABJM matrix model. Str denotes a super-trace in the super-representation \mathcal{R} . By noting that a representation of $U(2N)$ induces a super-representation $U(N|N)$ defined by the same Young tableaux \mathcal{R} we can also write [72]

$$\begin{aligned} \text{Str}_{\mathcal{R}} \begin{pmatrix} e^{\mu_i} & 0 \\ 0 & -e^{-\nu_j} \end{pmatrix} &= \sum_{\mathbf{k}} \frac{\chi_{\mathcal{R}}(\mathbf{k})}{z_{\mathbf{k}}} \prod_{\ell} \left(\text{Str} \begin{pmatrix} e^{\mu_i} & 0 \\ 0 & -e^{-\nu_j} \end{pmatrix}^{\ell} \right)^{k_{\ell}} \\ &= \sum_{\mathbf{k}} \frac{\chi_{\mathcal{R}}(\mathbf{k})}{z_{\mathbf{k}}} \prod_{\ell} \left(\text{tr} \left(e^{\ell \mu_i} \right) - (-1)^{\ell} \text{tr} \left(e^{\ell \nu_j} \right) \right)^{k_{\ell}}. \end{aligned} \quad (2.3.45)$$

This is the supergroup generalization of Frobenius formula and here $\mathbf{k} = (k_{\ell})$ is a vector of non-negative, integer entries, which can be regarded as conjugacy classes of the symmetric group. $\chi_{\mathcal{R}}(\mathbf{k})$ is the character of this conjugacy class in the representation \mathcal{R} , and

$$z_{\mathbf{k}} = \prod_{\ell} \ell^{k_{\ell}} k_{\ell}!. \quad (2.3.46)$$

Here we will consider Wilson loops with arbitrary winding number n . In the representation-basis these are defined by

$$W_n^{1/6} = \sum_{s=0}^{n-1} (-1)^s W_{R_{n,s}}^{1/6}, \quad (2.3.47)$$

where $R_{n,s}$ is a hook-representation with n boxes in total, $n-s$ boxes in the first row, and one box in the remaining rows. The case $n=1$ corresponds to the Wilson loop in the fundamental representation. In terms of matrix model vevs this is given by

$$\langle W_n^{1/6} \rangle = \langle \text{tr} \left(e^{n \mu_i} \right) \rangle_{\text{ABJM}}. \quad (2.3.48)$$

The 1/2 Wilson loop with winding n , as we can deduce from (2.3.45), given by

$$\langle W_n^{1/2} \rangle = \langle W_n^{1/6} \rangle - (-1)^n \langle \widehat{W}_n^{1/6} \rangle. \quad (2.3.49)$$

This means in general, as it is clear from (2.3.45), that the vevs of 1/2 BPS Wilson loops can be obtained from computing the 1/6 BPS Wilson loops.

Here we showed that the partition function as well as the operators for the 1/6 BPS Wilson loop and the 1/2 BPS Wilson loop can be written in terms of matrix models. These matrix models were used in [41, 36] to solve this problem at different coupling strength, by making use of the tools known for topological string theory. We will use these result and map them to a free Fermi gas which admits an expansion corresponding to the string coupling limit in ABJM theory.

In [44, 45] a matrix model describing Chern–Simons theory in $L(p, 1) = S^3/\mathbb{Z}_p$ has been derived. This matrix model is large N -dual to the topological string A-model on local $\mathbb{P}^1 \times \mathbb{P}^1$. The mirror geometry is encoded in the elliptic curve

$$y = \frac{z_1 x^2 + x + 1 - \sqrt{(1 + x + z_1 x^2)^2 - 4z_2 x^2}}{2} \quad (2.3.50)$$

where z_1, z_2 are the complex structure moduli. This moduli space has previously been analyzed in [45, 40].

The way [41] made use of this is by realizing the connection

$$Z_{\text{ABJM}}(N_1, N_2, g) = Z_{L(2,1)}(N_1, -N_2, g) \quad (2.3.51)$$

so that we are able to use the tools already available for the topological string to solve ABJM theory.

2.3.2 The geometry of ABJM theory

In [41, 36] the partition function and the Wilson loop vevs of ABJM theory are mapped, via the spectral curve of the lens space matrix model, to geometric invariants of the elliptic curve

$$H(X, Y) = X + \frac{1}{\varphi_1^2 X} + Y + \frac{1}{\varphi_2^2 Y} + 1 = 0, \quad (2.3.52)$$

which are in turn related to meromorphic differentials of the third kind². In particular, in the planar limit, the partition function and the Wilson loop vevs are related to periods of these differentials. The higher N corrections are related to these periods by a recursive procedure, which amounts to integration of the loop equations of the matrix model, described in section 2.1.3. In (2.3.52) X, Y are \mathbb{C}^* variables and (2.3.52) is the mirror curve of the local Calabi–Yau geometry of the B-model, namely $M_{cy} = \mathcal{O}(-K_{\mathbb{P}^1 \times \mathbb{P}^1}) \rightarrow \mathbb{P}^1 \times \mathbb{P}^1$, which is the total space of the anti canonical line bundle over $\mathbb{P}^1 \times \mathbb{P}^1$.

After multiplying (2.3.52) with XY , homogenizing it to a cubic with W , swapping W with $-Y$ and rescaling $X \mapsto X\varphi_1$, one obtains the curve

$$\tilde{H}(X, Y) = Y^2 - Y \left(1 + X\varphi_1 + X^2 \frac{\varphi_1^2}{\varphi_2^2} \right) + X^2 = 0. \quad (2.3.53)$$

A common parameterization of the \mathbb{C}^* variables arising in the definition of the curve is $X = e^u$ and $Y = e^v$. Then the relevant meromorphic differentials of the third kind are given by

$$\mu_k = v e^{ku} du = \log(Y) X^{k-1} dX, \quad k = 0, 1, \dots, \quad (2.3.54)$$

where

$$Y = \frac{a(X)}{2} \pm \frac{1}{2} \sqrt{\sigma(X)}. \quad (2.3.55)$$

This form is typical of local mirror geometries. With the above parameterization the discrimi-

² see [72] for a review.

nant is given as

$$\sigma(X) = \prod_{i=1}^4 (X - x_i) = a(X)^2 - 4X^2, \quad \text{with} \quad a(X) = 1 + X\varphi_1 + X^2 \frac{\varphi_1^2}{\varphi_2}. \quad (2.3.56)$$

The branch points involve square roots of the φ_i , but with an appropriate ordering one has

$$\varphi_1 = -\frac{1}{2} \sum_{i=1}^4 x_i, \quad \frac{\varphi_1}{\varphi_2} = \frac{1}{4}(x_1 + x_2 - x_3 - x_4), \quad x_1 = \frac{1}{x_2} =: a, \quad x_4 = \frac{1}{x_3} =: -b. \quad (2.3.57)$$

Note that (2.3.53,2.3.55) defines the same family of (hyper) elliptic curves as

$$y^2 = \sigma(x), \quad (2.3.58)$$

where we identified X, Y with x, y . This identification amounts to a compactification of the \mathbb{C}^* variables X, Y and does not affect integrals over closed cycles, up to one important subtlety: at $X \rightarrow \infty$, μ_0 behaves like

$$\mu_0(X) = \frac{2}{X} \left(\log \left(\frac{\varphi_1}{\varphi_2} \right) + \log(X) \right) + \frac{1}{X^2} \frac{\varphi_2^2}{\varphi_1} - \frac{1}{X^3} \left(\frac{\varphi_2^4}{\varphi_1^4} - \frac{\varphi_2^4}{2\varphi_1^2} + \frac{\varphi_2^2}{\varphi_1^2} \right) + \mathcal{O} \left(\frac{1}{X^4} \right). \quad (2.3.59)$$

In the compactification one has to regularize the form μ_0 to

$$\mu_0(x) = \mu_0(X)|_{x=X} - \frac{2}{x} \log(x). \quad (2.3.60)$$

Derivatives of $\mu_0(x)$ w.r.t. to φ_i are related to standard elliptic integrals on (2.3.58).

When the ranks of the nodes in ABJM theory are not identical (this is the so-called ABJ theory [73]), there are two 't Hooft parameters defined by

$$\lambda_i = \frac{N_i}{k}, \quad i = 1, 2. \quad (2.3.61)$$

In the Calabi–Yau picture, these parameters are mirror coordinates and as such they are identified with the periods

$$\lambda_i = \frac{1}{4\pi i} \int_{\mathcal{C}_i} \mu_0, \quad (2.3.62)$$

where the cycles have the geometry

$$\mathcal{C}_1 = (1/a, a), \quad \mathcal{C}_2 = (-b, -1/b). \quad (2.3.63)$$

The homology relations imply that the \mathcal{C}_i periods are non identical because of the pole in the μ_k . In particular for μ_0 it is clear from figure 2.3 and (2.3.59) that there is an exact relation between the periods (2.3.62)

$$\exp(2\pi i(\lambda_1 - \lambda_2)) = \frac{\varphi_1}{\varphi_2}. \quad (2.3.64)$$

For this reason, the ABJM slice

$$\lambda_1 = \lambda_2 \pmod{\mathbb{Z}} \quad (2.3.65)$$

can be identified with an algebraic submanifold of the complex deformation space of (2.3.52).

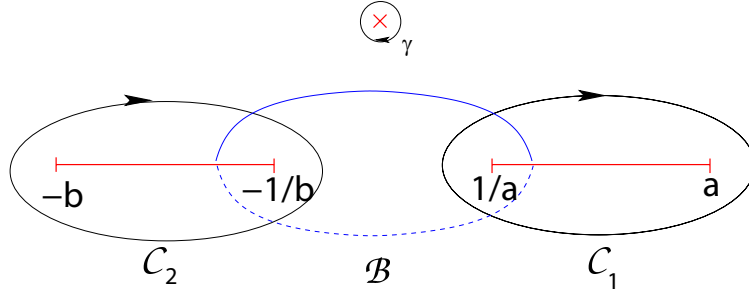


Figure 2.3: The cycles in the ABJM geometry in the x -plane. The non-vanishing residua of the forms at $x = \infty$

This submanifold is simply given by

$$\varphi_1 = \varphi_2 = \varphi = i\kappa. \quad (2.3.66)$$

In particular, in the slice one has

$$\partial_\varphi \mu_k = \omega_k = \frac{x^k}{\sqrt{\sigma(x)}} dx, \quad (2.3.67)$$

i. e. all closed integrals of μ_k on (2.3.53,2.3.55) are determined up to a constant by standard elliptic integrals on (2.3.58). For latter reference we note that the parameterization of the branch points by κ is

$$a(\kappa) = \frac{1}{2} \left(2 + i\kappa + \sqrt{\kappa(4i - \kappa)} \right), \quad b(\kappa) = \frac{1}{2} \left(2 - i\kappa + \sqrt{-\kappa(4i + \kappa)} \right). \quad (2.3.68)$$

On the slice (2.3.53) is an algebraic family of elliptic curves with monodromy group $\Gamma^0(4)$ and j -invariant

$$j = \frac{16 - 16\varphi^2 + \varphi^4}{1728\varphi^2(16 - \varphi^2)}. \quad (2.3.69)$$

This family is related to the $\Gamma_0(2)$ curve of pure $SU(2)$ SW-theory

$$y^2 = (x^2 - u)^2 - \Lambda^4 \quad (2.3.70)$$

by identifying

$$u = \pm \left(1 - \frac{\varphi^2}{8} \right) \Lambda^2. \quad (2.3.71)$$

Indeed, the period integrals of μ_0 are annihilated by a single Picard–Fuchs differential operator for M_{cy} , after identifying the Kähler classes of the \mathbb{P}^1 i. e. $T_1 = T_2$ (in the notation of [36]). It reads³

$$\mathcal{D} = (\varphi^2 \theta_\varphi^2 - 16(2\theta_\varphi - 1)^2) \theta_\varphi = \varphi(\varphi^2(\theta_\varphi + 1)^2 + 16\theta_\varphi^2) \partial_\varphi = \varphi \mathcal{D}_{hol} \partial_\varphi, \quad (2.3.72)$$

where $\theta_x = x d/dx$ is the logarithmic derivative. \mathcal{D}_{hol} annihilates the periods over the holomor-

³ The formulas $\theta_x = a\theta_y$ if $y = x^a$ and $[\theta_x, x^z] = ax^z$ make the comparison with [74] trivial.

phic differential ω_0 on (2.3.58), as a consequence of (2.3.67). The differential equation (2.3.72) has three critical points: $\varphi^2 = 0$, $\varphi^2 = 16$ and $\varphi^2 = \infty$. Let us describe the behavior of the periods at these points and determine the analytic continuations and the monodromy action. The weak coupling point of ABJM theory is the point $\varphi = 0$. In the $w = \varphi^2$ variable the period basis looks like

$$\Pi = \begin{pmatrix} \int_{\gamma} \mu_0 \\ \int_{\mathcal{B}} \mu_0 \\ \int_{\mathcal{C}} \mu_0 \end{pmatrix} = \begin{pmatrix} 1 \\ \partial_{\lambda} F^0 \\ \lambda \end{pmatrix}, \quad \text{with} \quad \begin{pmatrix} 1 \\ \lambda \\ \tilde{F}_{\lambda} \end{pmatrix} = \begin{pmatrix} 1 \\ \frac{\sqrt{w}}{8\pi i} [1 + \frac{w}{192} + \mathcal{O}(w^2)] \\ \frac{2\lambda}{\pi i} \log(w) + \frac{\sqrt{w}}{4\pi^2 i} [\frac{5}{588} w + \mathcal{O}(w^2)] \end{pmatrix}. \quad (2.3.73)$$

where

$$\partial_{\lambda} F^0 = \tilde{F}_{\lambda} - (2 + ib)\lambda - \frac{1}{2}, \quad b = \frac{4 \log(2) + 1}{\pi}. \quad (2.3.74)$$

The recursion defining λ can be summed up to yield [48]

$$\lambda = \frac{\kappa}{8\pi} {}_3F_2 \left(\frac{1}{2}, \frac{1}{2}, \frac{1}{2}; 1, \frac{3}{2}; -\frac{\kappa^2}{16} \right). \quad (2.3.75)$$

This function plays the role of the mirror map at the orbifold, while $\partial_{\lambda} F_w^0$ is the dual period. This pair defines the genus zero prepotential F_w^0 , by special geometry, as well as the polarization on the ABJM slice.

The point $\varphi^2 = \infty$ is the strong coupling point of ABJM theory, $\lambda \rightarrow \infty$. It corresponds to the large radius point of topological string theory. The topological string basis is obtained by the local limit of a compact Calabi–Yau manifold, and it is half integral in the homology of the curve (2.3.53)

$$\Pi = \begin{pmatrix} 1 & 0 & 0 \\ -1 & 1 & 0 \\ 0 & -\frac{1}{2} & 1 \end{pmatrix} \Pi_{ts}. \quad (2.3.76)$$

In the coordinates $z = \varphi^{-2}$ the topological string basis reads

$$\Pi_{ts} = \begin{pmatrix} 1 \\ T \\ \partial_T F_{gw}^0 \end{pmatrix} = \begin{pmatrix} 1 \\ \frac{1}{2\pi i} [\log(z) + 4z + \mathcal{O}(z^2)] \\ -\frac{1}{2} \left(\frac{1}{2\pi i} \right)^2 [\log^2(z) + 4z \log(z) + 8z + \mathcal{O}(z^2)] - \frac{1}{12} \end{pmatrix}. \quad (2.3.77)$$

Here, $Q = \exp(2\pi i T)$, and $\partial_T F_{gw}^0$ can be integrated to obtain the genus 0 prepotential

$$F_{gw}^0(Q) = -\frac{1}{6} T^3 - \frac{1}{12} T + c + \sum_{d=1}^{\infty} n_d^9 \text{Li}_3(q^d). \quad (2.3.78)$$

This is the generating function of $g = 0$ BPS invariants, summing over the degrees $d_1 + d_2 = d$ w.r.t. to both Kähler classes of the \mathbb{P}^1 's⁴. Near the conifold point, and in the $u = (1 - \frac{16}{\varphi^2})$

⁴ Up to a constant $c = \frac{\chi}{2(2\pi i)^3}$, which depends on the regularized Euler number of the local geometry for $\chi = 4$.

coordinates, the basis reads ⁵

$$\Pi_{ts} = \begin{pmatrix} 1 \\ \partial_{T_c} F_c^0 \\ T_c \end{pmatrix} = \begin{pmatrix} 1 \\ \frac{1}{2\pi^2 i} [4\pi T_c \log(u) + \frac{9}{16} u^2 + \mathcal{O}(u^3)] + 2biT_c + c \\ \frac{1}{4\pi} [u + \frac{5}{8} u^2 + \mathcal{O}(u^3)] \end{pmatrix}. \quad (2.3.79)$$

From this we get the $\Gamma^0(4)$ monodromies in the Π basis

$$M_{\varphi=0} = \begin{pmatrix} 1 & 0 & 0 \\ -1 & -1 & -4 \\ 0 & 0 & -1 \end{pmatrix}, \quad M_{\varphi^2=-16} = \begin{pmatrix} 1 & 0 & 0 \\ 0 & 3 & 4 \\ 0 & -1 & -1 \end{pmatrix}, \quad M_{\varphi=\infty} = \begin{pmatrix} 1 & 0 & 0 \\ 1 & 1 & 0 \\ -1 & -1 & 1 \end{pmatrix}. \quad (2.3.80)$$

One checks $(M_{\varphi^2=-16} M_{\varphi=\infty})^{-1} = M_{\varphi=0}$.

In topological string theory or $\mathcal{N} = 2$ 4d supersymmetric gauge theory, the coupling constants are complex. At the various critical points one has to chose appropriate coordinates, which are either invariant or reflect invariances of the theory under the local monodromy. For example, at large radius or the asymptotic free region of the gauge theory, one can chose T as the appropriate variable and the monodromy $T \rightarrow T + 1$ is understood as a shift in the NS B field of topological string or the θ -angle of Yang-Mills theory. The canonical choices of other coordinates in different regions in the moduli space correspond to a change of polarization.

Because in ABJM theory the coupling constant is real, there is *a priori* no need to consider the action of the monodromy. The polarization is picked once and for all at the weak coupling point. The choice made here is identical to the one made in topological string theory at this point in moduli space. However, as pointed out in [41], this polarization is not the one of topological string theory at large radius. The coupling of the ABJM theory λ behaves at large radius like

$$\lambda = \partial_T F_{gw}^0 - \frac{1}{2} T = -\frac{1}{2} T^2 - \frac{1}{2} T - \frac{1}{12} + \mathcal{O}(Q). \quad (2.3.81)$$

To obtain the famous $N^{3/2}$ scaling of the genus zero free energy $F^{(0)}$, it is crucial to integrate the B -cycle integral $\partial_\lambda F^{(0)}$ with respect to λ [36]. This yields⁶

$$F = g_s^{-2} F^{(0)} = \frac{\pi\sqrt{2}}{3} k^2 \hat{\lambda}^{\frac{3}{2}} + \mathcal{O}(\hat{\lambda}^0, e^{-2\pi\sqrt{2\hat{\lambda}}}). \quad (2.3.82)$$

The relation of the topological string theory to the ABJM theory at this point is therefore given by a change of polarization.

What is remarkable is that, despite the fact that the action of the monodromy does not have a clear interpretation in ABJM theory, the higher genus contributions to the partition function of the theory have the same modular invariance under $\Gamma^0(4)$ that they have in topological string theory. One might speculate that the monodromy at the strong coupling region reflects an invariance of the theory, so far not understood, which involves non-perturbative effects. Note that this monodromy does not change the leading $N^{3/2}$ behavior. A related issue concerns the $1/6$ BPS Wilson loop vev itself. This vev is obtained as an integral over the \mathcal{C} cycle. However, the integral of the same differential over the dual \mathcal{B} -cycle has no interpretation in ABJM theory. If the monodromy action had a meaning in ABJM theory, it would mix the two types of cycles.

⁵ The irrational constant $c = .3712268727\dots$ is fastest iterated using the Meijers function [74].

⁶ As further explained in [36] it is natural to shift λ and consider instead $\hat{\lambda} = \lambda - \frac{1}{24}$.

2.3.3 Wilson loops in the geometric description

The Wilson loop vevs have a genus expansion of the form,

$$\langle W_n^{1/6,1/2} \rangle = \sum_{g=0}^{\infty} g_s^{2g-1} \langle W_n^{1/6,1/2} \rangle_g, \quad (2.3.83)$$

and of course the ABJM matrix model correlators (2.3.48) have the same type of expansion. The first term in this expansion corresponds to the genus zero or planar vev. The exact planar vevs of 1/2 BPS and 1/6 BPS Wilson loops (for winding number $n = 1$) were obtained in [41], from the exact solution of the ABJM matrix model at large N . We will now review these results.

The planar limit of the matrix model is completely determined by the densities of eigenvalues in the cuts, which were also obtained explicitly in [41]:

$$\begin{aligned} \rho_1(X)dX &= \frac{1}{2i\pi^2\lambda} \tan^{-1} \left[\sqrt{\frac{\alpha X - 1 - X^2}{\beta X + 1 + X^2}} \right] \frac{dX}{X}, \\ \rho_2(Y)dY &= \frac{1}{2i\pi^2\lambda} \tan^{-1} \left[\sqrt{\frac{\beta Y + 1 + Y^2}{\alpha Y - 1 - Y^2}} \right] \frac{dY}{Y}, \end{aligned} \quad (2.3.84)$$

where

$$\alpha = a + \frac{1}{a}, \quad \beta = b + \frac{1}{b}. \quad (2.3.85)$$

These densities are normalized in such a way that their integrals over the cuts are equal to one. In (2.1.28) we defined the planar correlators in terms of integrals over a eigenvalue density, therefore here we have the relation

$$g_s^{-1} \langle \text{tr } e^{n\mu_i} \rangle_{g=0} = N \int_{\mathcal{C}_1} \rho_1(X) X^n dX. \quad (2.3.86)$$

Keeping track of the residue at $X = \infty$, analogously to (2.3.59), we can write simpler expressions for the densities which are valid in the compactified variables x, y . The planar 1/6 BPS Wilson loop vevs read in terms of those

$$g_s^{-1} \langle W_n^{1/6} \rangle_{g=0} = \frac{k}{2\pi^2} \int_{\mathcal{C}_1} \mu_n, \quad g_s^{-1} \langle \hat{W}_n^{1/6} \rangle_{g=0} = (-1)^n \frac{k}{2\pi^2} \int_{\mathcal{C}_2} \mu_n. \quad (2.3.87)$$

The planar 1/2 BPS Wilson loops is given by the γ -period, i. e. the residue at infinity,

$$g_s^{-1} \langle W_n^{1/2} \rangle_{g=0} = \frac{k}{2\pi^2} \oint_{\gamma} \mu_n. \quad (2.3.88)$$

Since the forms ω_n defined in (2.3.67) are not independent elements of the cohomology of the curve, one can relate all Wilson loop vevs to the integrals of μ_0 . Let us denote by

$$R_n(\varphi) = \oint_{\gamma} \mu_n \quad (2.3.89)$$

the residue of μ_n at $x = \infty$. Then we get a relation in homology of the form

$$\mathcal{L}_n \omega_0 - \omega_n = \partial_\varphi R_n(\varphi) x^3 dx, \quad (2.3.90)$$

where

$$\mathcal{L}_n = p_n^1(\varphi) \partial_\varphi + p_n^0(\varphi). \quad (2.3.91)$$

The coefficients $p_n^0(\varphi)$ and $p_n^1(\varphi)$ are polynomials in φ and can be obtained by the Griffiths reduction method. For the first few we get,

$$\begin{aligned} p_1^0 &= \frac{\varphi}{4}, & p_1^1 &= 0, & R_1 &= \frac{1}{2}\varphi, \\ p_2^0 &= 1, & p_2^1 &= 4\varphi - \frac{\varphi^3}{4}, & R_2 &= \frac{1}{4}\varphi^2, \\ p_3^0 &= \frac{9\varphi}{4} - \frac{\varphi^3}{8}, & p_3^1 &= 6\varphi^2 - \frac{3\varphi^4}{8}, & R_3 &= \frac{1}{2}\varphi - \frac{\varphi^3}{6}, \\ p_4^0 &= 1 + \frac{10\varphi^2}{3} - \frac{5\varphi^4}{24}, & p_4^1 &= \frac{16\varphi^2}{3} + 7\varphi^3 - \frac{11\varphi^5}{24}, & R_4 &= \varphi^2 + \frac{\varphi^4}{8}. \end{aligned} \quad (2.3.92)$$

This relates $\langle W_n^{1/6} \rangle_{g=0}$ to λ , e.g.

$$\langle W_1^{1/6} \rangle_{g=0} = \frac{1}{4} \int \kappa \lambda(\kappa) d\kappa + \frac{1}{2} \kappa. \quad (2.3.93)$$

The integration constant is zero as μ_1 has no constant residue.

The relations (2.3.90) are homological relations. They imply a differential relation between the \mathcal{B} -cycles integrals over μ_n and $\partial_\lambda F^0$. Since λ and $\partial_\lambda F^0$ are related by special geometry, the relations (2.3.90) imply, for each n , differential relations between the Wilson loop integrals over the \mathcal{C} and the \mathcal{B} cycles. These can be viewed as an extension of special geometry to the Wilson loop integrals.

We will now compute the vev (2.3.86) for any positive integer n , at leading order in the strong coupling expansion, extending the result for $n = 1$ obtained in [41]. In the form (2.3.86), these correlators are difficult to compute, but as in [75], their derivatives w.r.t. κ are easier to calculate and given by

$$g_s^{-1} \frac{\partial}{\partial \kappa} \langle W_n^{1/6} \rangle_{g=0} = \frac{k}{2\pi^2} \mathcal{I}_n, \quad (2.3.94)$$

where

$$\mathcal{I}_n = \frac{1}{2} \int_{1/a}^a \frac{X^n dX}{\sqrt{(\alpha X - 1 - X^2)(\beta X + 1 + X^2)}}, \quad (2.3.95)$$

which can be calculated in terms of elliptic integrals. The computation for $n = 1$ was done in [41], and in appendix B.1 we compute them for a positive integer n . In order to make contact with the Fermi gas approach, where subleading exponential corrections are neglected, we want to extract their leading exponential behavior in the strong coupling region $\kappa \gg 1$. One finds,

$$\mathcal{I}_n \approx \frac{i^n \kappa^{n-1}}{2} \left(\log \kappa - \frac{\pi i}{2} - H_{n-1} \right), \quad \kappa \gg 1, \quad (2.3.96)$$

where

$$H_n = \sum_{d=1}^n \frac{1}{d} \quad (2.3.97)$$

are harmonic numbers (for $n = 1$, we set $H_0 = 0$). It then follows that

$$g_s^{-1} \langle W_n^{1/6} \rangle_{g=0} = \frac{(i\kappa)^n k}{4\pi^2 n} \left(\log \kappa - \frac{\pi i}{2} - H_n \right) \left(1 + \mathcal{O} \left(\frac{1}{\kappa^2} \right) \right). \quad (2.3.98)$$

From this we deduce that the vev for the 1/2 BPS Wilson loop in terms of κ is

$$g_s^{-1} \langle W_n^{1/2} \rangle_{g=0} = -\frac{ik(i\kappa)^n}{4\pi n} \left(1 + \mathcal{O} \left(\frac{1}{\kappa^2} \right) \right). \quad (2.3.99)$$

This agrees with a result obtained in section 8.2 of [36], where the generating function of these vevs, with an extra $1/n$ factor, was shown to be a dilogarithm in the variable $i\kappa$.

The regime of large κ corresponds to the regime of large 't Hooft coupling [41], and one has from (2.3.75),

$$\lambda(\kappa) = \frac{\log^2(\kappa)}{2\pi^2} + \frac{1}{24} + \mathcal{O} \left(\frac{1}{\kappa^2} \right), \quad (2.3.100)$$

which is immediately inverted to

$$\kappa = e^{\pi\sqrt{2\lambda}} \left(1 + \mathcal{O} \left(e^{-2\pi\sqrt{2\lambda}} \right) \right). \quad (2.3.101)$$

It follows that the 1/6 Wilson loops go like,

$$\langle W_n^{1/6} \rangle \approx e^{n\pi\sqrt{2\lambda}}, \quad (2.3.102)$$

and for $n = 1$ this is in agreement with the AdS calculation in terms of fundamental strings [34, 76, 70].

Coming back to the results of section 2.1.3 we can make a general statement about the logarithmic structure of Wilson loop integrals at strong coupling. Since

$$G(\kappa) \sim \frac{1}{\log(\kappa)} + \mathcal{O}(\kappa^{-1}) \quad (2.3.103)$$

we see that the highest inverse powers of $1/\log(\kappa)$ at leading order in κ go as

$$\frac{1}{(\log(\kappa))^{3g-1}}. \quad (2.3.104)$$

For the 1/6 Wilson loop there will be a positive power of $\log(\kappa)$ at leading order due to the integration of the meromorphic differential $\omega_g(p)$ over the \mathcal{C} cycle. The structure can be checked e. g. at genus two, in the expression obtained from the Fermi gas approach in (3.3.117).

ABJM Wilson loops in the Fermi gas approach

3.1 Introduction

In section 2.1 we introduced matrix models and showed some ways to solve them. We also gave a short overview to ABJM theory in section 2.2 and showed in section 2.3 how localization techniques can be used to localize the partition function and certain Wilson loop operators in ABJM theory (or more generally CSM theories) to matrix integrals. Here we will use the formalism developed in [48] to compute the vevs of the $1/2$ and $1/6$ in the strong coupling limit. Wilson loops can already be computed in the matrix model picture and the exact planar result was obtained in [41]. Afterwards the first $1/N$ correction was computed in [36] by making use of the results in [61]. This could be extended to even higher genus by using the topological recursion presented in section 2.3.2, but it is computationally very hard to do these calculations. In the context of ABJM theory it is very important to understand the full $1/N$ expansion, since it gives quantitative information about the M–theory AdS dual.

These matrix models can, if all gauge groups are of equal rank, be rewritten in terms of a gas of free fermions. This is a statistical physics problem and can be solved by already well understood techniques, like the Wigner–Kirkwood and the Sommerfeld expansion. In order to compare the results obtained in this manner to results of M–theory, we need to obtain the large N expansion of the correlators we are considering. In terms of quantum statistical mechanics the grand canonical ensemble is a convenient way to extract this limit. Since the gas is non-interacting, this problem can be reduced to a quantum mechanical computation in the one–body problem, which can be done in a semiclassical expansion. First one needs to quantize the system via the Wigner phase space quantization, giving us a lot of control over the semiclassical expansion, which is what we are interested in. The reason is, that this expansion corresponds to the expansion in the Chern–Simons level of ABJM theory. The expectation values can be computed in this semiclassical expansion by means of the Wigner–Kirkwood expansion. One computes everything in the grand canonical ensemble, which is related to the canonical ensemble via an integral transform. This integral transform can be computed in a saddle point expansion, leading to a series in large N . Putting everything together, one is able to resum the whole series in N , up to exponentially suppressed terms. We extended this setup to include Wilson loops in the ABJM theory. In order to compute the expectation values of this operator, we need to perform a low temperature expansion, i. e. a Sommerfeld expansion, in the grand canonical ensemble. The resulting expressions in terms of number operators now need to

be extracted using the Wigner–Kirkwood expansion, which yield results in terms of integrals over the Fermi surface. In contrast to the computation of the free energies we now have an infinite series of quantum corrections. Even though it is a lot harder now, we were able to resum this up to exponentially suppressed corrections. We analyzed Wilson loop operators in ABJM theory, and showed that the expectation values can be written in terms of the Airy function. An interesting point is that the semiclassical expansion in the Fermi gas picture corresponds to an expansion in large coupling of the gauge theory. This could, in principle, be compared to computations on the gravity side of AdS/CFT. Genus by genus these results were already derived directly from the Matrix model via the topological recursion of Eynard and Orantin and we were successfully able match our results.

In section 3.2 we will review the basic tools needed for our formalism. We start with reviewing phase space quantization and give the definitions of statistical physics relevant for our purposes. After having these definitions set up, we show how to write a matrix model for a CSM theory in terms of the Fermi gas.

Section 3.3 is the core of this chapter. There we will do the actual computation of the vevs of the 1/2 and 1/6 Wilson loop operators in ABJM theory. In section 3.3.1 we show how we can include Wilson loops in the Fermi gas formalism. In order to conduct the computation of the vevs we need the full quantum corrected Hamiltonian of the fermionic system. Knowing this we then are able to calculate the corresponding Wigner–Kirkwood corrections for the quantum mechanical averages. This will be done in section 3.3.2. In 3.3.3 we will explain how to compute the integration over the quantum corrected Fermi surface in the presence of a Wilson loop operator. Finally, in section 3.3.4, we present the explicit results for Wilson loop vevs and a detailed comparison with the ’t Hooft expansion in the string coupling regime. In appendix B.1, we present the details of the matrix model computation for the 1/6 BPS Wilson loop correlator at arbitrary winding. Appendix B.2 summarizes the results of the ’t Hooft expansion at genus three and genus four.

3.2 The Fermi gas approach

3.2.1 Quantum mechanics in phase space

The following section is mainly based on the description given in [77, 78, 79] Usually, when using quantum mechanics, we introduce some kind of distribution on the configuration space.

But generally, if we start quantizing systems, given by a Hamiltonian, i. e. quantizing a system that is most naturally given by a set of conjugated variables q_i and p_i , because H is defined on the phase space. Having established that we are interested in distribution functions we might ask, why we do not introduce a distribution function $\rho_Q(q, p)$ which is defined on the whole phase space and not just some slice of it. This distribution should have the properties

$$\int dp \rho_Q(q, p) = \rho(q) = \langle q | \hat{\rho} | q \rangle \quad (3.2.1)$$

and

$$\int dq \rho(q, p) = \rho(p) = \langle p | \hat{\rho} | p \rangle, \quad (3.2.2)$$

in order to be natural. Furthermore it should be nonnegative

$$\rho_Q(q, p) \geq 0, \quad (3.2.3)$$

in order to be interpreted as a probability distribution. Two approaches fulfill some of these conditions are the *Wigner* distribution and the *Husini* distribution. The former one does not fulfill (3.2.3), while the latter one does not fulfill the conditions (3.2.1) and (3.2.2). During the remainder of this thesis we are only interested in the Wigner–distribution, therefore we are not pursuing the development of the Husini–distribution any further. The Wigner distribution is in some sense an intermediate between the position–space representation and the momentum–space representation. For a single particle in one dimension it is defined as

$$\rho_W(q, p) = \int_{-\infty}^{\infty} dq' e^{ipq'/\hbar} \left\langle q - \frac{q'}{2} \left| \hat{\rho} \right| q + \frac{q'}{2} \right\rangle. \quad (3.2.4)$$

More generally for any operator \hat{A} we define

$$A_W(q, p) = \int_{-\infty}^{\infty} dq' e^{ipq'/\hbar} \left\langle q - \frac{q'}{2} \left| \hat{A} \right| q + \frac{q'}{2} \right\rangle, \quad (3.2.5)$$

as its *Wigner transform*.

The Wigner transform of a product of two operators is given by

$$(\hat{A}\hat{B})_W = A_W \star B_W, \quad (3.2.6)$$

where the star operator is defined as

$$\star = \exp \left[\frac{i\hbar}{2} (\partial_q \partial_p - \partial_p \partial_q) \right]. \quad (3.2.7)$$

Having defined the Wigner transformation, we are able to introduce the phase-space equivalent of the trace over an operator in the phase–space quantization formalism

$$\text{Tr } \hat{A} = \int \frac{dqdp}{2\pi\hbar} A_W(q, p). \quad (3.2.8)$$

For only two operators the star product simplifies to a common multiplication under the integral [80]

$$\text{Tr } \hat{A}\hat{B} = \int \frac{dqdp}{2\pi\hbar} A_W(q, p) \star B_W(q, p) = \int \frac{dqdp}{2\pi\hbar} A_W(q, p) B_W(q, p). \quad (3.2.9)$$

The commutator is also easily extended to this formalism and one even immediately sees that the first order of its semiclassical expansion actually is the well known Poisson-bracket.

$$[A, B]_\star = A \star B - B \star A = i\hbar \{A, B\} + \mathcal{O}(\hbar^2). \quad (3.2.10)$$

If we compute the commutator of p and q we find the usual relation

$$[q, p]_\star = i\hbar. \quad (3.2.11)$$

3.2.2 Quantum Statistical Mechanics in phase space

We continue now with the description of quantum statistical mechanics of N –particle systems. The first step is the introduction of the Hilbert space of bosons and fermions, respectively. The

starting point is the basis

$$|\lambda_1, \dots, \lambda_N\rangle \quad (3.2.12)$$

of the space of eigenstates for an N -particle system of distinguishable particles.

In order to construct the Hilbert space of indistinguishable particles, we introduce a projection operator for totally (anti)symmetric states.

$$P_\eta = \frac{1}{N!} \sum_{\sigma \in S_N} \eta^{\epsilon(\sigma)} \sigma, \quad (3.2.13)$$

where

$$\eta = \pm 1 \quad (3.2.14)$$

for bosons and fermions, respectively. As a projection operator, it has the property

$$P_\eta^2 = P_\eta. \quad (3.2.15)$$

We obtain the appropriately (anti)symmetrized states by applying the (anti)symmetrization-operator to a state (3.2.12) and introduce therefore

$$|\lambda_1, \dots, \lambda_N\rangle = \sqrt{N!} P_\eta |\lambda_1, \dots, \lambda_N\rangle = \frac{1}{\sqrt{N!}} \sum_{\sigma \in S_N} \eta^{\epsilon(\sigma)} |\lambda_{\sigma(1)}, \dots, \lambda_{\sigma(N)}\rangle, \quad (3.2.16)$$

which forms a basis of the Hilbert space of bosons/fermions, depending on the choice of η . In this basis the resolution of the identity reads

$$\frac{1}{N!} \int d\lambda |\lambda_1, \dots, \lambda_N\rangle \langle \lambda_1, \dots, \lambda_N| = \mathbf{1}. \quad (3.2.17)$$

An n -body operator \mathcal{O} is an operator which is invariant under any permutation of the particles. It acts on a state of the Hilbert space \mathcal{H}_N of distinguishable particles as follows

$$\mathcal{O}|\lambda_1 \cdots \lambda_N\rangle = \frac{1}{k!} \sum_{1 \leq i_1 \neq \dots \neq i_k \leq N} \mathcal{O}(\lambda_{i_1}, \dots, \lambda_{i_k}) |\lambda_1 \cdots \lambda_N\rangle. \quad (3.2.18)$$

For a one-body operator this simplifies to

$$\mathcal{O}|\lambda_1 \cdots \lambda_N\rangle = \sum_{i=1}^N \mathcal{O}(\lambda_i) |\lambda_1 \cdots \lambda_N\rangle, \quad (3.2.19)$$

where $\mathcal{O}(\lambda)$ is an operator on the Hilbert space of a single particle.

A quantum mechanical statistical ensemble is described by a density matrix $\hat{\rho}$. The canonical partition function in terms of the density matrix is given by a trace

$$Z_N = \text{Tr}(\hat{\rho}), \quad (3.2.20)$$

while the thermal average of an n -body operator \mathcal{O} in the canonical ensemble is defined by

$$\langle \mathcal{O} \rangle_N = \text{Tr}(\hat{\rho} \mathcal{O}). \quad (3.2.21)$$

Here we are using *unnormalized* vevs. The partition function therefore is just the thermal

average over the identity.

After this definition, let us consider the canonical density matrix for a system of indistinguishable particles. It is given by

$$\rho_D(\{x_1, \dots, x_N\}, \{x'_1, \dots, x'_N\}; \beta) = \langle x_1 \cdots x_N | e^{-\beta \hat{H}} | x'_1 \cdots x'_N \rangle, \quad (3.2.22)$$

where \hat{H} is the total Hamiltonian of the N particles. Depending on what system we look at, namely bosons or fermions, we have to symmetrize or antisymmetrize the system appropriately in order to obtain [81]

$$\begin{aligned} \rho(\{x_1, \dots, x_N\}, \{x'_1, \dots, x'_N\}; \beta) &= \frac{1}{N!} \sum_{\sigma \in S_N} \eta^{\epsilon(\sigma)} \rho_D(\{x_1, \dots, x_N\}, \{x'_{\sigma(1)}, \dots, x'_{\sigma(N)}\}; \beta) \\ &= \frac{1}{N!} \langle x_1 \cdots x_N | e^{-\beta \hat{H}} | x'_1 \cdots x'_N \rangle. \end{aligned} \quad (3.2.23)$$

We want to compute vevs of a many-body operator in the canonical ensemble and because sometimes the operator in consideration only depends on a subsystem of the complete system, we need to introduce *density submatrices* or *reduced density matrices*¹. The reduced n -particle density matrix is defined by integrating out a certain number of states in an integral over the density matrix of indistinguishable particles

$$\begin{aligned} \rho_n(\{x_1, \dots, x_n\}, \{x'_1, \dots, x'_n\}; \beta) &= \\ &= \frac{N!}{(N-n)!} \int dx_{n+1} \cdots dx_N \rho(\{x_1, \dots, x_N\}, \{x'_1, \dots, x'_N\}; \beta). \end{aligned} \quad (3.2.24)$$

The vev of an operator acting on such a reduced subsystem can be computed in terms of the n -reduced density matrix by using the reduced density matrix and integrating over the remaining n variables like

$$\langle \mathcal{O} \rangle_N = \frac{1}{n!} \int dx_1 \cdots dx_n \mathcal{O}(x_1, \dots, x_n) \rho_n(\{x_1, \dots, x_n\}, \{x'_1, \dots, x'_n\}; \beta). \quad (3.2.25)$$

We note that, in a system of non-interacting particles, the density matrix (3.2.22) factorizes,

$$\rho_D(\{x_1, \dots, x_N\}, \{x'_1, \dots, x'_N\}; \beta) = \prod_{i=1}^N \rho(x_i, x'_i), \quad (3.2.26)$$

into a product of canonical density matrices $\rho(x, x')$ of the one-particle problem.

In our case it is more useful to work in the grand-canonical ensemble, because we want to extract the large N -behavior of the considered statistical mechanics system. In the grand canonical ensemble the reduced density matrix is defined as²

$$\rho_n^{\text{GC}}(\{x_1, \dots, x_n\}, \{x'_1, \dots, x'_n\}; \beta, z) = \sum_{N=n}^{\infty} z^N \rho_n(\{x_1, \dots, x_n\}, \{x'_1, \dots, x'_n\}; \beta). \quad (3.2.27)$$

¹ For further information see for example [81, 82]

² See for example [82]

Here

$$z = e^{\beta\mu} \quad (3.2.28)$$

denotes the usual *fugacity*. The vev of an n -body operator in this ensemble can be expressed in terms of a sum of canonical vevs over all particle numbers,

$$\langle \mathcal{O} \rangle^{\text{GC}} = \sum_{N=n}^{\infty} \langle \mathcal{O} \rangle_N z^N. \quad (3.2.29)$$

The grand partition function is given by a sum over N -particle partition functions, weighted with the N -th power of the fugacity

$$\Xi = 1 + \sum_{N=1} z^N Z_N. \quad (3.2.30)$$

According to [82, 83] the grand-canonical density matrix has a very simple form in the case of non-interacting gases:

$$\rho_n^{\text{GC}}(\{x_1, \dots, x_n\}, \{x'_1, \dots, x'_n\}; \beta, z) = \Xi \sum_{\sigma \in S_n} \eta^{\epsilon(\sigma)} \prod_{i=1}^n n(x_i, x'_{\sigma(i)}; \beta, z), \quad (3.2.31)$$

where Ξ is the grand-canonical partition function, and

$$n(x, x'; \beta, z) = \left\langle x \left| \frac{1}{z^{-1} e^{\beta \hat{H}} - \eta} \right| x' \right\rangle \quad (3.2.32)$$

is the occupation number operator in the position representation

The relationship (3.2.31) can be derived by using creation and annihilation operators [83]. Using the Landsberg's recursion relation the case $n = 1$ can also be derived. This relation is based on the analysis of the sum over permutations in terms of conjugacy classes, and it was originally derived for the canonical partition function of ideal quantum gases³. Generalizing this to density matrices is straightforward [85], and it yields

$$\rho_1(x, x'; \beta) = \sum_{\ell=1}^N \eta^{\ell-1} \rho(x, x'; \ell\beta) Z_{N-\ell}, \quad (3.2.33)$$

where $\rho(x, x'; \beta)$ is the density matrix for the one-particle problem. We now sum over all N with the fugacity z^N to obtain the grand-canonical, reduced density matrix

$$\begin{aligned} \rho_1^{\text{GC}}(x, x'; \beta, z) &= \sum_{N=1}^{\infty} \rho_1(x, x'; \beta) z^N = \eta \sum_{N=1}^{\infty} \sum_{\ell=1}^N Z_{N-\ell} z^{N-\ell} \langle x | e^{-\ell\beta\hat{H}} | x' \rangle (\eta z)^\ell \\ &= \eta \left(\sum_{M=0}^{\infty} Z_M z^M \right) \left\langle x \left| \sum_{\ell=1}^{\infty} (\eta z)^\ell e^{-\ell\beta\hat{H}} \right| x' \right\rangle \\ &= \Xi \left\langle x \left| \frac{1}{z^{-1} e^{\beta\hat{H}} - \eta} \right| x' \right\rangle. \end{aligned} \quad (3.2.34)$$

³ see for example [84]

We conclude from this that the vev of a one-body operator in the grand-canonical ensemble is given by

$$\frac{1}{\Xi} \langle \mathcal{O} \rangle^{\text{GC}} = \text{tr} \left(\frac{\mathcal{O}}{z^{-1} e^{\beta \hat{H}} - \eta} \right) \quad (3.2.35)$$

where the operator \mathcal{O} appearing inside the trace is understood as the operator restricted to the one-particle Hilbert space.

3.2.3 Large N expansion from the grand canonical ensemble

Sometimes it is easier to analyze a system in terms of the grand canonical ensemble. We for instance want to extract the large N expansion of the Fermi gas which is most conveniently done in the grand canonical ensemble. Here we will present how to use the definition of the grand canonical ensemble to extract the large N expansion.

We already introduced the grand canonical partition function in (3.2.30). Based on this we define is the *grand-canonical potential* which is given by the logarithm of the grand partition function

$$J(\mu) = \log \Xi. \quad (3.2.36)$$

If we want to find the canonical partition function for a given N from the grand partition function we can use the integral expression

$$Z(N) = \oint \frac{dz}{2\pi i} \frac{\Xi}{z^{N+1}}. \quad (3.2.37)$$

This is a very convenient definition, if we want to analyze the large N behavior, because in this case we can apply the saddle-point method to this problem by writing

$$Z(N) = \frac{1}{2\pi i} \int d\mu \exp[J(\mu) - \mu N]. \quad (3.2.38)$$

The saddle point of this expression is determined by the equation

$$N = \frac{\partial J}{\partial \mu}, \quad (3.2.39)$$

which defines a function $\mu_*(N)$. Plugging this in, the free energy in the limit $N \rightarrow \infty$ is given by

$$F(N) = J(\mu_*) - \mu_* N. \quad (3.2.40)$$

In [48] the following representation of the grand canonical potential $J(\mu)$ in terms of $\rho(E)$ has been shown to hold

$$J(\mu) = \int_0^\infty dE \rho(E) \log(1 + z e^{-E}). \quad (3.2.41)$$

3.2.4 Quantum corrections

The next step is to analyze the quantity (3.2.35). The idea is to find the semiclassical expansion of the vev and a way to achieve this is to first make a low temperature expansion in order to write this vev as an expansion in terms of ensembles at zero temperature. This is done via the *Sommerfeld expansion*. The zero-temperature vevs themselves now admit a semiclassical

expansion in \hbar which is captured by the *Wigner–Kirkwood* series [86]. This is the reason why introducing the Wigner–transform is useful for our formalism.

3.2.4.1 Wigner–Kirkwood expansion

Let \hat{H} be the Hamiltonian of our problem and H_W be the Wigner transform of it, which we defined in (3.2.5). If we have a quantity f , depending on \hat{H} , we can formally Taylor expand it like

$$f(\hat{H}) = \sum_{r=0}^{\infty} \frac{1}{r!} f^{(r)}(H_W) (\hat{H} - H_W(q, p))^r. \quad (3.2.42)$$

Having introduced this we can compute the Wigner transform

$$f(\hat{H})_W = \sum_{r=0}^{\infty} \frac{1}{r!} f^{(r)}(H_W) \mathcal{G}_r \quad (3.2.43)$$

of this expression, where

$$\mathcal{G}_r = \left[(\hat{H} - H_W(q, p))^r \right]_W \quad (3.2.44)$$

for $r \geq 2$ and

$$\mathcal{G}_0 = 1, \mathcal{G}_1 = 0. \quad (3.2.45)$$

Here the Wigner transform is evaluated at the same point q, p . These quantities can be computed by applying (3.2.6). The general expansion of this has the structure

$$\mathcal{G}_r = \sum_{n=\lceil \frac{r+2}{3} \rceil}^{\infty} \hbar^{2n} G_r^{(n)}, \quad r \geq 2. \quad (3.2.46)$$

This expansion tells us, that for any given order in \hbar only a finite number of \mathcal{G}_r contribute.

The first few orders are given by

$$\mathcal{G}_2 = -\frac{\hbar^2}{4} \left[\frac{\partial^2 H_W}{\partial q^2} \frac{\partial^2 H_W}{\partial p^2} - \left(\frac{\partial^2 H_W}{\partial q \partial p} \right)^2 \right] + \mathcal{O}(\hbar^4) \quad (3.2.47)$$

and

$$\mathcal{G}_3 = -\frac{\hbar^2}{4} \left[\left(\frac{\partial H_W}{\partial q} \right)^2 \frac{\partial^2 H_W}{\partial p^2} + \left(\frac{\partial H_W}{\partial p} \right)^2 \frac{\partial^2 H_W}{\partial q^2} - 2 \frac{\partial H_W}{\partial q} \frac{\partial H_W}{\partial p} \frac{\partial^2 H_W}{\partial q \partial p} \right] + \mathcal{O}(\hbar^4). \quad (3.2.48)$$

We will call the \mathcal{G}_r appearing here *Wigner–Kirkwood corrections* and the expansions *Wigner–Kirkwood expansions*. This expansion can be applied to any function of the Hamiltonian.

One operator, which is very important in the following, is the number operator

$$\hat{n}(E) = \Theta(E - \hat{H}), \quad (3.2.49)$$

where $\Theta(x)$ is the Heavyside step function. The trace of this operator counts the number of states up to a given energy E . We will denote this number by

$$n(E) = \text{Tr } \hat{n}(E). \quad (3.2.50)$$

This number corresponds to the Fermi-distribution at zero temperature. We then apply the Wigner–Kirkwood expansion (3.2.42) to (3.2.49) and find

$$\hat{n}(E)_W = \Theta(E - H_W) + \sum_{r=2}^{\infty} \frac{(-1)^r}{r!} \mathcal{G}_r \delta^{(r-1)}(E - H_W). \quad (3.2.51)$$

Having this expression, we can compute the trace over \hat{n} by virtue of (3.2.8), which results in

$$n(E) = \text{Tr} \hat{n}(E) = \int \frac{dqdp}{2\pi\hbar} \hat{n}_W(q, p) = \int_{H_W(q, p) \leq E} \frac{dqdp}{2\pi\hbar} + \sum_{r=2}^{\infty} \frac{(-1)^r}{r!} \int \frac{dqdp}{2\pi\hbar} \mathcal{G}_r \delta^{(r-1)}(E - H_W). \quad (3.2.52)$$

In the semiclassical limit the number of eigenstates is given by

$$n(E) \approx \int \frac{dqdp}{2\pi\hbar} \Theta(E - H(q, p)) = \frac{\text{Vol}(E)}{2\pi\hbar}, \quad (3.2.53)$$

which is just the volume of the phase space. The surface of this volume is defined by

$$H(q, p) = E \quad (3.2.54)$$

and is called the *Fermi surface* of the system.

Applying the expansion (3.2.43) to the canonical density matrix, yields

$$\left(e^{-\beta\hat{H}} \right)_W = \left(\sum_{r=0}^{\infty} \frac{(-\beta)^r}{r!} \mathcal{G}_r \right) e^{-\beta H_W}, \quad (3.2.55)$$

where β is the inverse temperature. The expression (3.2.55) can be viewed in the sense that the Wigner transform of the canonical density matrix is the generating function of the Wigner–Kirkwood corrections, defined in (3.2.44).

3.2.4.2 Sommerfeld expansion

In the problem of computing statistical-mechanical averages in the Fermi gas, we will have to perform a low-temperature expansion of expressions, involving the Fermi-distribution function. Let us say we have an integral of the form

$$I = \int_0^{\infty} \frac{g(E)}{e^{\beta(E-\mu)} + 1} dE, \quad (3.2.56)$$

where $g(E)$ is some C^∞ -function, and want to expand it in a low temperature. This amounts to a power expansion in large β and will result in

$$I = \int_0^{\mu} g(E) dE + \sum_{n=1}^{\infty} \frac{1}{\beta^{2n}} \left(2 - \frac{1}{2^{2n-2}} \right) \zeta(2n) g^{(2n-1)}(\mu), \quad (3.2.57)$$

which we will call the *Sommerfeld expansion*. What this does for us is, it expresses quantities in a finite temperature distribution as a power series of terms in a zero-temperature distribution. Which means, we obtain an expression in the eigenvalue distribution operator defined in (3.2.49) after performing the Sommerfeld expansion. In (3.2.43) we showed how to expand the vev of

such an operator by means of the Wigner–Kirkwood expansion. This makes it clear how to approach a computation in a Fermi-distribution.

We also want to mention that the Sommerfeld expansion can also be written as the operator expansion

$$\frac{1}{e^{\beta(\hat{H}-\mu)} + 1} = \frac{\pi\partial_\mu}{\beta} \operatorname{csc}\left(\frac{\pi\partial_\mu}{\beta}\right) \Theta(\mu - \hat{H}). \quad (3.2.58)$$

Let us now come back to the expression (3.2.35). Here we will only consider $\eta = -1$ and set $\beta = 1$ for simplicity. We can use (3.2.8) to write (3.2.35) as

$$\frac{1}{\Xi} \langle \mathcal{O} \rangle^{\text{GC}} = \operatorname{tr} \left(\frac{\mathcal{O}}{e^{\hat{H}-\mu} + 1} \right) = \pi\partial_\mu \operatorname{csc}(\pi\partial_\mu) n_{\mathcal{O}}(\mu), \quad (3.2.59)$$

where

$$\begin{aligned} n_{\mathcal{O}}(\mu) &= \int \frac{dqdp}{2\pi\hbar} \Theta(\mu - \hat{H})_W \mathcal{O}_W \\ &= \int \frac{dqdp}{2\pi\hbar} \Theta(\mu - \hat{H}_W)_W \mathcal{O}_W + \sum_{r=2}^{\infty} \frac{(-1)^r}{r!} \int \frac{dqdp}{2\pi\hbar} \mathcal{G}_r \delta^{(r-1)}(\mu - H_W) \mathcal{O}_W. \end{aligned} \quad (3.2.60)$$

Here we used, in the first line, the fact (3.2.9), that the star product drops out if there are only two operators under the trace. The second line is obtained by the Wigner–Kirkwood expansion of the number operator (3.2.51).

3.2.5 Fermi Gas for Chern Simons Matter theories

We will now review the Fermi gas approach to $\mathcal{N} \geq 3$ Chern–Simons–matter theories, developed in [48]. But let us start with showing how it works for ABJM theory, before we generalize it afterwards. The partition function of ABJM theory can be written as a matrix model [32] given by the partition function

$$Z_{\text{ABJM}}(N) = \frac{1}{N!^2} \int \frac{d^N \mu}{(2\pi)^N} \frac{d^N \nu}{(2\pi)^N} \frac{\prod_{i < j} \left[2 \sinh \left(\frac{\mu_i - \mu_j}{2} \right) \right]^2 \left[2 \sinh \left(\frac{\nu_i - \nu_j}{2} \right) \right]^2}{\prod_{i,j} \left[2 \cosh \left(\frac{\mu_i - \nu_j}{2} \right) \right]^2}, \quad (3.2.61)$$

as we have shown in section 2.3.1.

We relate the rank of the gauge group N and the Chern–Simons level k by

$$\lambda = \frac{N}{k}. \quad (3.2.62)$$

Now we use the Cauchy identity

$$\begin{aligned} \frac{\prod_{i < j} \left[2 \sinh \left(\frac{\mu_i - \mu_j}{2} \right) \right] \left[2 \sinh \left(\frac{\nu_i - \nu_j}{2} \right) \right]}{\prod_{i,j} 2 \cosh \left(\frac{\mu_i - \nu_j}{2} \right)} &= \det_{ij} \frac{1}{2 \cosh \left(\frac{\mu_i - \nu_j}{2} \right)} \\ &= \sum_{\sigma \in S_N} (-1)^{\epsilon(\sigma)} \prod_i \frac{1}{2 \cosh \left(\frac{\mu_i - \nu_{\sigma(i)}}{2} \right)}. \end{aligned} \quad (3.2.63)$$

In this equation, S_N is the permutation group of N elements, and $\epsilon(\sigma)$ is the signature of the

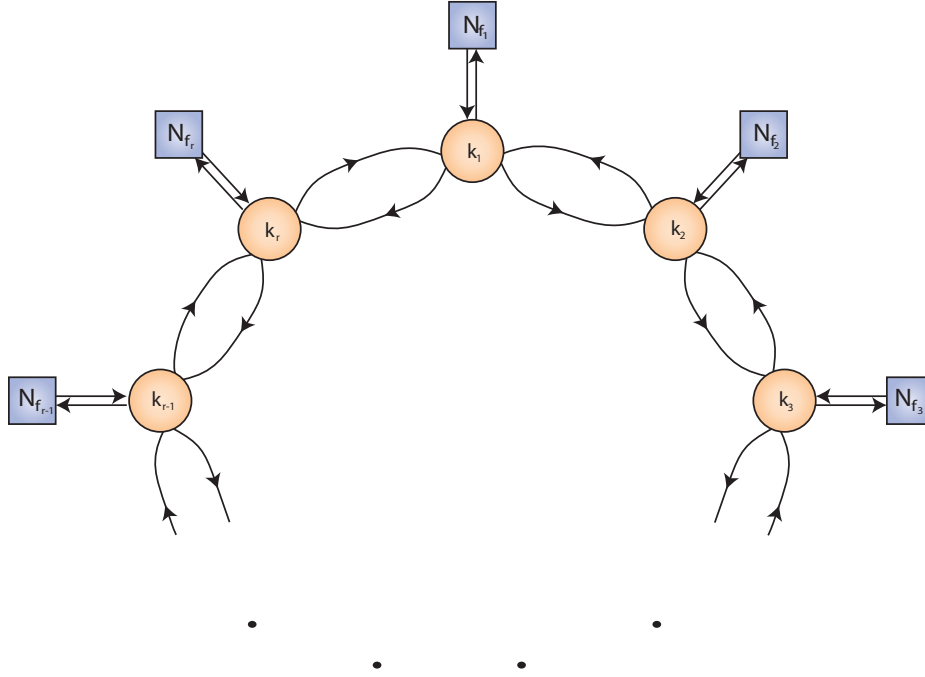


Figure 3.1: Necklace quiver

permutation σ . By using this it is possible to bring (3.2.61) into the form

$$Z(N) = \frac{1}{N!} \sum_{\sigma \in S_N} (-1)^{\epsilon(\sigma)} \int \frac{d^N x}{(2\pi k)^N} \frac{1}{\prod_i 2 \cosh \left(\frac{x_i}{2} \right) 2 \cosh \left(\frac{x_i - x_{\sigma(i)}}{2} \right)}. \quad (3.2.64)$$

This suggests the definition of

$$\rho(x_1, x_2) = \frac{1}{2\pi k} \frac{1}{\left(2 \cosh \frac{x_1}{2} \right)^{\frac{1}{2}}} \frac{1}{\left(2 \cosh \frac{x_2}{2} \right)^{\frac{1}{2}}} \frac{1}{2 \cosh \frac{x_1 - x_2}{2}}, \quad (3.2.65)$$

so that we can write (3.2.61) as

$$Z(N) = \frac{1}{N!} \sum_{\sigma \in S_N} (-1)^{\epsilon(\sigma)} \int d^N x \prod_i \rho(x_i, x_{\sigma(i)}). \quad (3.2.66)$$

We will consider the generalization of ABJM theory given by necklace quivers with r nodes [87, 88], and with fundamental matter in each node, as depicted in figure 3.1. These theories have a gauge group

$$U(N)_{k_1} \times U(N)_{k_2} \times \cdots \times U(N)_{k_r} \quad (3.2.67)$$

and each node will be labeled with the letter $a = 1, \dots, r$. There are bifundamental chiral superfields A_{aa+1} , B_{aa-1} connecting adjacent nodes, and in addition we will suppose that there are N_{f_a} matter superfields (Q_a, \tilde{Q}_a) in each node, in the fundamental representation. We will write

$$k_a = n_a k, \quad (3.2.68)$$

and we will assume that

$$\sum_{a=1}^r n_a = 0. \quad (3.2.69)$$

According to the general localization computation in section 2.3, the matrix model computing the \mathbb{S}^3 partition function of a necklace quiver is given by

$$Z(N) = \frac{1}{(N!)^r} \int \prod_{a,i} d\lambda_{a,i} \frac{\exp\left[\frac{in_a k}{4\pi} \lambda_{a,i}^2\right]}{2\pi} \frac{\exp\left[\frac{in_a k}{4\pi} \lambda_{a,i}^2\right]}{\left(2 \cosh \frac{\lambda_{a,i}}{2}\right)^{N_{f_a}}} \prod_{a=1}^r \frac{\prod_{i<j} \left[2 \sinh\left(\frac{\lambda_{a,i}-\lambda_{a,j}}{2}\right)\right]^2}{\prod_{i,j} 2 \cosh\left(\frac{\lambda_{a,i}-\lambda_{a+1,j}}{2}\right)}. \quad (3.2.70)$$

The building block of the integrand in (3.2.70) is the following N -dimensional kernel, associated to an edge connecting the nodes a and b :

$$K_{ab}(\lambda_1, \dots, \lambda_N; \mu_1, \dots, \mu_N) = \frac{1}{N!} \prod_{i=1}^N e^{-U_a(\lambda_i)} \frac{\prod_{i<j} 2 \sinh\left(\frac{\lambda_i-\lambda_j}{2k}\right) 2 \sinh\left(\frac{\mu_i-\mu_j}{2k}\right)}{\prod_{i,j} 2 \cosh\left(\frac{\lambda_i-\mu_j}{2k}\right)}. \quad (3.2.71)$$

Here,

$$U_a(\lambda) = -\frac{in_a}{4\pi k} \lambda^2 + N_{f_a} \log\left(2 \cosh \frac{\lambda}{2k}\right) \quad (3.2.72)$$

and will be interpreted as a one-body potential for a Fermi gas with N particles. We denoted by λ_i the variables corresponding to the a node, and by μ_i those corresponding to the b node, after rescaling them as $\mu, \lambda \rightarrow \mu/k, \lambda/k$.

We now want to interpret the kernel (3.2.71) as a matrix element

$$K_{ab}(\lambda_1, \dots, \lambda_N; \mu_1, \dots, \mu_N) = \frac{1}{N!} \{\lambda_1, \dots, \lambda_N | \hat{\rho}_{ab} | \mu_1, \dots, \mu_N\}, \quad (3.2.73)$$

in terms of a non-symmetrized density matrix $\hat{\rho}_{ab}$ (i. e. a density matrix for distinguishable particles). We first notice that

$$\frac{1}{N!} \{\lambda_1, \dots, \lambda_N | \hat{\rho}_{ab} | \mu_1, \dots, \mu_N\} = \frac{1}{N!} \sum_{\sigma \in S_N} (-1)^{\epsilon(\sigma)} \rho_{ab}(\lambda_1, \dots, \lambda_N; \mu_{\sigma(1)}, \dots, \mu_{\sigma(N)}). \quad (3.2.74)$$

We also look at (3.2.71) and use the Cauchy identity (3.2.63) on it

$$\begin{aligned} K_{ab}(\lambda_1, \dots, \lambda_N; \mu_1, \dots, \mu_N) &= \frac{1}{N!} \prod_{i=1}^N e^{-U_a(\lambda_i)} \det_{ij} \left(\frac{1}{2 \cosh \frac{\lambda_i - \mu_j}{2k}} \right) \\ &= \frac{1}{N!} \sum_{\sigma \in S_N} (-1)^{\epsilon(\sigma)} \prod_{i=1}^N e^{-U_a(\lambda_i)} \prod_{i=1}^N t\left(\frac{\lambda_i - \mu_{\sigma(j)}}{k}\right) \end{aligned} \quad (3.2.75)$$

where we denoted

$$t(x) = \frac{1}{2 \cosh \frac{x}{2}}. \quad (3.2.76)$$

By comparing with (3.2.74), it follows that

$$\rho_{ab}(\lambda_1, \dots, \lambda_N; \mu_1, \dots, \mu_N) = \prod_{i=1}^N e^{-U_a(\lambda_i)} \prod_{i=1}^N t\left(\frac{\lambda_i - \mu_i}{k}\right). \quad (3.2.77)$$

Since the density matrix is completely factorized, the N -particle system is an ideal gas, albeit with a non-trivial one-particle Hamiltonian. By taking the Wigner transform of this expression, with

$$\hbar = 2\pi k, \quad (3.2.78)$$

we see that ρ_{ab} defines an N -body Hamiltonian

$$\rho_{ab}^W = e_{\star}^{-H_{N,W}^{ab}}, \quad (3.2.79)$$

where

$$H_{N,W}^{ab} = \sum_{i=1}^N H_W^{ab}(i). \quad (3.2.80)$$

The one-particle Hamiltonian H_W^{ab} is defined by

$$e_{\star}^{-H_W^{ab}} = e^{-U_a(q)} \star e^{-T(p)} \quad (3.2.81)$$

and

$$T(p) = \log\left(2 \cosh \frac{p}{2}\right). \quad (3.2.82)$$

We can now repeatedly use the resolution of the identity (3.2.17) to write the matrix integral (3.2.70) as

$$Z(N) = \text{tr}(\hat{\rho}), \quad (3.2.83)$$

where $\hat{\rho}$ is the density matrix

$$\hat{\rho} = \hat{\rho}_{12} \hat{\rho}_{23} \cdots \hat{\rho}_{r-1r} \hat{\rho}_{r1}, \quad (3.2.84)$$

and this defines the one-particle Hamiltonian H_W by

$$e_{\star}^{-H_W} = e_{\star}^{-H_W^{12}} \star e_{\star}^{-H_W^{23}} \star \cdots \star e_{\star}^{-H_W^{r-1r}} \star e_{\star}^{-H_W^{r1}}. \quad (3.2.85)$$

For necklace theories without fundamental matter it is easy to see that the total, one-particle Hamiltonian is given by [48]

$$e_{\star}^{-H_W} = \frac{1}{2 \cosh \frac{p}{2}} \star \frac{1}{2 \cosh \frac{p-n_1 q}{2}} \star \frac{1}{2 \cosh \frac{p-(n_1+n_2)q}{2}} \star \cdots \star \frac{1}{2 \cosh \frac{p-(n_1+\cdots+n_{r-1})q}{2}}. \quad (3.2.86)$$

3.2.5.1 The Fermi Surface

Here will will briefly present the computation the free energy of ABJM theory as it was done in [48]. Later, in section 3.3.3, we will go into more detail about this and conduct the computation with the relevant operator insertion to obtain the vev of a Wilson loop operator. In the case of ABJM theory the Hamiltonian is written in terms of the functions $U(q)$ and $T(p)$,

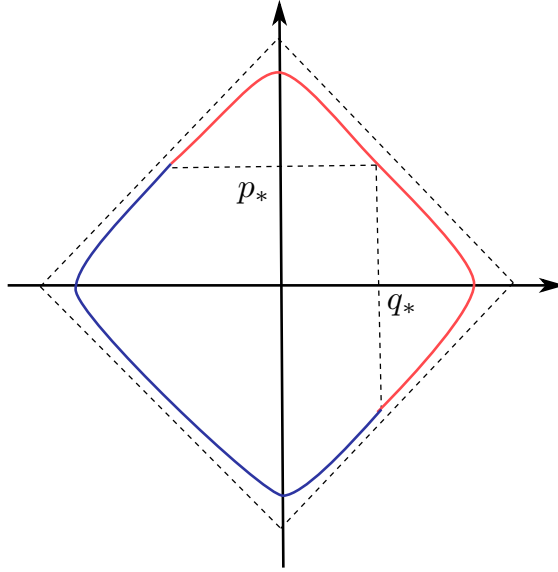


Figure 3.2: The regions in the Fermi surface.

which have the asymptotic behavior

$$U(q) = \log 2 \cosh \frac{q}{2} = \frac{q}{2} + \sum_{k=1}^{\infty} \frac{(-1)^{k+1}}{k} e^{-kq}, \quad (3.2.87a)$$

$$U'(q) = \frac{1}{2} \tanh \frac{q}{2} = \frac{1}{2} + \sum_{k=1}^{\infty} (-1)^k e^{-kq} \quad (3.2.87b)$$

$$U''(q) = \frac{1}{4 \cosh^2 \frac{q}{2}} = \sum_{k=1}^{\infty} k (-1)^{k+1} e^{-kq}. \quad (3.2.87c)$$

This is analogous for T , where only q and p have to be exchanged. Higher derivatives of these functions are zero up to exponentially suppressed terms when going to infinity. This will lead to a great simplification of the expressions at large E . Let us now present the relevant computations to find the phase space volume.

We want to compute the volume defined in (3.2.53), which is given by the area enclosed by the curve

$$H_W(q, p) = E. \quad (3.2.88)$$

Let us fix a point (q_*, p_*) on the curve in such a way that

$$p_* = E. \quad (3.2.89)$$

Then, by considering the asymptotics of H , the relation

$$q_* = E + \mathcal{O}(e^{-E}) \quad (3.2.90)$$

holds. This point divides the curve (3.2.88) in a manner described in section 3.2.5.1 in which we also use the division shown in figure 3.2. Once again, we are able to use the the asymp-

otics (3.2.87) to solve the curve for q and p in the correct regions. The full volume will be pieced together like

$$\text{Vol}(E) = 4 \text{Vol}_I(E) + 4 \text{Vol}_{II}(E), \quad (3.2.91)$$

where

$$\text{Vol}_I(E) = \int_0^{q_*(E)} p(E, q) dq \quad \text{and} \quad \text{Vol}_{II}(E) = \int_0^{p_*(E)} q(E, p) dp - p_* q_*. \quad (3.2.92)$$

Here $p(E, q)$ and $q(E, p)$ are the local solutions of the curve.

Let us now consider region I , where we can write

$$T(p) = \frac{p}{2} + \mathcal{O}(e^{-E}), \quad T'(p) = \frac{1}{2} + \mathcal{O}(e^{-E}) \quad (3.2.93)$$

and

$$T^{(n)}(p) = 0 + \mathcal{O}(e^{-E}). \quad (3.2.94)$$

This shows that, up to exponentially suppressed corrections, there are no contributions from derivatives of $T(p)$ which are of higher order than one in this region. We should only keep the terms $(T'(p))^n$ with $n \geq 1$ and are therefore left with a Hamiltonian of the form

$$H_W(q, p) = \frac{p}{2} + U(q) - \frac{\hbar^2}{48} U''(q) + \frac{1}{2} \sum_{n=1}^{\infty} \hbar^{2n} c_n U^{2n}(q) + \mathcal{O}(e^{-E}). \quad (3.2.95)$$

In this region we can solve the equation (3.2.88) for p in terms of q . Doing this also for the case where q and p are exchanged and integrating the expressions in (3.2.92) yields the full volume

$$\text{Vol}(E) = 8E^2 - \frac{4\pi^2}{3} + \frac{\hbar^2}{24} + \mathcal{O}(Ee^{-E}). \quad (3.2.96)$$

We now need to further analyze the terms containing

$$\delta(E - H_W(q, p)) \quad (3.2.97)$$

and higher order derivatives, which appear in the Wigner–Kirkwood expansion of $n(E)$. The result is that, up to exponentially suppressed contributions, they do not give any further terms.

Putting everything together we conclude

$$n(E) = \frac{\text{Vol}(E)}{2\pi\hbar} + \mathcal{O}(Ee^{-E}) = \frac{2E^2}{\pi^2 k} - \frac{1}{3k} + \frac{k}{24} + \mathcal{O}(Ee^{-E}). \quad (3.2.98)$$

The grand canonical potential of ABJM theory, when using the formula (3.2.41) while noting the relation

$$\rho(E) = \frac{dn(E)}{dE}, \quad (3.2.99)$$

can be put into the form

$$J_{\text{ABJM}}(\mu) = \frac{2\mu^3}{3k\pi^2} + \mu \left(\frac{1}{3k} + \frac{k}{24} \right) + A(k) + J_{\text{np}}(\mu) \quad (3.2.100)$$

where $J_{\text{np}}(\mu)$ denotes the nonperturbative expansion and $A(k)$ is

$$A(k) = \frac{2\zeta(3)}{\pi^2 k} - \frac{k}{12} + \frac{\pi^2 k^3}{4320} + \mathcal{O}(k^5) \quad (3.2.101)$$

which can be interpreted as the resummation of the constant map contribution expanded around $k = 0$ (see [89, 48]). Using the integral representation of the Airy function

$$\text{Ai}(z) = \frac{1}{2\pi i} \int_{\mathcal{C}} dt \exp\left(\frac{t^3}{3} - zt\right), \quad (3.2.102)$$

where \mathcal{C} is a contour in the complex plane going from $e^{-i\pi/3}\infty$ to $e^{i\pi/3}\infty$ and (3.2.38) it finally follows that the partition function can be written as the Airy function

$$Z_{\text{ABJM}} = C^{-1/3} e^{A(k)} \text{Ai}\left[C^{-1/3}\left(N - \frac{1}{3k} - \frac{k}{24}\right)\right], \quad (3.2.103)$$

where C is

$$C = \frac{2}{\pi^2 k}, \quad (3.2.104)$$

which is a result first derived in [43] for ABJM theory and then rederived in the Fermi gas approach in [48] for a class of $\mathcal{N} \geq 3$ theories.

3.2.5.2 Derivation of the $N^{3/2}$ behaviour of ABJM theory

Having introduced the formalism so far is quite useful in order to derive the $N^{3/2}$ scaling behavior of M2-branes described in [42]. From (3.2.98) we know that the leading behavior of $n(E)$. Using the relation (3.2.99) and plugging the result into (3.2.41), we find

$$J(\mu) \approx \frac{4}{\pi k} \int_0^\infty \log(1 + ze^{-E}) E dE = -\frac{2}{\pi k} \Gamma(s+1) \text{Li}_3(-e^\mu). \quad (3.2.105)$$

Using the relation for the saddle point (3.2.39), we find

$$N(\mu) \approx \frac{2}{\pi k} \Gamma(s+1) \text{Li}_2(-e^\mu). \quad (3.2.106)$$

As large N corresponds to large μ , we have

$$J(\mu) \approx \frac{2}{3\pi^2 k} \mu^3, \quad N(\mu) \approx \frac{2}{\pi^2 k} \mu^2. \quad (3.2.107)$$

Using (3.2.40) we find for the free energy

$$F(N) \approx -\frac{\pi\sqrt{2k}}{3} N^{3/2}, \quad (3.2.108)$$

which concludes our derivation of the $N^{3/2}$ -behavior of ABJM theory. This behavior also holds for more general CSM theories as shown in [48].

3.3 Wilson loops in the Fermi gas approach

3.3.1 Incorporating Wilson loops

In this section we will show how it is possible to map the calculations of vevs of Wilson loop operators to the calculation of statistical–mechanical averages in the Fermi gas approach. For simplicity, we restrict ourselves to ABJM theory. The general $\mathcal{N} \geq 3$ quiver can be obtained by a straightforward generalization.

The ABJM quiver is defined by two nodes with Chern–Simons levels k and $-k$ (as we mentioned before, and without loss of generality, we will take k , the level in the first node, to be positive). The one–body Hamiltonians associated to the edges are given by

$$e_{\star}^{-H_W^{12}} = e^{\frac{ig^2}{2h}} \star \frac{1}{2 \cosh \frac{p}{2}}, \quad e_{\star}^{-H_W^{21}} = e^{-\frac{ig^2}{2h}} \star \frac{1}{2 \cosh \frac{p}{2}}. \quad (3.3.1)$$

Let us consider a 1/6 BPS Wilson loop with winding number n for the first node. As shown in [32] and reviewed above, this corresponds to inserting

$$\mathcal{O}_n = \sum_{i=1}^N e^{n\lambda_i/k} \quad (3.3.2)$$

into the matrix integral, after rescaling $\lambda \rightarrow \lambda/k$. The unnormalized vev can be written, in the language of many–body physics, as

$$\langle \mathcal{O}_n \rangle = \frac{1}{N!^2} \int d\lambda d\mu \{ \lambda_1 \cdots \lambda_N | \mathcal{O}_n \hat{\rho}_{12} | \mu_1 \cdots \mu_N \} \{ \mu_1 \cdots \mu_N | \hat{\rho}_{21} | \lambda_1 \cdots \lambda_N \}. \quad (3.3.3)$$

If we integrate over μ by using the resolution of the identity, we find

$$\langle \mathcal{O}_n \rangle = \frac{1}{N!} \int d\lambda \{ \lambda_1 \cdots \lambda_N | \mathcal{O}_n \hat{\rho}_{12} \hat{\rho}_{21} | \lambda_1 \cdots \lambda_N \} = \text{tr} (\mathcal{O}_n \hat{\rho}_{12} \hat{\rho}_{21}), \quad (3.3.4)$$

which is the vev of the one–body operator (3.3.2) in an ideal Fermi gas of N particles with a one–body Hamiltonian given by

$$e_{\star}^{-H_W} = \frac{1}{2 \cosh \frac{p-q}{2}} \star \frac{1}{2 \cosh \frac{p}{2}}. \quad (3.3.5)$$

Notice that this Hamiltonian is *not* Hermitian. This stems from the fact that the vev of a 1/6 BPS operator is not real. After a canonical transformation,

$$q \rightarrow q + p, \quad p \rightarrow p, \quad (3.3.6)$$

we obtain a more convenient form,

$$e_{\star}^{-H_W} = \frac{1}{2 \cosh \frac{q}{2}} \star \frac{1}{2 \cosh \frac{p}{2}} = e_{\star}^{-U(q)} \star e_{\star}^{-T(p)} \quad (3.3.7)$$

where $T(p)$ is given in (3.2.82) and

$$U(q) = \log \left(2 \cosh \frac{q}{2} \right). \quad (3.3.8)$$

After this canonical transformation, the insertion of the 1/6 BPS Wilson loop corresponds to considering in the Fermi gas a one-body operator of the form

$$\mathcal{O}_n = \exp \left(\frac{n(q+p)}{k} \right), \quad (3.3.9)$$

which we have written already in the one-particle sector.

Since the vev of a 1/2 BPS Wilson loop can be computed by considering the vev of the 1/6 BPS Wilson loop and its conjugate, as we can see from (2.3.49), we will only analyze the case of the 1/6 BPS Wilson loops, and deduce the vev of the 1/2 BPS Wilson loops from (2.3.49).

3.3.2 Quantum Hamiltonian and Wigner–Kirkwood corrections

In the Fermi gas approach of [48], the full quantum Hamiltonian contains \hbar corrections and it is not known in closed form. Its semiclassical expansion can be obtained by using the Baker–Campbell–Hausdorff (BCH) formula as applied to the \star -product in (3.3.7). It was shown in [48] that, in the calculation of the grand potential of the system, up to exponentially small corrections in the chemical potential, only the first quantum correction is needed. For the calculation of the Wilson loop vev on the other hand, we will need an infinite series of terms appearing in the semiclassical expansion. These terms are of the form

$$U^{(n)}(q) (T'(p))^n, \quad T^{(n)}(p) (U'(q))^n. \quad (3.3.10)$$

The coefficients of these terms can be determined in closed form by exploiting some particular cases of the BCH formula (see [90] for examples of such calculations). We will now determine these coefficients.

In our problem we will analyze the behavior of the \star product

$$e_\star^A \star e_\star^B, \quad (3.3.11)$$

where

$$A = -U(q), \quad B = -ap, \quad (3.3.12)$$

and a being some constant is the case relevant for our analysis. The function $U(q)$ is arbitrary in this analysis. Here we choose the representation of p so that, B acts as the derivative $ia\hbar\partial_q$, hence the commutator reads

$$[A, B]_\star = ia\hbar U'(q). \quad (3.3.13)$$

Further nesting of this commutator with B yields only terms proportional to higher derivatives of U . As a result we can use a simpler version of the BCH formula which is given [90] by

$$Z = \log_\star \left(e_\star^A \star e_\star^B \right) = B + A \frac{B]_\star}{1 - e^{-B]_\star}}, \quad (3.3.14)$$

where $B]_\star$ is to be understood as the operation of performing a \star -commutator with B (acting on the left), and its n -th power is obtained by nesting the the \star -commutator n times in the

above manner⁴. The function appearing in this expression is given by the generating function of the Bernoulli numbers

$$\frac{x}{1 - e^{-x}} = \sum_{n=0}^{\infty} c_n x^n = 1 + \frac{x}{2} + \frac{x^2}{12} + \dots \quad (3.3.15)$$

where

$$c_n = \frac{B_n(-1)^n}{n!} \quad (3.3.16)$$

depends on the Bernoulli numbers B_n . The Bernoulli numbers have the property, that they are only non-vanishing for even numbers, with the exception of B_1 . Hence all the powers in this series are even except for the second term. Using this expansion, we then conclude that

$$Z = -ap - \sum_{n \geq 0} c_n (-i\hbar a)^n U^{(n)}(q). \quad (3.3.17)$$

In our case the asymptotics of the Hamiltonian tell us that we should analyze the case $T(p) = p/2$. In this case only the terms of the form

$$U^{(n)}(q) (T'(p))^n \quad (3.3.18)$$

survive in the BCH expansion, which can easily be seen by analyzing the nested commutators. This choice corresponds to taking $a = 1/2$ in the above formula. Putting all of this together we find that for the choices made in (3.3.12) these terms appear in the Hamiltonian in the form

$$T(p) + U(q) + \sum_{n \geq 1} \frac{B_n}{n!} (i\hbar)^n U^{(n)}(q) (T'(p))^n. \quad (3.3.19)$$

The case

$$A = -T(p), \quad B = -aq, \quad (3.3.20)$$

can be calculated in a similar way by exchanging p and q .

Here, where $U(q)$ is given by (3.3.8), the derivatives of $U(q)$ can be written in terms of polylogarithms. For the second derivative a calculation yields

$$U''(q) = \frac{1}{4 \cosh^2 \frac{q}{2}} = -\text{Li}_{-1}(-e^q). \quad (3.3.21)$$

Generally higher order derivatives of U can be written in terms of polylogarithms in the following way

$$U^{(m)}(q) = -\text{Li}_{1-m}(-e^q), \quad m \geq 2. \quad (3.3.22)$$

We will now compute all the Wigner–Kirkwood corrections for the simplified Hamiltonian considered above, which is obtained from the equation

$$e_{\star}^{-H_{\text{W}}} = e^{-U(q)} \star e^{-ap}. \quad (3.3.23)$$

In section 3.2.4.1 we introduced the Wigner–Kirkwood expansion, where we derived an expression for the generating function of the Wigner–Kirkwood corrections. These corrections are

⁴ Like $A(B)_{\star}^N = [[A, B]_{\star}, \dots, B]_{\star}$

obtained by computing the Wigner transform of the canonical density matrix

$$e_{\star}^{-tH_W}, \quad (3.3.24)$$

presented in (3.2.55). To calculate (3.3.24), we use the following trick, inspired by similar calculations in [90]. Assuming the general asymptotic structure appearing in the integration over the Fermi surface, let us suppose that we can write (3.3.24) as

$$e_{\star}^{-tH_W} = e_{\star}^{-tG(q)} \star e_{\star}^{-tap} \quad (3.3.25)$$

by using the BCH formula. If this assumption holds, the \star -product can be evaluated by the usual shift of the derivative into the arguments,

$$e_{\star}^{-tH_W} = e_{\star}^{-tG(q)} e^{\frac{i\hbar}{2} \overleftarrow{\partial}_q \overrightarrow{\partial}_p} e_{\star}^{-tap} = \exp\left(-tap - te^{\frac{\xi t}{2} \partial} G(q)\right). \quad (3.3.26)$$

where we have defined

$$\xi = -ia\hbar. \quad (3.3.27)$$

On the other hand, we can use the BCH formula (3.3.14) to find an alternative and explicit expression for $G(q)$,

$$e_{\star}^{-tG(q)} \star e_{\star}^{-tap} = \exp_{\star} \left(-tap - t \sum_{m \geq 0} c_m (t\xi)^m G^{(m)}(q) \right). \quad (3.3.28)$$

By construction, this equals $e_{\star}^{-tH_W}$ in (3.3.26). On the other hand, we already derived (3.3.17), which states

$$H_W = ap + \sum_{n \geq 0} c_n \xi^n U^{(n)}(q). \quad (3.3.29)$$

Comparing these results we deduce

$$\frac{\xi t \partial}{1 - e^{-\xi t \partial}} G(q) = \frac{\xi \partial}{1 - e^{-\xi \partial}} U(q), \quad (3.3.30)$$

which we formally solve for $G(q)$ and for which we find

$$G(q) = \frac{1}{t} \frac{1 - e^{-\xi t \partial}}{1 - e^{-\xi \partial}} U(q). \quad (3.3.31)$$

Plugging this back into (3.3.26), we conclude that

$$e_{\star}^{-tH_W} = \exp \left(-tap - \frac{e^{\frac{\xi t}{2} \partial} - e^{-\frac{\xi t}{2} \partial}}{1 - e^{-\xi \partial}} U(q) \right). \quad (3.3.32)$$

The second term in the exponent can, as done before, be computed by using the generating function of the Bernoulli polynomials,

$$\frac{ze^{-zt}}{1 - e^{-z}} = \sum_{n \geq 0} B_n(t) (-1)^n \frac{z^n}{n!}. \quad (3.3.33)$$

Applying this definition we find,

$$\frac{1}{t} \frac{e^{\frac{\xi t}{2} \partial} - e^{-\frac{\xi t}{2} \partial}}{1 - e^{-\xi \partial}} U(q) = \sum_{m \geq 0} \frac{B_{m+1}(t/2) - B_{m+1}(-t/2)}{t} \frac{(-1)^m}{(m+1)!} \xi^m U^{(m)}(q). \quad (3.3.34)$$

Let us make some consistency checks. Comparison with (3.2.55) we conclude that exponent in (3.3.32) should be of the form

$$-tH_W + \mathcal{O}(t^2), \quad (3.3.35)$$

due to vanishing $\mathcal{G}_0 = 1$, $\mathcal{G}_1 = 0$.

And indeed, because

$$\frac{B_{m+1}(t/2) - B_{m+1}(-t/2)}{m+1} = B_m t + \mathcal{O}(t^3) \quad (3.3.36)$$

a direct computation yields the result

$$ap + \frac{1}{t} \frac{e^{\frac{\xi t}{2} \partial} - e^{-\frac{\xi t}{2} \partial}}{1 - e^{-\xi \partial}} U(q) = H_W(q, p) + \mathcal{O}(t^2), \quad (3.3.37)$$

we expected. The expression (3.3.32) generates all the functions \mathcal{G}_r by expanding in t , and one can verify the results, at the very first orders, against the explicit expression in terms of \star -products given in (3.2.46).

Let us further analyze the expression given in (3.3.32). The operator appearing in this expression can be written as

$$\frac{e^{\frac{\xi t}{2} \partial} - e^{-\frac{\xi t}{2} \partial}}{1 - e^{-\xi \partial}} U(q) = \frac{1}{1 - e^{-\xi \partial}} \left[U\left(q + \frac{\xi t}{2}\right) - U\left(q - \frac{\xi t}{2}\right) \right], \quad (3.3.38)$$

by shifting the exponentials of derivatives into the argument of $U(q)$. The denominator can again be formally expanded in terms of Bernoulli numbers

$$\sum_{\ell \geq 0} \frac{B_\ell (-1)^\ell}{\ell!} \xi^{\ell-1} \partial^{\ell-1} \left[U\left(q + \frac{\xi t}{2}\right) - U\left(q - \frac{\xi t}{2}\right) \right], \quad (3.3.39)$$

but we have to be careful, since in this expansion the expression ∂^{-1} appears in the term $\ell = 0$. This term has to be properly interpreted and defined. We already expressed the operator in (3.3.38) in terms of Bernoulli numbers in (3.3.34). Comparing the two expressions, we see that this terms stands for

$$\frac{1}{\xi} \partial^{-1} \left[U\left(q + \frac{\xi t}{2}\right) - U\left(q - \frac{\xi t}{2}\right) \right] = t \sum_{g=0}^{\infty} \frac{1}{(2g+1)!} \left(\frac{t\xi}{2}\right)^{2g} U^{(2g)}(q). \quad (3.3.40)$$

Writing this as an integral gives us

$$\begin{aligned} & \sum_{g=0}^{\infty} \frac{1}{(2g+1)!} \left(\frac{t\xi}{2}\right)^{2g} U^{(2g)}(q) \\ &= \frac{1}{t\xi} \int_{\Lambda}^q \left[U\left(q' + \frac{\xi t}{2}\right) - U\left(q' - \frac{\xi t}{2}\right) \right] dq' + \sum_{g=0}^{\infty} \frac{1}{(2g+1)!} \left(\frac{t\xi}{2}\right)^{2g} U^{(2g)}(\Lambda), \end{aligned} \quad (3.3.41)$$

where Λ is an appropriate reference point.

As we will see in the next subsection, we need the expression of the canonical density matrix for the value

$$t = \frac{2n}{k}, \quad (3.3.42)$$

where n is the winding of the Wilson loop operator. This can be evaluated in principle with (3.3.32) and (3.3.39). In this case we have

$$\xi t/2 = -n\pi i \quad (3.3.43)$$

and if we analyze $U(q)$, which can be written like

$$U(q) = \frac{q}{2} + \log(1 + e^{-q}) \quad (3.3.44)$$

and also analyze the shift in (3.3.32) like it is done in (3.3.39) we find

$$U(q - n\pi i) - U(q + n\pi i) = -n\pi i \operatorname{sgn}(q) \quad q \neq 0, \quad (3.3.45)$$

due to the identity

$$U(q \pm n\pi i) = \pm n\pi i + \log(1 + (-1)^n), \quad (3.3.46)$$

which is singular for odd n .

This analysis implies that we are resumming the series of semiclassical corrections beyond its radius of convergence, and a regularization is needed. In order to resolve this, we first, notice that, in the polygonal limit $|q| \rightarrow \infty$, we can use the asymptotics of $U(q)$ as given in (3.2.87a)

$$U(q) \approx \frac{|q|}{2} + \mathcal{O}\left(e^{-|q|}\right). \quad (3.3.47)$$

In this limit, the second term in the exponent of (3.3.32) is given, for $q \neq 0$, by

$$-t|q| - \frac{t\xi}{2} \operatorname{sgn}(q), \quad (3.3.48)$$

since only $U(q)$ and its first derivative survive. Therefore, we want to calculate the correction to this polygonal limit for the value of t given by (3.3.42). In fact, this correction is given by a distribution supported at $q = 0$. We will show now how it can be obtained. The first term of (3.3.39) can be split like shown in (3.3.44) in the following way, for $q > 0$

$$U(q) = \frac{q}{2} + \tilde{U}(q), \quad \tilde{U}(q) = \log(1 + e^{-q}). \quad (3.3.49)$$

We have to calculate the sum appearing in the r. h. s. of (3.3.40), which we write as

$$\frac{q}{2} + \sum_{g=0}^{\infty} \frac{1}{(2g+1)!} \left(\frac{t\xi}{2}\right)^{2g} \tilde{U}^{(2g)}(q). \quad (3.3.50)$$

Since this function, as well as all its derivatives, vanish at infinity, we take $\Lambda = \infty$ as a reference point. For the particular value (3.3.43), we obtain from (3.3.41)

$$\sum_{g=0}^{\infty} \frac{1}{(2g+1)!} \left(\frac{t\xi}{2}\right)^{2g} \tilde{U}^{(2g)}(q) = \frac{1}{t\xi} \int_{\infty}^q \left[\tilde{U}\left(q + \frac{\xi t}{2}\right) - \tilde{U}\left(q - \frac{\xi t}{2}\right) \right] = 0 \quad (3.3.51)$$

since the integrand vanishes. We conclude that the term with $\ell = 0$ in (3.3.39) is given by

$$\frac{t}{2}q, \quad q > 0. \quad (3.3.52)$$

A similar reasoning for $q < 0$ shows that the first term in (3.3.39), for the value (3.3.42) of t , is

$$- \frac{n\pi i}{\xi} |q|. \quad (3.3.53)$$

The second term in (3.3.39) involves the derivative of this first term. Equivalently, it can be computed as the monodromy of $U(q)$,

$$U\left(q + \frac{\xi t}{2}\right) - U\left(q - \frac{\xi t}{2}\right) = -n\pi i \operatorname{sgn}(q). \quad (3.3.54)$$

We then see from (3.3.39) that the full series of corrections involves the distribution $\mathcal{S}(q)$ defined as

$$\mathcal{S}(q) = \sum_{\ell \geq 0} \frac{B_{\ell}(-1)^{\ell}}{\ell!} \xi^{\ell-1} \partial^{\ell-1} \operatorname{sgn}(q) = \frac{1}{1 - e^{-\xi\partial}} \operatorname{sgn}(q) = \frac{|q|}{\xi} + \frac{1}{2} \operatorname{sgn}(q) + \mathcal{O}(\xi). \quad (3.3.55)$$

To calculate $\mathcal{S}(q)$, we take a derivative w. r. t. q , and we multiply both sides by $1 - e^{-\xi\partial}$. We obtain the equation

$$\mathcal{T}(q) - \mathcal{T}(q - \xi) = \delta(q) + \delta(-q), \quad (3.3.56)$$

where

$$\mathcal{T}(q) = \mathcal{S}'(q). \quad (3.3.57)$$

The Fourier transform of (3.3.56) gives

$$\widehat{\mathcal{T}}(\omega) = \sqrt{\frac{2}{\pi}} \frac{1}{1 - e^{i\xi\omega}}. \quad (3.3.58)$$

We now set

$$\xi = -i\vartheta, \quad \vartheta = \pi k, \quad (3.3.59)$$

and solve for $\mathcal{T}(q)$ by doing an inverse Fourier transform. This transform is in principle ill-defined due to the pole at $\omega = 0$, but we can regularize it in a standard way by taking a

principal value at the origin (or an extra derivative w. r. t. q). We obtain in this way

$$\mathcal{T}(q) = -\frac{\text{P}}{2\pi} \int d\omega e^{-i\omega q} \frac{e^{-\omega\vartheta/2}}{\sinh\left(\frac{\omega\vartheta}{2}\right)} = \frac{i}{\vartheta} \coth\left(\frac{\pi q}{\vartheta}\right). \quad (3.3.60)$$

We now integrate w.r.t. q to obtain $\mathcal{S}(q)$. The result is, after fixing the appropriate value for the integration constant,

$$\mathcal{S}(q) = \frac{1}{2} + \frac{i}{\pi} \log\left(2 \sinh\left(\frac{\pi q}{\vartheta}\right)\right). \quad (3.3.61)$$

To see that this is a natural regularization, and to fix the integration constant, we note that for $q > 0$ this can be written as

$$\mathcal{S}(q) = \frac{q}{\xi} + \frac{1}{2} + \frac{i}{\pi} \log\left(1 - e^{-2\pi q/\vartheta}\right), \quad (3.3.62)$$

while for $q < 0$ we find,

$$\mathcal{S}(q) = -\frac{q}{\xi} + \frac{1}{2} + \frac{i}{\pi} \log(-1) + \frac{i}{\pi} \log\left(1 - e^{2\pi q/\vartheta}\right), \quad (3.3.63)$$

i. e.

$$\mathcal{S}(q) = \frac{|q|}{\xi} + \frac{1}{2} \text{sgn}(q) + \frac{i}{\pi} \log\left(1 - e^{2\pi|q|/\vartheta}\right), \quad (3.3.64)$$

so that, for $q \neq 0$, and ξ small, we find,

$$\mathcal{S}(q) \approx \frac{|q|}{\xi} + \frac{1}{2} \text{sgn}(q), \quad (3.3.65)$$

which is consistent with (3.3.55) and also gives the polygonal limit we need, cf. (3.3.48).

Even though it might not be clear at a first glance that an infinite sum of distributions (3.3.55) can be resummed to a smooth function of q , but this is common in the context of the semiclassical approximation of Wigner functions. It is performed by means of Fourier transforms, as we have just done [91]. For example, the ground state of a harmonic oscillator in the Wigner formulation involves the Gaussian

$$f_{\text{W}}(q, p) = f(q)f(p), \quad f(q) = \frac{1}{\sqrt{\pi\hbar}} e^{-q^2/\hbar}. \quad (3.3.66)$$

But

$$\hat{f}(\omega) = \frac{1}{\sqrt{2\pi}} e^{-\hbar\omega^2/4} = \frac{1}{\sqrt{2\pi}} \sum_{\ell=0}^{\infty} \frac{(-1)^\ell \hbar^\ell}{4^\ell \ell!} \omega^{2\ell} \quad (3.3.67)$$

which has inverse Fourier transform

$$\sum_{\ell=0}^{\infty} \frac{(-1)^\ell \hbar^\ell}{4^\ell \ell!} \delta^{2\ell}(q). \quad (3.3.68)$$

In the classical limit $\hbar \rightarrow 0$ we have a localized particle at the origin, and the \hbar corrections give an infinite sum of distributions which can be obtained from the smooth Gaussian in (3.3.66).

We conclude that, for the simplified Hamiltonian (3.3.23), the canonical density matrix with

t given in (3.3.42) is

$$e_{\star}^{-\frac{2n}{k}H_W} = \exp \left[-\frac{n}{k}p + \frac{n\pi i}{2} - n \log \left(2 \sinh \left(\frac{q}{k} \right) \right) \right], \quad (3.3.69)$$

at least with the natural regularization procedure explained above.

3.3.3 Integrating over the Fermi surface

We are now ready to calculate the vev of the $1/6$ BPS Wilson loop with winding number n in the Fermi gas approach. The corresponding one-body operator is given in (3.3.9). The first step is then to calculate (3.2.60) for this operator, i. e.

$$n_{\mathcal{O}_n}(\mu) = \int \frac{dqdp}{2\pi\hbar} \Theta(\mu - H_W) e^{\frac{n(q+p)}{k}} + \sum_{r \geq 1} \frac{(-1)^r}{r!} \frac{d^{r-1}}{d\mu^{r-1}} \int \frac{dqdp}{2\pi\hbar} \delta(\mu - H_W) \mathcal{G}_r e^{\frac{n(q+p)}{k}}. \quad (3.3.70)$$

Notice that, since the Hamiltonian is complex, the Fermi surface

$$H_W(q, p) = \mu \quad (3.3.71)$$

is in principle a surface in complex space. However, up to exponentially small corrections, we can recover a real Hamiltonian by a Wick rotation of the Planck constant, $\hbar \rightarrow -i\hbar$, so that $i\hbar$ is real. After this rotation, the integration process is well defined, and we can rotate back at the end of the calculation. Equivalently, it can be easily seen from our computations, that this can be done by integrating over appropriate paths in the complexified phase space.

The first integral is over the region enclosed by the Fermi surface. However, by integrating w. r. t. p or q one can reduce the integral to a boundary integral over the Fermi surface, plus a bulk contribution which is easy to calculate. As in [48] and briefly described in section 3.2.5.1, we will divide the boundary of the Fermi surface in appropriate regions. The quantum Hamiltonian reads,

$$H_W = T(p) + U(q) + \frac{i\hbar}{4} U'(q) T'(p) + \dots \quad (3.3.72)$$

where the corrections are exponentially small. The point in the Fermi surface with p coordinate

$$p_* = \mu + \frac{i\hbar}{8} \quad (3.3.73)$$

has a q coordinate of the form

$$q_* = \mu + \frac{i\hbar}{8} + \mathcal{O}(e^{-\mu}). \quad (3.3.74)$$

It is easy to see that the leading contribution to the Wilson loop is obtained by subtracting the contribution of the bulk region

$$-p_* \leq p \leq p_*, \quad -q_* \leq q \leq q_* \quad (3.3.75)$$

to the contribution of the boundary (of course, in writing this inequalities, we assume that we have performed a Wick rotation and that $i\hbar$ is real). But, if we restrict ourselves to terms which are proportional to $\exp(2n\mu/k)$, the only contribution comes from the boundary shown in red

in 3.2. This region can be divided in turn in two regions: a region where

$$p > p_*, \quad -q_* \leq q \leq q_*, \quad (3.3.76)$$

and the region obtained by exchanging p and q ,

$$q > q_*, \quad -p_* \leq p \leq p_*. \quad (3.3.77)$$

They give the same contribution, so we will restrict ourselves to the first region and then multiply the result by two. Along the curve bounding the region (3.3.76) we can neglect exponentially small terms in p , i.e. we can assume that $T(p) = p/2$. We can then write

$$p(\mu, q) = 2\mu + (2H_W - p), \quad (3.3.78)$$

where

$$2H_W - p = U(q) + \frac{i\hbar}{4}U'(q) + \dots \quad (3.3.79)$$

only depends on q and it has been computed in (3.3.19), with $T(p) = p/2$. We want to calculate the first term in (3.3.70),

$$\int \frac{dqdp}{2\pi\hbar} e^{\frac{n(q+p)}{k}} \Theta(\mu - H_W) = \frac{k}{n} \int \frac{dq}{2\pi\hbar} e^{\frac{q}{k}} \left(e^{\frac{np(\mu, q)}{k}} - 1 \right) \quad (3.3.80)$$

and we restrict to terms which are proportional to $\exp(2n\mu/k)$, so we keep only the first term. After plugging in the value of $p(\mu, q)$, we find

$$\frac{k}{2\pi n\hbar} e^{\frac{2n\mu}{k}} \int_{-q_*}^{q_*} dq e^{\frac{n(p+q)}{2k}} e^{-\frac{2n}{k}H_W}. \quad (3.3.81)$$

Notice that the p dependence in this and similar expressions cancels trivially. It is easy to see that all \hbar corrections to the Hamiltonian contribute to this integral, even if we neglect exponentially small corrections.

Let us now consider the Wigner–Kirkwood corrections to (3.3.70) along the curve bounding the region (3.3.76). By writing

$$\delta(\mu - H_W(q, p)) = \frac{1}{\left| \frac{\partial H_W(q, p)}{\partial p} \right|} \delta(p - p(\mu, q)) = 2\delta(p - p(\mu, q)) \quad (3.3.82)$$

we obtain

$$\begin{aligned} & 2 \sum_{r \geq 1} \frac{(-1)^r}{r!} \frac{d^{r-1}}{d\mu^{r-1}} e^{\frac{2n\mu}{k}} \int_{-q_*}^{q_*} \frac{dq}{2\pi\hbar} \mathcal{G}_r e^{\frac{n(q+p)}{k}} e^{-\frac{2n}{k}H_W} \\ &= \frac{k}{n} e^{\frac{2n\mu}{k}} \sum_{r \geq 1} \frac{(-1)^r}{r!} \left(\frac{2n}{k} \right)^r \int_{-q_*}^{q_*} \frac{dq}{2\pi\hbar} \mathcal{G}_r e^{\frac{n(q+p)}{k}} e^{-\frac{2n}{k}H_W}. \end{aligned} \quad (3.3.83)$$

This combines with (3.3.81) to produce,

$$\frac{k}{2\pi n\hbar} e^{\frac{2n\mu}{k}} \sum_{r \geq 0} \frac{(-1)^r}{r!} \left(\frac{2n}{k} \right)^r \int_{-q_*}^{q_*} dq \mathcal{G}_r e^{\frac{n(q+p)}{k}} e^{-\frac{2n}{k}H_W} = \frac{k}{2\pi n\hbar} e^{\frac{2n\mu}{k}} \int_{-q_*}^{q_*} dq e^{\frac{n(q+p)}{k}} e^{-\frac{2n}{k}H_W}. \quad (3.3.84)$$

Using (3.3.69) we find that this integral equals

$$\frac{k}{2\pi n\hbar} i^n e^{\frac{2n\mu}{k}} \int_{-q_*}^{q_*} dq \frac{e^{nq/k}}{\left(2 \sinh\left(\frac{q}{k}\right)\right)^n}, \quad (3.3.85)$$

where

$$q_* \approx \mu + \frac{\pi i k}{4}. \quad (3.3.86)$$

There is a singularity of the integrand for $q = 0$. However, as we will see, this can be avoided in a natural way. Also notice that, as $q_* \rightarrow \infty$, the integral diverges due to the upper integration limit, but it is not divergent when we send the lower integration limit to infinity. In fact, doing this only introduces exponentially small corrections (which we are neglecting anyway), and up to these corrections we can just compute,

$$k I_n = \int_{-\infty - \frac{\pi i k}{4}}^{q_*} dq \frac{e^{nq/k}}{\left(2 \sinh\left(\frac{q}{k}\right)\right)^n}. \quad (3.3.87)$$

To calculate this integral, we make the following change of variables

$$u = e^{q/k}, \quad (3.3.88)$$

so that

$$I_n = \int_0^{u_*} du \frac{u^{n-1}}{(u - u^{-1})^n}. \quad (3.3.89)$$

It is actually simpler to calculate the generating functional,

$$\mathcal{I} = \sum_{n=1}^{\infty} I_n z^n = \int_0^{u_*} du \frac{zu}{u^2(1-z) - 1} \approx \frac{1}{2} \frac{z}{1-z} \log(-u_*^2) + \frac{1}{2} \frac{z}{1-z} \log(1-z), \quad (3.3.90)$$

where

$$-u_*^2 = e^{2\mu/k} e^{-\frac{i\pi}{2}} \quad (3.3.91)$$

and we have again neglected exponentially small corrections. We now take into account that

$$-\frac{\log(1-z)}{1-z} = \sum_{n=1}^{\infty} H_n z^n, \quad (3.3.92)$$

where H_n are harmonic numbers, to obtain

$$k I_n = \mu - \frac{i\pi k}{4} - \frac{k}{2} H_{n-1}. \quad (3.3.93)$$

Notice that the integrand above has poles at $u^2 = (1-z)^{-1}$, and we have chosen an integration contour in the complex u -plane which avoids these poles. This is natural since the upper limit of integration, u_* , is in fact complex.

Putting all together, we obtain

$$\frac{k}{2\pi n\hbar} e^{\frac{2n\mu}{k}} i^n \left(\mu - \frac{\pi i k}{4} - \frac{k}{2} H_{n-1} \right). \quad (3.3.94)$$

As we explained above, there is an identical contribution from the region obtained by exchanging $p \leftrightarrow q$. Finally, one has to subtract the contribution from the bulk region, which gives

$$-\int_{-q_*}^{q_*} \int_{-p_*}^{p_*} \frac{dqdp}{2\pi\hbar} e^{\frac{n(p+q)}{k}} = -\frac{k^2}{2\pi n^2 \hbar} e^{\frac{2n\mu}{k} + \frac{i n \hbar}{4k}} + \dots = -\frac{i^n k^2}{2\pi n^2 \hbar} e^{\frac{2n\mu}{k}} + \dots \quad (3.3.95)$$

where the dots denote subleading exponentially small corrections. Therefore, up to these corrections, we find

$$n_{\mathcal{O}_n}(\mu) \approx \frac{k}{2\pi n \hbar} e^{\frac{2n\mu}{k}} i^n \left(2\mu - \frac{\pi i k}{2} - k H_n \right). \quad (3.3.96)$$

As we will see in a moment, this is in precise agreement with the result obtained in the 't Hooft expansion at genus zero.

According to (3.2.59), in order to find the full statistical-mechanical average, we just have to take into account the finite temperature corrections encoded in the Sommerfeld expansion. We then find,

$$\frac{1}{\Xi} \langle \mathcal{O}_n \rangle^{\text{GC}} = \pi \partial_\mu \csc(\pi \partial_\mu) n_{\mathcal{O}_n}(\mu), \quad (3.3.97)$$

with the value obtained in (3.3.96), which we will write as

$$n_{\mathcal{O}_n}(\mu) \approx (A(k)\mu + B(k)) e^{\frac{2n\mu}{k}}. \quad (3.3.98)$$

Here $A(k)$ and $B(k)$ are given by

$$A(k) = \frac{i^n}{2\pi^2 n}, \quad B(k) = -\frac{k}{4\pi^2 n} i^{n+1} \left(\frac{\pi}{2} - i H_n \right). \quad (3.3.99)$$

Putting things together, we find

$$\frac{1}{\Xi} \langle \mathcal{O}_n \rangle^{\text{GC}} = \frac{2\pi n}{k} \csc \frac{2\pi n}{k} \left[\left(\mu + \frac{k}{2n} - \pi \cot \frac{2\pi n}{k} \right) A(k) + B(k) \right] e^{\frac{2n}{k} \mu}, \quad (3.3.100)$$

where Ξ is the grand-canonical partition function calculated in [48], which is given by

$$\Xi = \exp \left(\frac{2\mu^3}{3\pi^2 k} + \frac{\mu}{3k} + \frac{\mu k}{24} \right), \quad (3.3.101)$$

up to exponentially small corrections and an overall, μ -independent constant. (3.3.100) gives then the exact grand canonical correlator at all k , up to exponentially small corrections in μ . To get the original normalized Wilson loop correlator, we have to perform the inverse transformation

$$\langle W_n^{1/6} \rangle = \frac{1}{2\pi i Z} \int d\mu e^{-\mu N} \langle \mathcal{O}_n \rangle^{\text{GC}}, \quad (3.3.102)$$

where Z denotes the partition function of the theory, which is itself given by

$$Z(N) = \frac{1}{2\pi i} \int d\mu e^{-\mu N} \Xi(\mu). \quad (3.3.103)$$

Given the definition of the Airy function in (3.2.102) and the explicit form of the partition

function (3.2.103), we are able to rewrite the integral (3.3.102), due to the exponential form of (3.3.100), in terms of quotients of Airy functions,

$$\begin{aligned} \langle W_n^{1/6} \rangle &= -C^{-1/3} A_1(k) \frac{\text{Ai}'\left[C^{-1/3}\left(N - \frac{k}{24} - \frac{6n+1}{3k}\right)\right]}{\text{Ai}\left[C^{-1/3}\left(N - \frac{k}{24} - \frac{1}{3k}\right)\right]} \\ &\quad + A_2(k) \frac{\text{Ai}\left[C^{-1/3}\left(N - \frac{k}{24} - \frac{6n+1}{3k}\right)\right]}{\text{Ai}\left[C^{-1/3}\left(N - \frac{k}{24} - \frac{1}{3k}\right)\right]}, \end{aligned} \quad (3.3.104)$$

where the prime denotes the derivative of the Airy function, and

$$C = \frac{2}{\pi^2 k}. \quad (3.3.105)$$

The functions $A_1(k)$ and $A_2(k)$ are defined as

$$A_1(k) = \frac{2\pi n}{k} \csc \frac{2\pi n}{k} A(k), \quad (3.3.106)$$

$$A_2(k) = \frac{2\pi n}{k} \csc \frac{2\pi n}{k} \left[\left(\frac{k}{2n} - \pi \cot \frac{2\pi n}{k} \right) A(k) + B(k) \right]. \quad (3.3.107)$$

Once the answer for the 1/6 BPS Wilson loop correlator is found, we can obtain the expectation value of the 1/2 BPS Wilson loop via (2.3.49)

$$\langle W_n^{1/2} \rangle = \frac{1}{4} \csc \frac{2\pi n}{k} \frac{\text{Ai}\left[C^{-1/3}\left(N - \frac{k}{24} - \frac{6n+1}{3k}\right)\right]}{\text{Ai}\left[C^{-1/3}\left(N - \frac{k}{24} - \frac{1}{3k}\right)\right]}. \quad (3.3.108)$$

Notice that the Airy functions in the denominators of (3.3.104) and (3.3.108) come from the partition function [43, 48].

We should emphasize that (3.3.104) and (3.3.108) are exact results at all orders in the $1/N$ expansion, up to exponentially small corrections. We will now extract from it some results on the 't Hooft genus expansion and test it with known results at low genus.

3.3.4 Genus expansion

In order to extract the 't Hooft expansion of the Wilson loop correlator, we have to expand (3.3.104) in powers of $1/k$. Since we are working in the $1/N$ expansion and k is generic, the results we will obtain are valid in the strong 't Hooft coupling regime

$$\lambda \gg 1. \quad (3.3.109)$$

The 't Hooft expansion of the Wilson loop vevs from the ABJM matrix model has been reviewed and extended in section 2.3.1. Therefore, we can compare the genus expansions we obtain from (3.3.104) with the results known from these computations. We will do the expansions explicitly for genus zero, genus one, and genus two. In appendix B.1, we will summarize the results for few more higher genus expansions.

— *Genus zero*

To test the agreement between the results of ABJM matrix model and the Fermi gas approach, it will be more convenient to expand the Airy functions in (3.3.104) in terms of the κ -variable (2.3.100) where only positive powers of κ are relevant at strong coupling. From (3.2.39) we find the relation

$$N = \frac{2\mu^2}{\pi^2 k} + \frac{k}{24} + \frac{1}{3k} \quad (3.3.110)$$

for the saddle point. Furthermore the κ -parameter in the matrix model is given by e^μ in the Fermi gas. Knowing this, we are able to compare our results.

For genus zero we find,

$$g_s^{-1} \langle W_n^{1/6} \rangle_{g=0} = \frac{i^n \kappa^n k}{4\pi^2 n} \left(\log \kappa - \frac{i\pi}{2} - H_n \right). \quad (3.3.111)$$

This agrees with the result (2.3.98) obtained with standard matrix model techniques.

The strong coupling expansion of this result can be obtained by expanding the Airy functions in (3.3.104) in terms of the 't Hooft coupling λ in the regime (3.3.109),

$$\begin{aligned} \langle W_n^{1/6} \rangle_{g=0} &= 2\pi i^{n+1} \left(\frac{\sqrt{\lambda}}{2\sqrt{2}\pi n} - \left(\frac{H_n}{4\pi^2 n} + \frac{i}{8\pi n} + \frac{1}{96} \right) + \left(\frac{i}{192} + \frac{\pi n}{4608} + \frac{H_{n-1}}{96\pi} \right) \frac{1}{\sqrt{2\lambda}} \right. \\ &\quad \left. - \left(\frac{i\pi n}{18432} + \frac{\pi^2 n^2}{663552} + \frac{nH_{n-1}}{9216} \right) \frac{1}{\lambda} + \mathcal{O}(\lambda^{-3/2}) \right) e^{\pi n \sqrt{2\lambda}}. \end{aligned} \quad (3.3.112)$$

Once we have obtained the result for the expectation value of the 1/6 BPS Wilson loop, the result for the 1/2 BPS Wilson loop follows from (2.3.49) by incorporating the result of the other node of the ABJM quiver gauge theory.

— *Genus one*

As the next step of our checks, we would like to compare the results of the Fermi gas approach and the ABJM matrix model at genus one. Expanding (3.3.104) in terms of κ , we find the following expression

$$\begin{aligned} \langle W_n^{1/6} \rangle_{g=1} &= -i^{n+1} \kappa^n \left[\frac{n \log \kappa}{12\pi} - \frac{in}{24} - \frac{2nH_n + 3n - 3}{24\pi} \right. \\ &\quad \left. + \left(\frac{3n+1}{24 \log \kappa} - \frac{1}{8 \log^2 \kappa} \right) \left(\frac{i}{2} + \frac{H_{n-1}}{\pi} \right) \right]. \end{aligned} \quad (3.3.113)$$

Using (2.3.49) we obtain for the vev of the 1/2 BPS Wilson loop at genus one,

$$\langle W_n^{1/2} \rangle_{g=1} = -i^n \kappa^n \left[\frac{2n \log^2 \kappa - (3n+1) \log \kappa + 3}{24 \log^2 \kappa} \right]. \quad (3.3.114)$$

The genus one result for the 1/6 Wilson loop correlator with winding one was first found in [36] by analyzing the ABJM matrix model. If we set $n = 1$ in (3.3.113), we find precise agreement between our results and those of [36]. We can also easily compute the genus one, 1/2 BPS

Wilson loop correlator with arbitrary winding from the ABJM matrix model, using (2.1.69), and the result is in agreement with the general expression (3.3.114).

Expanding the Airy functions in (3.3.104) directly in terms of the 't Hooft coupling λ in the region (3.3.109), we find the following expansion for the 1/6 BPS Wilson loop expectation value

$$\begin{aligned}
 \langle W_n^{1/6} \rangle_{g=1} = & -\frac{i^{n+1}\lambda}{2\pi} \left(\frac{\pi n}{3\sqrt{2\lambda}} - \left(\frac{2nH_n + 3n - 3}{12} + \frac{i\pi n}{12} + \frac{\pi^2 n^2}{144} \right) \frac{1}{\lambda} + \left(\frac{(3n+1)i}{24} + \frac{i\pi^2 n^2}{288} + \frac{\pi^3 n^3}{6912} \right. \right. \\
 & + \frac{n(n-1)\pi}{96} + \frac{(3n+1)H_{n-1}}{12\pi} + \frac{\pi n^2 H_{n-1}}{144} \left. \right) \frac{1}{\lambda\sqrt{2\lambda}} - \left(\frac{i}{16\pi} + \frac{i\pi(3n+1)n}{1152} \right. \\
 & + \frac{\pi^2 n^2 (n-1)}{9216} + \frac{i\pi^3 n^3}{27648} + \frac{i\pi^4 n^4}{995328} + \frac{(3n+1)nH_{n-1}}{576} + \frac{H_{n-1}}{8\pi^2} + \frac{\pi^2 n^3 H_{n-1}}{13824} \left. \right) \frac{1}{\lambda^2} \\
 & + \mathcal{O}(\lambda^{-5/2}) \Big) e^{\pi n \sqrt{2\lambda}}. \tag{3.3.115}
 \end{aligned}$$

Similar to the genus zero result, the expansion of the 1/2 BPS Wilson loop correlator with winding n is automatically obtained by applying (2.3.49).

— Genus two

As our last check, we consider ABJM Wilson loop correlators at genus two. Expanding (3.3.104) in terms of κ , we have

$$\begin{aligned}
 g_s^{-1} \langle W_n^{1/6} \rangle_{g=2} = & -\frac{i^n \kappa^n k}{2\pi n} \left[-\frac{7n^4 \log \kappa}{720\pi} + \frac{7in^4}{1440} - \frac{23n^3}{720\pi} + \frac{n^4}{48\pi} + \frac{7n^4 H_n}{720\pi} \right. \\
 & + \frac{n^2}{\log \kappa} \left(-\frac{in(3n+1)}{288} + \frac{11}{576\pi} + \frac{5n}{96\pi} - \frac{n^2}{64\pi} - \frac{n(3n+1)H_n}{144\pi} \right) \\
 & + \frac{n^2}{\log^2 \kappa} \left(\frac{i}{1152} + \frac{in}{64} + \frac{in^2}{128} - \frac{7}{96\pi} - \frac{n}{96\pi} + \frac{H_{n-1}}{576\pi} + \frac{nH_n}{32\pi} + \frac{n^2 H_n}{64\pi} \right) \\
 & + \frac{n}{\log^3 \kappa} \left(-\frac{i}{1152} - \frac{in}{96} - \frac{5in^2}{192} + \frac{5n}{64\pi} - \frac{H_{n-1}}{576\pi} - \frac{nH_{n-1}}{48\pi} - \frac{5n^2 H_n}{96\pi} \right) \\
 & + \frac{n}{\log^4 \kappa} \left(\frac{i}{96} + \frac{5in}{128} + \frac{H_{n-1}}{48\pi} + \frac{5nH_{n-1}}{64\pi} \right) \\
 & \left. - \frac{5n}{\log^5 \kappa} \left(\frac{i}{128} + \frac{H_{n-1}}{64\pi} \right) \right]. \tag{3.3.116}
 \end{aligned}$$

For $n = 1$, the above expression specializes to

$$\begin{aligned}
 g_s^{-1} \langle W_{n=1}^{1/6} \rangle_{g=2} = & -\frac{i\kappa k}{2\pi} \left[-\frac{7 \log \kappa}{720\pi} + \frac{7i}{1440} - \frac{1}{720\pi} + \frac{1}{\log \kappa} \left(-\frac{i}{72} + \frac{1}{36\pi} \right) + \frac{1}{\log^2 \kappa} \left(\frac{7i}{288} - \frac{7}{192\pi} \right) \right. \\
 & \left. + \frac{1}{\log^3 \kappa} \left(-\frac{43i}{1152} + \frac{5}{192\pi} \right) + \frac{19i}{384 \log^4 \kappa} - \frac{5i}{128 \log^5 \kappa} \right]. \tag{3.3.117}
 \end{aligned}$$

The 't Hooft expansion at strong coupling at genus two is found from (3.3.104),

$$\begin{aligned}
 \langle W_n^{1/6} \rangle_{g=2} &= \frac{i^{n+1} \lambda}{(2\pi)^3} \left(\frac{7\pi^3 n^3}{45\sqrt{2\lambda}} - \left(\frac{\pi^2 n^2 (7nH_n + 15n - 23)}{90} + \frac{7i\pi^3 n^3}{180} + \frac{7\pi^4 n^4}{2160} \right) \frac{1}{\lambda} \right. \\
 &+ \left(\frac{\pi n (3n+1)(3n-7)}{72} + \frac{\pi n^2 (3n+1)H_{n-1}}{18} + \frac{i\pi^2 n^2 (3n+1)}{36} \right. \\
 &\left. \left. + \frac{\pi^3 n^3 (7nH_n + 15n - 30)}{2160} + \frac{7i\pi^4 n^4}{4320} + \frac{7\pi^5 n^5}{103680} \right) \frac{1}{\lambda\sqrt{2\lambda}} + \mathcal{O}(\lambda^{-2}) \right) e^{\pi n \sqrt{2\lambda}}. \quad (3.3.118)
 \end{aligned}$$

The result for the 1/2 BPS Wilson loop is immediately obtained by applying (2.3.49) to (3.3.116), as in the previous cases.

We can now use the results of sections 2.1.3 and 2.3.3 for the 't Hooft expansion of 1/2 BPS Wilson loops, and study the expression derived there for genus two in the strong coupling region. We have checked explicitly that the strong coupling expansion of $W_2(p)$ agrees with the vev for the 1/2 BPS Wilson loop obtained from the Fermi gas result (3.3.116).

Since we have the exact result (up to exponentially small corrections) for the Wilson loop correlator (3.3.104), we can extract the leading and next to the leading terms of the 't Hooft expansion at arbitrary genus and strong coupling, as it was done in [92] for the 1/2 BPS Wilson loop of $\mathcal{N} = 4$ SYM theory. For the 1/6 BPS Wilson loop correlator with arbitrary winding n , we find

$$\begin{aligned}
 \langle W_n^{1/6} \rangle_g &= -i^{n+1} \frac{n^{2g-1}}{\sqrt{2}} a_g \sqrt{\lambda} e^{\pi n \sqrt{2\lambda}} \\
 &+ i^{n+1} \frac{n^{2g-2}}{2\pi} \left[\left(nH_{n-1} + i\frac{\pi n}{2} + \frac{\pi^2 n^2}{24} \right) a_g + \frac{3n+1}{12} a_{g-1} + c_g \right] \frac{e^{\pi n \sqrt{2\lambda}}}{\sqrt{\lambda}} \\
 &+ \mathcal{O}(\lambda^{-3/2}) e^{\pi n \sqrt{2\lambda}}, \quad (3.3.119)
 \end{aligned}$$

where a_g and c_g are given by

$$a_g = \frac{2(2^{2g-1} - 1)}{(2g)!} B_{2g}, \quad (3.3.120)$$

$$c_g = \sum_{m=0}^g \frac{2(2^{2m-1} - 1) 2^{2(g-m)}}{(2m)! (2g-2m)!} B_{2m} B_{2g-2m}. \quad (3.3.121)$$

Using (2.3.49), the leading and next to the leading terms of the 1/2 BPS Wilson loop correlator are found

$$\begin{aligned}
 \langle W_n^{1/2} \rangle_g &= -\frac{n^{2g-1}}{4} a_g e^{\pi n \sqrt{2\lambda}} \\
 &+ \frac{n^{2g-2}}{2\pi} \left(\frac{\pi^2 n^2}{48} a_g + \frac{3n+1}{24} a_{g-1} \right) \frac{e^{\pi n \sqrt{2\lambda}}}{\sqrt{2\lambda}} + \mathcal{O}(\lambda^{-2}) e^{\pi n \sqrt{2\lambda}}. \quad (3.3.122)
 \end{aligned}$$

It turns out that the 1/2 Wilson loop correlator does not involve c_g coefficients. At every genus,

the ratio of the leading terms of the 1/6 and 1/2 Wilson loop expectation values is given by

$$\frac{\langle W_n^{1/6} \rangle_g}{\langle W_n^{1/2} \rangle_g} = \frac{i^{n+1} \sqrt{\lambda}}{4\sqrt{2}} + \mathcal{O}(\lambda^0). \quad (3.3.123)$$

This ratio was first found in [41] at genus zero for the trivial winding, and (3.3.123) generalizes this result for arbitrary genus and winding.

Quantum Geometry of del Pezzo surfaces in the Nekrasov–Shatashvili limit

4.1 Introduction

In this chapter we will consider the *Nekrasov–Shatashvili* limit, i.e. we set one of the deformation parameters, say ϵ_1 , in (1.0.3) to zero and expand in the remaining one $\epsilon_2 = \hbar$. In [20] Nekrasov and Shatashvili conjectured that this limit leads to a description of the presented setup as a quantum integrable system. Looking at the expansion given in (1.0.3), we see that the Nekrasov–Shatashvili limit is encoded in the terms $F^{(n,0)}$ of the full free energy.

We base our calculation on the results of [19], where branes were studied in the context of refined topological strings. Branes probe the geometry in a quantum mechanical way, which was analyzed in [18] for the B–model on Calabi–Yau geometries given by

$$uv = H(x, p; z), \tag{4.1.1}$$

where $H(x, p; z) = 0$ defines a Riemann surface. The wave function $\Psi(x)$ which describes such branes satisfies the operator equation

$$\hat{H}\Psi(x) = 0 \tag{4.1.2}$$

where \hat{H} is defined via the position space representation of p if interpreted as the momentum

$$\hat{H} = H(x, i\hbar\partial_x). \tag{4.1.3}$$

\hat{H} reduces to the Riemann surface (4.1.1) in the semiclassical limit. In case of the unrefined topological string one obtains further corrections in g_s to \hat{H} , so that the relation (4.1.2) is only true to leading order.

In the refined topological string two types of branes exist which correspond to $M5$ branes wrapping different cycles in the M–theory lift. The way these branes probe the geometry is a key ingredient for deriving the results in this article.

A refinement of the topological B–model in terms of a matrix model has been conjectured in [93]. This refinement, based on the matrix model description of the topological B–model, amounts to deforming the Vandermonde determinant in the measure by a power of $\beta = -\frac{\epsilon_1}{\epsilon_2}$.

By virtue of this matrix model the time dependent Schrödinger equation

$$\hat{H}\Psi = \epsilon_1\epsilon_2 \sum f_I(t) \frac{\partial\Psi}{\partial t_I} \quad (4.1.4)$$

can be derived. \hbar is either identified with ϵ_1 or with ϵ_2 , depending on which brane the wavefunction describes.

In the Nekrasov–Shatashvili limit we have $g_s \rightarrow 0$, therefore this picture simplifies immensely and relation (4.1.3) is true up to normal ordering ambiguities. This can be seen from the Schrödinger equation (4.1.4)

From the result of moving the branes around cycles of the geometry one can deduce that the free energy in the Nekrasov–Shatashvili limit can be computed via the relation of special geometry between A- and B-cycles. We will have to introduce a deformed differential over which periods of these cycles are computed.

This setup is conjectured to be true generally and in this paper we want to check it for more general geometries. Furthermore we aim to clear up the technical implementations of this computation. This means we want to identify the right parameters of the models and compute the free energies in a more concise way. In case of local Calabi–Yau geometries, we find two different kind of moduli. These are normalizable and non-normalizable moduli. In order to successfully compute the free energies, we have to keep this difference in mind, especially because the non-normalizable moduli will not obtain any quantum corrections.

In the context of Seiberg–Witten theory an interpretation of these distinction exists in the sense that the normalizable moduli are related to the Coulomb parameters while the non-normalizable are identified as mass parameters of the gauge theory, which appear as residues of the meromorphic differential defined on the Seiberg–Witten curve.

We use the relations introduced in [19] and apply them to the case of mirror duals of toric varieties. In order to compute higher order corrections to the quantum deformed meromorphic differential, we derive certain differential operators of order two. Based on [94] this method has been used in [19] for the cubic matrix model and it has been applied in [95] to the case of toric geometries. We find that these operators act only on the normalizable moduli. There are some advantages in using these operators, one is that we are able to compute the free energies in different regions of the moduli space, another is that we do not have to actually solve the period integrals. This method of computing the higher order corrections also clears up their structure. Namely, the mass parameters will not obtain any quantum corrections, while the periods, do.

We will compute the free energies in the Nekrasov–Shatashvili limit of the topological string on local Calabi–Yau geometries with del Pezzo surfaces or mass deformations thereof as the base. For the local \mathbb{P}^2 we also compute it at different points in moduli space namely, not only the large radius point, but also at the orbifold point and the conifold locus. For local \mathbb{F}_0 we also will not only solve the model at large radius, but also at the orbifold point.

In section 4.2 we will provide an overview of the geometric structures we are using. In 4.3 we introduce the Nekrasov–Shatashvili limit and motivate a quantum special geometry, which we use to finally solve the topological string in the Nekrasov–Shatashvili limit in section 4.4.

4.2 Geometric setup

4.2.1 Branes and Riemann surfaces

We want to strengthen the conjecture made in [19] and clear up some technical details of this computation along the way. Let us therefore briefly review the geometric setup which we consider here.

Similarly to computations that were performed in [96] we want to compute the instanton series of the topological string A-model on non-compact Calabi-Yau spaces X , which are given as the total space of the fibration of the anti-canonical line bundle

$$\mathcal{O}(-K_B) \rightarrow B \quad (4.2.1)$$

over a Fano variety B . By the adjunction formula this defines a non-compact Calabi-Yau d -fold for $(d - 1)$ -dimensional Fano varieties. *Del Pezzo* surfaces are two-dimensional smooth Fano manifolds and they enjoy a finite classification. These consists of \mathbb{P}^2 and blow-ups of \mathbb{P}^2 in up to $n = 8$ points, called \mathcal{B}_n , as well as $\mathbb{P}^1 \times \mathbb{P}^1$.

As a result of mirror symmetry we are able to compute the amplitudes in the topological string B-model, where the considered geometry is given by

$$uv = H(e^p, e^x; z_I) \quad (4.2.2)$$

with $u, v \in \mathbb{C}$, $e^p, e^x \in \mathbb{C}^*$ and z_I are complex structure moduli. Furthermore $H(e^p, e^x; z_I) = 0$ is the defining equation of a Riemann surface.

The analysis in the following relies heavily on the insertion of branes into the geometry and their behavior when moved around cycles. Let us continue along the lines of [18] with the description of the influence branes have if we insert them into this geometry. In particular let us consider 2-branes. If we fix a point (p_0, x_0) on the (p, x) -plane these branes will fill the subspace of fixed p_0, x_0 , where u and v are restricted by

$$uv = H(p_0, x_0). \quad (4.2.3)$$

The class of branes in which we are interested, corresponds to fixing (p_0, x_0) in a manner so that they lie on the Riemann surface, i. e.

$$H(p_0, x_0) = 0. \quad (4.2.4)$$

By fixing the position of the brane like this, the moduli space of the brane is given by the set of admissible points, meaning it can be identified with the Riemann surface itself.

Following from an analysis of the worldvolume theory of these branes, one can argue that the two coordinates x and p have to be noncommutative. Namely, this means that they fulfill the commutator relation

$$[x, p] = g_s, \quad (4.2.5)$$

where g_s is the coupling constant of the topological string, which takes the role of the Planck constant.

The leading order part of such a brane’s partition function is given by

$$\Psi_{\text{cl.}}(x) = \exp\left(\frac{1}{g_s} \int^x p(y) dy\right). \quad (4.2.6)$$

This looks a lot like the first order term of a WKB approximation if we would identify $H(x, p)$ with the Hamiltonian of the quantum system. All of this suggests that $\Psi(x)$ is a wave-function for the quantum Hamiltonian H . As a result, we are expecting a relation of the form

$$\hat{H}(x, p)\Psi(x) = 0, \quad (4.2.7)$$

which can be considered as $H(x, p) = 0$ written as a condition on operators. Unfortunately it is generally not possible to derive this Hamiltonian, because we do not have control over the higher order g_s -corrections to it. But this is the story for the unrefined case. In the Nekrasov–Shatashvili limit of the refined topological string this problem disappears as we will show later on.

4.2.1.1 Mirror symmetry for non-compact Calabi-Yau spaces

We want to analyze toric del Pezzo surfaces and mass deformations thereof. These kind of geometries are related to Riemann surfaces defined by equations like (4.2.2) via mirror symmetry. Given the toric data of a non-compact Calabi-Yau space, there exists a construction which gives the defining equation for the Riemann surface.

The A-model geometry of a noncompact toric variety is given by a quotient

$$M = (\mathbb{C}^{k+3} \setminus \mathcal{SR})/G, \quad (4.2.8)$$

where $G = (\mathbb{C}^*)^k$ and \mathcal{SR} is the Stanley-Reisner ideal. The group G acts on the homogeneous coordinates x_i via

$$x_i \rightarrow \lambda_\alpha^{l_i^\alpha} x_i \quad (4.2.9)$$

where $\alpha = 1, \dots, k$ and $\lambda_\alpha \in \mathbb{C}^*$, $l_i^\alpha \in \mathbb{Z}$. The Stanley-Reisner ideal needs to be chosen in a way that the variety M exists. The toric variety M can also be viewed as the vacuum field configuration of a 2d abelian (2,2) gauged linear σ -model. In this picture the coordinates $x_i \in \mathbb{C}^*$ are the vacuum expectation values of chiral fields. These fields transform as

$$x_i \rightarrow e^{il_i^\alpha \epsilon_\alpha} x_i \quad (4.2.10)$$

under the gauge group $U(1)^k$, where again $l_i^\alpha \in \mathbb{Z}$ and $\alpha = 1, \dots, k$, while $\epsilon_\alpha \in \mathbb{R}$.

The vacuum field configurations are the equivalence classes under the gauge group, which fulfill the D -term constraints

$$D^\alpha = \sum_{i=1}^{k+3} l_i^\alpha |x_i|^2 = r^\alpha, \quad \alpha = 1, \dots, k \quad (4.2.11)$$

where the r^α are the Kähler parameters. In string theory r^α is complexified to $T^\alpha = r^\alpha + i\theta^\alpha$.

The Calabi-Yau condition $c_1(TM) = 0$ is equivalent to the anomaly condition

$$\sum_{i=1}^{k+3} l_i^\alpha = 0, \quad \alpha = 1, \dots, k. \quad (4.2.12)$$

Looking at (4.2.11), we see that negative entries in the l -vectors lead to noncompact directions in M .

But we are going to do computations in the topological string B-model defined on the mirror W of M . We will now describe briefly how W will be constructed. Let us define $x_i := e^{y_i} \in C^*$, where $i = 1, \dots, k+3$ are homogeneous coordinates. Using the charge vectors l^α , we define coordinates z_α by setting

$$z_\alpha = \prod_{i=1}^{k+3} x_i^{l_i^\alpha}, \quad \alpha = 1, \dots, k. \quad (4.2.13)$$

These coordinates are called *Batyrev coordinates* and are chosen so that $z_\alpha = 0$ at the large complex structure point. In terms of the homogeneous coordinates a Riemann surface can be defined by writing

$$H = \sum_{i=1}^{k+3} x_i. \quad (4.2.14)$$

Using (4.2.13) to eliminate the x_i and setting one $x_i = 1$, we are able to parameterize the Riemann surface (4.2.14) via two variables, which we call $X = \exp(x)$ and $P = \exp(p)$. Finally, the mirror dual W is given by the equation

$$uv = H(e^x, e^p; z_I) \quad I = 1, \dots, k. \quad (4.2.15)$$

4.3 The refinement

This was the story for the unrefined case, but we actually are interested in the refined topological string. Let us therefore introduce the relevant changes that occur when we consider the refinement of the topological string. According to [97], the partition function of the topological A-model on a Calabi-Yau X is equal to the partition function of M-theory on the space

$$X \times TN \times S^1 \quad (4.3.1)$$

where TN is a Taub-NUT space, with coordinates z_1, z_2 . The TN is fibered over the S^1 so that, when going around the circle, the coordinates z_1 and z_2 are twisted by

$$z_1 \rightarrow e^{i\epsilon_1} z_1 \quad \text{and} \quad z_2 \rightarrow e^{i\epsilon_2} z_2. \quad (4.3.2)$$

This introduces two parameters ϵ_1 and ϵ_2 and unless $\epsilon_1 = -\epsilon_2$ supersymmetry is broken. But if the Calabi-Yau is non-compact we are able to relax this condition, because an additional $U(1)_R$ -symmetry, acting on X , exists.

General deformations in ϵ_1 and ϵ_2 break the symmetry between z_1 and z_2 of the Taub-NUT space in (4.3.1). As a result we find two types of branes in the refinement of the topological string. In the M-theory setup the difference is given by the cigar subspaces $\mathbb{C} \times S^1$ in $TN \times S^1$ of (4.3.1), which the M5-brane wraps.

The classical partition function of an ϵ_i -brane is now given by

$$\Psi_{i,\text{cl.}(x)} = \exp\left(\frac{1}{\epsilon_i}W(x)\right), \quad (4.3.3)$$

where $W(x)$ is the superpotential of the $\mathcal{N} = (2, 2)$, $d = 2$ world-volume theory on the brane and which is identified with the p -variable in (4.2.15) as

$$W(x) = -\int^x p(y)dy. \quad (4.3.4)$$

This is quite similar to (4.2.6) and still looks like the leading order contribution of a WKB expansion where only the coupling changed.

This suggests that the $\epsilon_{1/2}$ -branes themselves also behave like quantum objects and if we have again say an ϵ_1 -brane with only one point lying on the Riemann surface parameterized by (p, x) then the two coordinates are again noncommutative, i. e.

$$[x, p] = \epsilon_1 = \hbar. \quad (4.3.5)$$

We will show later that the free energy of the refined topological string can be extracted from a brane-wave function like this in a limit where we send either one of the ϵ -parameters to zero. The limit of ϵ_i to zero means that one of the branes of the system decouples. In the next section we will describe the relevant limit.

4.3.1 The Nekrasov-Shatashvili limit

In [20] the limit where one of the deformation parameters is set to zero was introduced. The free energy in this so called *Nekrasov-Shatashvili* limit is defined by

$$\mathcal{W}(\hbar) = \lim_{\epsilon_2 \rightarrow 0} \epsilon_1 \epsilon_2 F. \quad (4.3.6)$$

where \mathcal{W} is the called the *twisted superpotential*. This \mathcal{W} can be expanded in \hbar like

$$\mathcal{W}(\hbar) = \sum_{n=0} \hbar^{2n} \mathcal{W}^{(n)} \quad (4.3.7)$$

where the $\mathcal{W}^{(i)}$ can be identified like

$$\mathcal{W}^{(i)} = F^{(i,0)} \quad (4.3.8)$$

with the free energy in the expansion (1.0.3).

Because we are only computing amplitudes in this limit, we present a convenient definition of the instanton numbers, tailored for usage in this limit. We define the parameters

$$\epsilon_L = \frac{\epsilon_1 - \epsilon_2}{2}, \quad \epsilon_R = \frac{\epsilon_1 + \epsilon_2}{2} \quad (4.3.9)$$

and accordingly

$$q_{1,2} = e^{\epsilon_{1,2}}, \quad q_{L,R} = e^{\epsilon_{L,R}}. \quad (4.3.10)$$

Using this definition the free energy at large radius has the following expansion

$$F^{hol}(\epsilon_1, \epsilon_2, t) = \sum_{\substack{j_L, j_R=0 \\ k=1}}^{\infty} \sum_{\beta \in H_2(M, \mathbb{Z})} (-1)^{2(j_L+j_R)} \frac{N_{j_L j_R}^\beta}{k} \frac{\sum_{m_L=-j_L}^{j_L} q_L^{km_L}}{2 \sinh\left(\frac{k\epsilon_1}{2}\right)} \frac{\sum_{m_R=-j_R}^{j_R} q_R^{km_R}}{2 \sinh\left(\frac{k\epsilon_2}{2}\right)} e^{-k\beta \cdot t} \quad (4.3.11)$$

in terms of BPS numbers $N_{j_L j_R}^\beta$.

By a change of basis of the spin representations

$$\sum_{g_L, g_R} n_{g_L, g_R}^\beta I_L^{g_L} \otimes I_R^{g_R} = \sum_{j_L, j_R} N_{j_L, j_R}^\beta \left[\frac{j_L}{2} \right]_L \otimes \left[\frac{j_R}{2} \right]_R \quad (4.3.12)$$

we introduce the instanton numbers n_{g_R, g_L}^β , which are more convenient to extract from our computations. With the sum over the spin states given by the expression

$$\sum_{m=-j}^j q^{km} = \frac{q^{j+\frac{k}{2}} - q^{-j-\frac{k}{2}}}{q^{\frac{k}{2}} - q^{-\frac{k}{2}}} = \chi(q^{\frac{k}{2}}) \quad (4.3.13)$$

we write down the relation between $N_{j_L j_R}^\beta$ and the numbers n_{g_R, g_L}^β defined in (4.3.12) explicitly [15, 98]

$$\sum_{j_L, j_R} (-1)^{2(j_L+j_R)} N_{j_L j_R}^\beta \chi(q_L^{\frac{k}{2}}) \chi(q_R^{\frac{k}{2}}) = \sum_{g_L, g_R} n_{g_L, g_R}^\beta (q_L^{\frac{1}{2}} - q_L^{-\frac{1}{2}})^{2g_L} (q_R^{\frac{1}{2}} - q_R^{-\frac{1}{2}})^{2g_R} . \quad (4.3.14)$$

Since we do not consider the full refined topological string we want to see how this expansion looks like in the Nekrasov-Shatashvili limit. Writing (4.3.11) in terms of n_{g_L, g_R}^β and taking the Nekrasov-Shatashvili limit (4.3.6), we find

$$\mathcal{W}(\hbar, t) = \hbar \sum_{\substack{g=0 \\ k=1}}^{\infty} \sum_{\beta \in H_2(M, \mathbb{Z})} \frac{\hat{n}_g^\beta (q^{\frac{k}{4}} - q^{-\frac{k}{4}})^{2g}}{k^2 2 \sinh\left(\frac{k\hbar}{2}\right)} e^{-k\beta \cdot t} \quad (4.3.15)$$

where $\hbar = \epsilon_1$ and

$$\hat{n}_g^\beta = \sum_{g_L + g_R = g} n_{g_L, g_R}^\beta . \quad (4.3.16)$$

4.3.2 Schrödinger equation from the β -ensemble

In [18] the authors described the behavior of branes by analyzing the relevant insertions into the matrix model description of the topological string B-model. In [93] a conjecture has been made about a matrix model description of the refined topological B-model, which we now want to use as described in [19] to derive a Schrödinger equation for the brane-wavefunction of an ϵ_1 or ϵ_2 -brane. This matrix model takes the form of a deformation of the usual matrix model, describing the unrefined topological string where the usual Vandermonde-determinant is not taken to the second power anymore, but to the power 2β where

$$\beta = -\frac{\epsilon_1}{\epsilon_2} . \quad (4.3.17)$$

This clearly has the unrefined case as its limit, when $\epsilon_1 \rightarrow -\epsilon_2$. Matrix models of this type are called β -ensembles.

The partition function of this matrix model is

$$Z = \int d^N z \prod_{i < j} (z_i - z_j)^{-2\epsilon_1/\epsilon_2} e^{-\frac{2}{\epsilon_2} \sum_i W(z_i)}. \quad (4.3.18)$$

The free energy of this matrix model can be expanded in g_s and β in the following way

$$F = \sum_{n,g=0} \gamma^{2n} g_s^{2n+2g-2} F_{n,g} \quad (4.3.19)$$

where we defined

$$\gamma = \sqrt{\beta} - \sqrt{\beta^{-1}}. \quad (4.3.20)$$

Here we used

$$\epsilon_1 = i\sqrt{\beta}g_s \quad \epsilon_2 = -i\frac{g_s}{\sqrt{\beta}}. \quad (4.3.21)$$

This gives the expansion (1.0.3) in terms of ϵ_1 and ϵ_2 if we identify

$$F_{n,g} = (-1)^n F^{(n,g)}. \quad (4.3.22)$$

Based on this matrix model description the following equation for brane wave-functions has been derived in [19]

$$\left(-\epsilon_\alpha^2 \frac{\partial^2}{\partial x^2} + W'(x)^2 + f(x) + g_s^2 \sum_{n=0}^g x^n \partial_{(n)} \right) \Psi_\alpha(x) = 0. \quad (4.3.23)$$

Now let us take the Nekrasov-Shatashvili limit. Here we consider the case

$$\hbar = \epsilon_1, \quad \text{and} \quad \epsilon_2 \rightarrow 0. \quad (4.3.24)$$

Due to the identity $g_s^2 = -\epsilon_1\epsilon_2$, the term containing g_s^2 vanishes leaving us with a time independent Schrödinger equation. (For a more detailed explanation of what is meant by this see [19].) We are left with a time-independent Schrödinger equation for the ϵ_1 -brane, where the ϵ_2 -brane decouples.

If we now interpret

$$i\hbar \frac{\partial}{\partial x} = \hat{p} \quad (4.3.25)$$

as the position-space representation of the momentum operator \hat{p} this yields the form

$$(\hat{p}^2 + (W'(x))^2 + f(x))\Psi(x) = 0, \quad (4.3.26)$$

where $\Psi(x) = \Psi_2(x)$ is the brane partition function of the brane which does not decouple when taking the Nekrasov-Shatashvili limit.

In the limit $\hbar \rightarrow 0$ this equation becomes classical and we are left with the defining equation of the Riemann surface

$$p^2 + W'(x)^2 + f(x) = 0. \quad (4.3.27)$$

Having such a matrix model description, we are able to describe the effect the insertion of

branes into the geometry has. In the unrefined case, the meromorphic differential λ acquires a pole with residue g_s at the point the brane was inserted. Therefore by going around the position x_0 of this brane, we pick up

$$\oint_{x_0} \lambda = g_s. \quad (4.3.28)$$

This behavior is captured by the Kodaira-Spencer scalar field ϕ on Σ by the relation

$$\delta\lambda = \partial\phi. \quad (4.3.29)$$

Via bosonization we can relate this to the insertion of the brane insertion operator

$$\psi(x) = e^{\phi/g_s} \quad (4.3.30)$$

which is a fermion. In terms of periods this means

$$\oint_{x_0} \partial\phi\psi(x_0) = g_s\psi(x_0). \quad (4.3.31)$$

In analogy to (4.3.3) we define the brane insertion operator in the refined case as

$$\psi_\alpha(x) = \exp(\phi(x)/\epsilon_\alpha) \quad \alpha = 1, 2 \quad (4.3.32)$$

and the Riemann surface is deformed in a similar manner by an ϵ_i -brane inserted at the point x_0

$$\oint_{x_0} \partial\phi\psi_i(x_0) = \frac{g_s^2}{\epsilon_i}\psi_i(x_0). \quad (4.3.33)$$

4.3.3 Special geometry

Up to now we learned that the branes we are considering act like quantum theoretic objects. In order to make use of this, we derived Schrödinger equations for the wave functions of ϵ_1 - and ϵ_2 -branes, respectively. However we are actually interested in deriving free energies.

This will be achieved by a deformed version of special geometry. But to make things more clear let us put this into a more general context and give a very short introduction to special geometry. Via special geometry we are able to derive the genus zero contribution of the full free energy which we will call the prepotential.

We start with introducing the *periods* of the holomorphic three-form Ω of a Calabi-Yau threefold X . The first step is choosing a basis of three cycles A^I and B_J , where $I, J = 0, \dots, h^{2,1}$, with intersection numbers

$$A^I \cap B_J = -B_J \cap A^I, \quad A^I \cap A^J = B_I \cap B_J = 0. \quad (4.3.34)$$

The dual cohomology basis spanning $H^3(X, \mathbb{Z})$

$$(\alpha_I, \beta^I), \quad I = 0, 1, \dots, h^{2,1}(X) \quad (4.3.35)$$

is given by Poincaré duality

$$\int_{A^I} \alpha_I = \delta_I^J, \quad \int_{B_J} \beta^J = -\delta_I^J \quad (4.3.36)$$

and satisfies the relations

$$\int_X \alpha_I \wedge \beta^J = \delta_I^J \quad \text{and} \quad \int_X \beta^J \wedge \alpha_I = -\delta_I^J \quad (4.3.37)$$

while all other combinations vanish.

Now we are able to define the *periods* of the holomorphic 3-form Ω by

$$X^I = \int_{A^I} \Omega, \quad \mathcal{F}_I = \int_{B^I} \Omega. \quad (4.3.38)$$

These periods carry information about the complex structure deformations. The holomorphic three-form Ω , as an element of $H^3(X, \mathbb{C})$, can be expressed in terms of the basis (4.3.35) in the following way

$$\Omega = X^I \alpha_I - \mathcal{F}_I \beta^I. \quad (4.3.39)$$

The X^I can locally serve as homogeneous coordinates of the moduli space \mathcal{M} . From these we choose a nonzero coordinate, e. g. X^0 and define

$$t^a = \frac{X^a}{X^0}, \quad a = 1, \dots, h^{2,1}(X) \quad (4.3.40)$$

which are flat coordinates for the moduli space \mathcal{M} . The X_I and \mathcal{F}^I are not independent and we can derive from the fact

$$\int_X \Omega \wedge \frac{\partial}{\partial X^I} \Omega = 0, \quad \int_X \Omega \wedge \frac{\partial}{\partial X^I} \frac{\partial}{\partial X^J} \Omega = 0 \quad (4.3.41)$$

that a holomorphic function \mathcal{F} exists, which we will call the *prepotential*. This prepotential obeys the relations

$$\mathcal{F} = \frac{1}{2} X^I \mathcal{F}_I, \quad \mathcal{F}_I = \partial_{X^I} \mathcal{F}, \quad (4.3.42)$$

which imply that \mathcal{F} is homogeneous of degree two in X^I . In flat coordinates we define

$$\mathcal{F}(X_I) = (X^0)^2 F(t^I), \quad (4.3.43)$$

which fulfills the relations

$$F_I = \frac{\partial F}{\partial t^I}. \quad (4.3.44)$$

Since we are analyzing local Calabi-Yau spaces we have to consider *rigid special geometry*. Here we will analyze only the B-model topological string on local Calabi-Yau threefolds X which are given by the equation

$$uv = H(e^x, e^p; z_I) \quad (4.3.45)$$

as we stated before in section 4.2. The holomorphic three-form Ω in this case is given by

$$\Omega = \frac{du}{u} \wedge dx \wedge dp. \quad (4.3.46)$$

The three-cycles on X descend to one-cycles on the Riemann surface Σ given by the equation

$$H(e^x, e^p; z_I) = 0. \quad (4.3.47)$$

Furthermore we find the relation that the periods of the holomorphic three form on the full Calabi-Yau threefold descend to periods of a meromorphic one-form λ , on only the Riemann surface Σ . This one-form is given by

$$\lambda = p dx . \quad (4.3.48)$$

Hence we can concentrate on the geometry of Riemann surfaces. There are $2g$ compact one-cycles on a genus g surface. These form a basis with the elements A^i and B_i , where i runs from 1 to g . We demand their intersections to be

$$A^i \cap B_j = \delta_j^i \quad (4.3.49)$$

or more generally equal to n_j^i , with n_j^i being an integer.

Having found this basis, we define the periods of the meromorphic one-form

$$x^i = \oint_{A^i} \lambda, \quad p_i = \oint_{B_i} \lambda, \quad (4.3.50)$$

analogously to (4.3.38). Here the x^i are normalizable moduli of the Calabi-Yau manifold. But we are considering non-compact Calabi-Yau manifolds and the non-compactness leads to additional non-normalizable moduli. These are mere parameters, not actual moduli of the geometry.

The normalizable moduli are related to the Coulomb parameters in Seiberg-Witten theory, e. g. pure $SU(N)$ Seiberg-Witten theories have an $N - 1$ Coulomb parameters, which correspond to the $g = N - 1$ period integrals over the A -cycles of the genus g Seiberg-Witten curve.

We already introduced the meromorphic differential λ coming from a reduction of the holomorphic three-form on the Riemann surface Σ . In Seiberg-Witten theory one can have additional periods on Σ for theories with matter. These periods arise because λ has poles in this case and the residues correspond to *mass parameters*. This explains why we need to separate two types of moduli in terms of a physical interpretation.

4.3.4 Quantum special geometry

In [19] it was derived that the free energies of the topological string in the Nekrasov-Shatashvili limit can be derived by taking the defining equation for the Riemann surface and use it as the Hamiltonian of the system, which is then quantized. In this case the non-vanishing ϵ -parameter will take the role of the Planck constant. Which parameter we choose does not affect the computation, so let us set

$$\hbar = \epsilon_1 . \quad (4.3.51)$$

The ϵ_2 -parameter will be sent to zero, which amounts to the decoupling of the ϵ_2 -branes. In order to quantize this system we interpret x and p as canonically conjugated coordinates and lift them to operators \hat{x} and \hat{p} . On these operators we impose the commutation relation

$$[\hat{x}, \hat{p}] = i\hbar \quad (4.3.52)$$

so that \hat{p} will be

$$\hat{p} = i \frac{\partial}{\partial x} \quad (4.3.53)$$

in x -space. The reasoning behind this is that the ϵ_i -branes still behave like quantum mechanical objects.

We quantize the system as described above by letting the defining equation for the Riemann surface become the differential equation

$$H(x, i\hbar\partial_x)\Psi(x) = 0. \quad (4.3.54)$$

One way to solve this differential equation is the WKB method, where we use the ansatz

$$\Psi(x, \hbar) = \exp\left(\frac{1}{\hbar}S(x, \hbar)\right), \quad (4.3.55)$$

where S has an \hbar expansion by itself

$$S(x, \hbar) = \sum_{n=0}^{\infty} S_n(x)\hbar^n. \quad (4.3.56)$$

We solve this equation order by order in \hbar . This structure is very reminiscent of what we described in section 4.3. The Schrödinger equation constructed there was solved by brane wave functions and comparing this to (4.3.3) we see that to leading order we can identify

$$S_0(x) = -\int^x p(x')dx' \quad (4.3.57)$$

so that the derivative of the leading order approximation of S can be identified as being the momentum

$$S'_0(x) = -p(x). \quad (4.3.58)$$

Following this logic, we can use the derivative of S to define a *quantum differential* by setting

$$\partial S = \partial_x S(x, \hbar)dx. \quad (4.3.59)$$

But now we need to interpret the meaning of this quantum deformation and in order to do that, we need to analyze the behavior of brane monodromies on the Riemann surface. We define the combination of A and B cycles of the Riemann surface

$$\gamma_A = \sum_I \iota^I A_I, \quad \gamma_B = \sum_I \mathbf{m}_I B^I \quad (4.3.60)$$

around which we will move the branes. These monodromies change the phase of the partition function as

$$\mathcal{M}_{\gamma_A} : Z_{\text{top}}(\mathbf{a}) \rightarrow \exp\left(\frac{1}{\epsilon_\alpha} \sum_I \iota^I a_I\right) Z_{\text{top}}(\mathbf{a}) \quad (4.3.61)$$

if we move the brane around the A -cycle while it changes in the manner

$$\mathcal{M}_{\gamma_B} : Z_{\text{top}}(\mathbf{a}) \rightarrow Z_{\text{top}}\left(\mathbf{a} + \frac{g_s^2}{\epsilon_\alpha} \mathbf{m}\right) = \exp\left(\frac{g_s^2}{\epsilon_\alpha} \sum_I \mathbf{m}_I \frac{\partial}{\partial a_I}\right) Z_{\text{top}}(\mathbf{a}) \quad (4.3.62)$$

if we move the brane around the B -cycle.

The monodromy around γ_B acts on Z as a multiplication of

$$\exp\left(\sum_I \frac{1}{\epsilon_\alpha} \mathbf{m}_I a_D^I\right) \quad (4.3.63)$$

so that a comparison yields

$$a_D^I = g_s^2 \frac{\partial}{\partial a_I}. \quad (4.3.64)$$

From observation made in [18], we have

$$\Psi_2(x) = \langle e^{-\frac{1}{\hbar}\phi(x)} \rangle = e^{\frac{1}{\hbar} \int^x \partial S} \quad (4.3.65)$$

and therefore

$$Z_{\text{top}}(\mathbf{a}) \rightarrow e^{\frac{1}{\hbar} \oint_{\gamma_B} \partial S} Z_{\text{top}}(\mathbf{a}). \quad (4.3.66)$$

The partition function itself is given by

$$Z_{\text{top}}(\mathbf{a}; \epsilon_1, \epsilon_2) = \exp\left(\sum_{g=0}^{\infty} g_s^{2g-2} \mathcal{F}^{(g)}(\mathbf{a}; \hbar)\right) \quad (4.3.67)$$

which can be written as

$$Z_{\text{top}}(\mathbf{a}; \epsilon_1 = 0, \epsilon_2 = \hbar) = \exp(\mathcal{W}(\mathbf{a}; \hbar)) \quad (4.3.68)$$

in the Nekrasov-Shatashvili limit. We consider this as a deformation in \hbar of the genus zero amplitude of the unrefined topological string. As a result we can see now how the monodromy acts on the partition function

$$Z_{\text{top}}(\mathbf{a}) \rightarrow \exp\left(\sum_I \mathbf{m}_I \partial_{a_I} \mathcal{W}(\mathbf{a}; \hbar)\right) Z_{\text{top}}(\mathbf{a}). \quad (4.3.69)$$

This has to be consistent with (4.3.66) and leads to the relations

$$\oint_{B^I} \partial S = \partial_{a_I} \mathcal{W}(\mathbf{a}; \hbar) \quad (4.3.70)$$

where

$$\oint_{A_I} \partial S = a_I(\hbar). \quad (4.3.71)$$

These are \hbar deformed quantum periods. This coincides with the special geometry relations presented in 4.3.3.

Doing this suggests that we are able to extend special geometry to a quantum deformed special geometry by lifting the classical periods to quantum periods by means of the quantum differential ∂S . We therefore define

$$a_I(z_J; \hbar) = \oint_{A_I} \partial S \quad \text{and} \quad a_D^I(z_J; \hbar) = \oint_{B^I} \partial S \quad I = 1, \dots, n, \quad (4.3.72)$$

which contain the classical periods as the leading order term of the semiclassical expansion.

The argument above leads us to conjecture that the relations between the quantum periods

are just the common special geometry relations, although with quantum deformed differential ∂S and prepotential $\mathcal{W}(\hbar)$

$$\frac{\partial \mathcal{W}(\hbar)}{\partial a_I(z_J; \hbar)} = a_D^I(z_J; \hbar). \quad (4.3.73)$$

Using the WKB ansatz we plug (4.3.55) into (4.3.54). This results in a sequence of S'_n , which are the corrections to the quantum periods

$$a_I^{(n)}(z_J; \hbar) = \oint_{A_I} S'_n(x) dx \quad \text{and} \quad a_D^I(z_J; \hbar) = \oint_{B_I} S'_n(x) dx, \quad I = 1, \dots, n. \quad (4.3.74)$$

Another method to solve eq. (4.3.54) is the use of so called *difference equations* to solve for Ψ , which has been done in [19]. This solves the problem perturbatively in the moduli z_J , while it is exact in \hbar . On the other hand the WKB ansatz is exact in the moduli z_J , while perturbative in \hbar . Solving the Schrödinger equation via a difference equation is best shown by giving examples, which can be found in sections 4.4.1, 4.4.2 and 4.4.4.

At large radius the A-periods can be expanded like

$$a^{(n)}(z_J; \hbar) = \sum_m \text{Res}_{x=x_0}(\partial_m S'_n(x; z_J)) \frac{z^m}{m!} \quad (4.3.75)$$

for $n > 0$ and a suitably chosen point x_0 . In the case $n = 0$ the leading order of the integrand has a branch cut so that we cannot just take the residues.

After having explained how the WKB expansion is used, some comments about the quantization of this system are in order. The perturbative quantization condition for this problem is given by (see [94])

$$\oint_B \partial S = 2\pi\hbar \left(n + \frac{1}{2} \right) \quad n = 0, 1, 2, \dots \quad (4.3.76)$$

However in [99] it was shown that this is not a sufficient condition, because the B-periods have poles at infinitely many values of the coupling constant. Hence this condition has to be extended to a nonperturbative condition. The authors made the conjecture that the nonperturbative part is actually controlled by the unrefined topological string, somewhat dual to the observations made in [98].

Another approach has been suggested in [100], where the condition

$$\exp(\partial_{a_I} \mathcal{W}(\mathbf{a}, \hbar)) = 1 \quad (4.3.77)$$

was used as the starting point for defining a nonperturbative completion.

4.3.5 Genus 1-curves

4.3.5.1 Elliptic curve mirrors and closed modular expressions

The next step would be to actually compute the genus zero amplitudes. In order to do that a method has been developed in [101], based on the work of [102][103]. The B-period is given in this formalism via the relation

$$\frac{\partial}{\partial a} a_D(a, \mathbf{m}) = -\frac{1}{2\pi i} \tau(t, \mathbf{m}) \quad (4.3.78)$$

and the prepotential $F^{(0,0)}$ can be calculated by making use of the relation

$$\frac{\partial^2}{\partial a^2} F^{(0,0)}(t, \mathbf{m}) = -\frac{1}{2\pi i} \tau(a, \mathbf{m}) \quad (4.3.79)$$

between $F^{(0,0)}$ and the τ -function of an elliptic curve. This function is defined by

$$\tau = \frac{\int_b \omega}{\int_a \omega} \quad (4.3.80)$$

where a and b are an integer basis of $H^1(\mathcal{C}, \mathbb{Z})$ of the elliptic curve.

The elliptic curve needs to be given in Weierstrass form

$$y^2 = 4x^3 - g_2(u, m)x - g_3(u, m) \quad (4.3.81)$$

which is achieved by applying Nagell's algorithm. Here u is the complex structure parameter of the curve and m are isomonodromic deformations.

The local flat coordinate at a cusp point in the moduli space is the period over a vanishing cycle μ . It can be obtained near such a point u, \mathbf{m} by integrating

$$\frac{dt}{du} = \sqrt{\frac{E_6(\tau)g_2(u, \mathbf{m})}{E_4(\tau)g_3(u, \mathbf{m})}}. \quad (4.3.82)$$

Here the functions E_4 and E_6 are the Eisenstein series. Note that the g_i , while not invariants of the curve, can be rescaled by

$$g_i \rightarrow \lambda^i(u, \mathbf{m})g_i. \quad (4.3.83)$$

However the scaling function $\lambda(u, \mathbf{m})$ is very restricted by the requirement not to introduce new poles, zeros or branch cuts for the periods in the u, \mathbf{m} parameter space. In practice the remaining freedom is easily fixed, by matching $\frac{dt}{du}$ to the leading behavior of the period integral at the cusp. E.g. near the large complex structure cusp, we match the leading behavior

$$\frac{dt}{du} = \frac{1}{2\pi i} \int_{\mu} \frac{dx}{y} = \frac{1}{u} + \dots. \quad (4.3.84)$$

and use the fact that the integration constant vanishes. This yields the period that is usually called $a(u, \mathbf{m})$ in Seiberg-Witten theory. Similarly at the conifold cusp, we can match similarly t to the vanishing period $a_D(u, \mathbf{m})$ at that cusp.

We find the relation between τ and t, \mathbf{m} by the fact that the j function has the universal behavior

$$j = 1728 \frac{E_4^3(\tau)}{E_4^3(\tau) - E_6^2(\tau)} = \frac{1}{q} + 744 + 196\,884q + 21\,493\,760q^2 + \mathcal{O}(q^3) \quad (4.3.85)$$

where $q = \exp(2\pi i \tau)$ which can then be inverted to obtain $\tau(j)$. The function j on the other hand can also be written in terms of t, \mathbf{m}

$$j = 1728 \frac{g_2^3(t, \mathbf{m})}{\Delta(t, \mathbf{m})} \quad (4.3.86)$$

with $\Delta(t, \mathbf{m}) = g_2^3(t, \mathbf{m}) - 27g_3^2(t, \mathbf{m})$, so that we can easily find an expression of τ in terms of t, \mathbf{m} .

With the formalism described above it is hence possible to write for all B-model curves and Seiberg Witten curves of genus one the classical vanishing period as well as the classical dual period (see [102, 103] for more details regarding the latter period) at each cusp point. Alternatively one can write a differential operator, which is of third order in the derivatives w.r.t. u [96]

$$\mathcal{D}^{(3)}(u, \mathbf{m}) \int_{a,b} \lambda = 0 . \tag{4.3.87}$$

4.3.5.2 Special geometry

In this article we are only concerned with Riemann surfaces of genus one. As mentioned above this means effectively we only have two compact cycles. We will denote the periods around these a and a_D . The special geometry relation is given by

$$a_D = \frac{\partial F}{\partial a} . \tag{4.3.88}$$

At large radius we choose the periods in such a manner that we have a single logarithm in u for the a -period, while we get squares of logarithms for the a_D -period. In this paper \tilde{u} will correspond to the the compact toric divisors inside the diagram. Generally, we have to rescale it to find the moduli u which gives the leading log-behavior of the periods at large radius. But we are considering local Calabi-Yau manifolds which generally have additional non-normalizable parameters. We will associate these parameters with the remaining noncompact toric divisors and call them mass parameters, denoted by m_i . Let us give an example. In figure 4.1, we

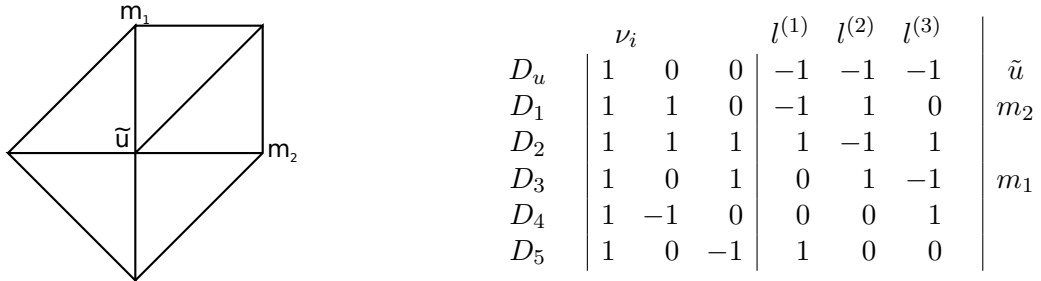


Figure 4.1: local \mathcal{B}_2 . In the first column we denote the divisors and in the fourth column the moduli and parameters associated with them.

have given the data for local \mathcal{B}_2 , which will be analyzed later on in (4.4.6). Here we have one normalizable moduli \tilde{u} and two mass parameters m_1, m_2 . Looking at Batyrev’s coordinates, we find three coordinates

$$z_1 = \frac{x_2 x_5}{x_0 x_1}, \quad z_2 = \frac{x_1 x_3}{x_0 x_2}, \quad z_3 = \frac{x_2 x_4}{x_0 x_3} \tag{4.3.89}$$

where x_0 is associated with D_u and therefore with \tilde{u} . Analogously for the two mass parameters. Setting the remaining x_i to one and defining $u = 1/\tilde{u}$, we obtain the relation

$$z_1 = \frac{u}{m_2}, \quad z_2 = u m_1 m_2, \quad z_3 = \frac{u}{m_1} . \tag{4.3.90}$$

The definition of u follows from demanding the behavior given in (4.3.84). The operator $\Theta_u = u\partial_u$ can also be written in terms of Batyrev coordinates which leads to

$$\Theta_u = \Theta_{z_1} + \Theta_{z_2} + \Theta_{z_3} . \quad (4.3.91)$$

4.3.5.3 Quantum Geometry

In [104] the connection between the dual toric diagrams which show the base of an $T^2 \times \mathbb{R}$ -fibration to (p, q) -branes was interpreted. The result was that moving the external lines in \mathbb{R}^2 requires an infinite amount of energy compared to the internal lines. The degrees of freedom related to the external lines are the mass parameters or non-normalizable moduli. Thus it makes sense to consider them as being non-dynamical. We assume that the quantum deformed periods remain non-dynamical, meaning that they do not obtain quantum corrections and for genus one only a and a_D will be quantum corrected.

As mentioned already, the quantum corrections to the periods can be extracted from the meromorphic forms, derived by the WKB ansatz which we use to solve the Schrödinger equation. For the A-periods, this reduces to residues, except for the logarithmic part of the classical contribution. Often it is possible to match the contributions from the residues to the different A-periods, but in some examples even this is not easily possible. For the B-periods it is even harder, because we generally have to find different parameterizations, giving different contributions, which have to be summed up in order to find the full result. The local \mathbb{P}^2 like it was solved in [19], is a good example for this, as well as the local \mathbb{F}^1 , see section 4.4.4.2. Actually, this problem even appears for the local \mathbb{F}_0 (see section 4.4.2, but because it is very symmetric we do not actually have to do any additional computations in order to solve this problem).

We want to avoid this complications, therefore we use a different approach. It is possible to derive differential-operators that give quantum corrections by acting on the classical periods. It turns out, that these operators are only of second order.

Having found these operators, the strategy is to apply them to the solution of the Picard-Fuchs system and build up the quantum corrections. The idea is that the operator is exact under the period integral, so that we can use partial integration to derive it.

The quantum periods $a(u, \mathbf{m}; \hbar)$ will be build up from the classical one $a(u, \mathbf{m})$ in the manner

$$a(u, \mathbf{m}; \hbar) = [1 + \sum_{i=1}^{\infty} \hbar^{2i} \mathcal{D}_{2i}] a(u, \mathbf{m}) =: \mathcal{D}^{(2)}(u, \mathbf{m}, \hbar) a(u, \mathbf{m}) . \quad (4.3.92)$$

The individual \mathcal{D}_i are second order differential operators in u given by

$$\mathcal{D}_i = a_i(u, \mathbf{m}) \Theta_u + b_i(u, \mathbf{m}) \Theta_u^2 \quad (4.3.93)$$

where $\Theta_u = u\partial_u$ and $a_i(u, \mathbf{m})$ and $b_i(u, \mathbf{m})$ are rational functions in their arguments. We do not have proven that this is always true, but for the examples we considered it has always been a viable ansatz. We derive such operators by taking the full WKB function under an integral with a closed contour and then applying partial integration.

The same holds for the dual period

$$a_D(u, \mathbf{m}; h) = \mathcal{D}^{(2)}(u, \mathbf{m}, h) a_D(u, \mathbf{m}) . \quad (4.3.94)$$

This approach has been introduced in [94] and used in [19] for the geometry corresponding

to a matrix model with a cubic potential. It also has been applied to the local \mathbb{F}_0 and local \mathbb{P}^2 in [95]. We are going to apply in even more examples while assuming that the operator is, at least at order \hbar^2 , always of order two. It would be very interesting to provide a proof for this conjecture.

4.4 Examples

4.4.1 The resolved Conifold

Let us start with a simple example, namely the resolved conifold. Its charge-vector is given by

$$l = (-1, -1, 1, 1). \quad (4.4.1)$$

Using the given charge vector we find for the Batyrev coordinate

$$z = \frac{x_3 x_4}{x_1 x_2} \quad (4.4.2)$$

which leads to the mirror curve

$$uv = 1 + e^x + e^p + ze^x e^{-p}. \quad (4.4.3)$$

Due to the adjacency of x and p in the last term of the sum we have quantum corrections in the Hamiltonian, due to the normal ordering ambiguities. The quantum Hamiltonian is

$$H = 1 + e^x + e^p + ze^{-\hbar/2} e^x e^{-p}. \quad (4.4.4)$$

This Hamiltonian leads to the difference equation

$$V(X) = -1 - X - z \frac{X e^{-\hbar/2}}{V(x - \hbar)} \quad (4.4.5)$$

where $X = e^x$ and $V(x) = \psi(x + \hbar)/\psi(x)$. The A -period does not obtain any quantum corrections and is therefore given by

$$a = \log(z). \quad (4.4.6)$$

After defining $Q = e^a$ we can invert this and find for the mirrormap $z = Q$. The B -period up to the fourth order in Q is

$$\tilde{a}_D = \frac{q^{1/2} \log q}{q - 1} Q + \frac{1}{2} \frac{q \log q}{q^2 - 1} Q^2 + \frac{1}{3} \frac{q^{3/2} \log q}{q^3 - 1} Q^3 + \frac{1}{4} \frac{q^2 \log q}{q^4 - 1} Q^4 + \mathcal{O}(Q^5) \quad (4.4.7)$$

where $q = e^{\hbar}$. The structure is very suggestive and leads us to assume the full form to be

$$a_D = \log q \sum_{i=1}^{\infty} \frac{1}{i} \frac{Q^i}{q^{i/2} - q^{-i/2}}. \quad (4.4.8)$$

The resolved conifold does not have a compact B-cycle and therefore only has a mass-parameter. But according to [105] the double-logarithmic solution can be generated by the

Frobenius method. The fundamental period for the resolved conifold is

$$\varpi(z; \rho) = \sum_{n=0}^{\infty} \frac{z^{n+\rho}}{\Gamma(1-n-\rho)^2 \Gamma(1+n+\rho)^2} \quad (4.4.9)$$

and

$$\partial_{\rho}^2 \varpi(z; \rho) \Big|_{\rho=0} = \log^2(z) + 2z + \frac{z^2}{2} + \frac{2z^3}{9} + \frac{z^4}{8} + \mathcal{O}(z^5) \quad (4.4.10)$$

generates the B-period. The non-logarithmic part of this is indeed given by the semiclassical limit of (4.4.7). Therefore, we define

$$a_D = \frac{1}{2} \log^2(z) + \tilde{a}_D \quad (4.4.11)$$

and use this formally as our dual period. Integrating the special geometry relations gives us the free energy in the Nekrasov-Shatashvili limit

$$\mathcal{W} = \hbar \sum_{i=1}^{\infty} \frac{1}{i^2} \frac{Q^i}{q^{i/2} - q^{-i/2}}. \quad (4.4.12)$$

The full free energy can be computed via the refined topological vertex and is

$$F_{\text{RTV}} = - \sum_{i=1}^{\infty} \frac{1}{i} \frac{Q^i}{(q^{\frac{i}{2}} - q^{-\frac{i}{2}})(t^{\frac{i}{2}} - t^{-\frac{i}{2}})} \quad (4.4.13)$$

with

$$q = e^{\epsilon_1} \quad \text{and} \quad t = e^{\epsilon_2}. \quad (4.4.14)$$

The Nekrasov-Shatashvili limit is defined in (4.3.6) and plugging in the free energy of the refined conifold into this, we find

$$\mathcal{W}_{\text{RTV}} = -\epsilon_2 \sum_{i=1}^{\infty} \frac{1}{i} \frac{Q^i}{t^{\frac{i}{2}} - t^{-\frac{i}{2}}} \left(\lim_{\epsilon_1 \rightarrow 0} \frac{\epsilon_1}{q^{\frac{i}{2}} - q^{-\frac{i}{2}}} \right) = -\epsilon_2 \sum_{i=1}^{\infty} \frac{1}{i^2} \frac{Q^i}{t^{\frac{i}{2}} - t^{-\frac{i}{2}}} \quad (4.4.15)$$

which is exactly the result we found using the quantum periods. This also fits nicely in the expansion presented in (4.3.15) with the only nonvanishing *instanton number* being $\hat{n}_0 = 1$.

4.4.2 local \mathbb{F}_0

We begin with presenting the Mori cone for the toric geometry depicted in fig. (4.2)

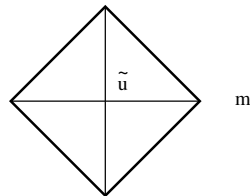


Figure 4.2: Polyhedron 2 depicting the toric geometry \mathbb{F}_0 .

$$\begin{array}{c} D_u \\ D_1 \\ D_2 \\ D_3 \\ D_4 \end{array} \left| \begin{array}{ccc} \nu_i & & \\ 1 & 0 & 0 \\ 1 & 1 & 0 \\ 1 & 0 & 1 \\ 1 & -1 & 0 \\ 1 & 0 & -1 \end{array} \right| \begin{array}{cc} l^{(1)} & l^{(2)} \\ -2 & -2 \\ 1 & 0 \\ 0 & 1 \\ 1 & 0 \\ 0 & 1 \end{array} \Bigg| . \quad (4.4.16)$$

From the toric data we find the complex structure moduli at the large radius point

$$z_1 = \frac{m}{\tilde{u}^2}, \quad z_2 = \frac{1}{\tilde{u}^2}. \quad (4.4.17)$$

After setting $u = \frac{1}{\tilde{u}^2}$ the mirror curve in these coordinates is given by

$$-1 + e^x + e^p + mu e^{-x} + u e^{-p} = 0. \quad (4.4.18)$$

Hence the Schrödinger equation for the brane wave function corresponding to this reads

$$(-1 + e^x + mu e^{-x})\Psi(x) + \Psi(x + \hbar) + u \Psi(x - \hbar) = 0. \quad (4.4.19)$$

The coefficients of the classical Weierstrass normal form are

$$g_2(u, m) = 27u^4(1 - 8u - 8mu + 16u^2 - 16mu^2 + 16m^2u^2), \quad (4.4.20a)$$

$$g_3(u, m) = 27u^6(1 - 12u - 12mu + 48u^2 + 24mu^2 + 48m^2u^2 - 64u^3 + 96mu^3 + 96m^2u^3 - 64m^3u^3). \quad (4.4.20b)$$

4.4.2.1 Difference equation

Defining the function

$$V(x) = \frac{\Psi(x + \hbar)}{\Psi(x)}, \quad (4.4.21)$$

we obtain the difference equation

$$V(x) = 1 - e^x + mu e^{-x} + \frac{u}{V(x - \hbar)}, \quad (4.4.22)$$

which can be expanded around $u = 0$. Doing this leads to a power series for $V(x)$

$$V(x) = 1 - X + mu e^{-x} + \frac{u}{1 - q^{-1}e^x} + \mathcal{O}(u^2), \quad (4.4.23)$$

where we defined $q = e^{\hbar}$.

We see in (4.4.21) that V includes the wavefunction ψ , which includes the quantum differential we seek. This has been already used in section 4.4.1, when we solved the resolved conifold, but let us see how we can actually extract it from this expression by integrating over $\log V$

$$\int \log(V(x)) = \int S'(x)dx + \sum_{n=2}^{\infty} \frac{\hbar^n}{n!} \int S^{(n)}(x)dx \quad (4.4.24)$$

where we used $\Psi(x) = e^{\frac{1}{\hbar} \sum_{i=0}^{\infty} S_i(x)\hbar^i}$. Integrating around a closed contour the last part vanishes

because we have for $n \geq 2$

$$\oint dx S^{(n)}(x) = [S^{(n-1)}], \quad (4.4.25)$$

so that indeed

$$\oint \partial S = \oint \log(V(X)) \quad (4.4.26)$$

and we can use this quantity to define the quantum differential for closed contours.

Computing the contour integral around the A_I cycles leads to

$$\frac{1}{2\pi i} \oint_{A_I} \log(V(x; z_I)) dx = \frac{1}{2\pi i} \oint_{A_I} \log(V(x; 0)) dx + \sum_n \frac{1}{n!} \text{Res}_{X=X_0} \frac{1}{X} \partial_{z^n} \log(V(X; z)) \quad (4.4.27)$$

$$\propto \log(z_I) + \tilde{a} \quad (4.4.28)$$

where we defined $X = e^x$ and X_0 is a appropriately chosen pole.

In this case the A-Period is is given by

$$a = \log u + 2(m+1)u + \left(3m^2 + 2m \left(q + \frac{1}{q} + 4 \right) + 3 \right) u^2 + \mathcal{O}(u^3) \quad (4.4.29)$$

The B-periods are more complicated to obtain. Due to the symmetry of this case, we find the contributions to the B-period by taking an integral and symmetrizing with respect to $u \leftrightarrow um$. This is due to the symmetry of local \mathbb{F}_0 and as a result we only have to do the integration once in order to obtain the final result.

We regularize the integrals using the boundaries δ and Λ . Using these we extract the finite (and real) part of the integral.

The B -period of local \mathbb{F}_0 is given by

$$a_D = -\frac{1}{2} \log(u) \log(mu) - \frac{1}{2} \log(mu^2) a + \tilde{a}_D \quad (4.4.30)$$

where the non-logarithmic part of the B -periods is given by

$$\tilde{a}_{\text{int}} = \int_{\delta}^{\Lambda} \log(V(x)) dx \quad (4.4.31)$$

$$= 4 \left(\frac{q+1}{q-1} \log q \right) z_2 + 4z_1^2 + \left(4 + 2 \frac{(5q^2 + 8q + 5) \log q}{q^2 - 1} \right) z_2^2 + \left(8 + 4 \frac{(q+1)^3}{(q-1)q} \log q \right) z_1 z_2 + \mathcal{O}(z_i^3). \quad (4.4.32)$$

In this expression we had to symmetrize with respect to $\hbar \rightarrow -\hbar$ to get rid of the odd sector in \hbar . That is expected because we only integrated over a small portion of the surface and are going to piece together the full period by symmetry considerations. Symmetrizing with respect

to the variables u and um finally yields

$$\begin{aligned} \tilde{a}_D = & -\frac{(m+1)(q+1)\log(q)}{q-1}u - 2(1+m)^2u^2 + \\ & -\frac{(m^2q(5q^2+8q+5) + 4m(q+1)^4 + q(5q^2+8q+5))\log(q)}{2q(q^2-1)}u^2 + \mathcal{O}(u^3). \end{aligned} \quad (4.4.33)$$

Due to the symmetry of local \mathbb{F}_0 we only had to compute one integral. But generally we would have to find the right parameterizations and piece together the results to yield the full periods. This will also become an issue for the A-periods in more complicated cases. We define the single valued quantity

$$Q_t = \exp(a). \quad (4.4.34)$$

The special geometry relations in this variable are

$$Q_t \partial_{Q_t} \mathcal{W}(Q_1, Q_2; q) = \tilde{a}_D(Q_t, Q_m; q) \quad (4.4.35)$$

which yields

$$\mathcal{W}(Q_1, Q_2; q) = \frac{1+q}{1-q}(Q_1+Q_2) + \frac{1}{4} \frac{1+q^2}{1-q^2}(Q_1^2+Q_2^2) + \frac{(1+q)(1+q^2)}{q(1-q)}Q_1Q_2 + \mathcal{O}(Q_i^3), \quad (4.4.36)$$

if we drop the classical terms.

One advantage of this method is that it is exact in \hbar from the beginning. In the following cases it will be very hard though to extract the correct contributions to the periods from the quantum differential form. The information we find due to this method can be obtained in any case, because at the large radius point the BPS numbers have the property

$$N_{j_L, j_R}^\beta = 0 \text{ for } \beta > \beta^{\max}(j_L, j_R) \quad (4.4.37)$$

for finite $\beta^{\max}(j_L, j_R)$. As a result we can reconstruct the data, found in this section by a computation perturbative in \hbar .

If we want to compute amplitudes at different point in moduli space we also have the problem that it is quite hard to compute the amplitudes exactly in \hbar , because we cannot properly attribute the contours. Hence, for the next section, we will use another approach, namely the differential operators, which map the classical periods to the higher order corrections.

4.4.2.2 Operator approach

From the Schrödinger equation given above we find for the zeroth order WKB function

$$S'_0(x) = \log \left(-\frac{e^{-x}}{2} \left(-e^x + e^{2x} + mu + \sqrt{(-e^x + e^{2x} + mu)^2 - 4e^{2x}u} \right) \right). \quad (4.4.38)$$

The operator mapping the zeroth to the second order periods is given by

$$\mathcal{D}_2 = \frac{1}{6}(-u - mu)\Theta_u + \frac{1}{12}(1 - 4u - 4mu)\Theta_u^2, \quad (4.4.39)$$

with $\theta_u = u\partial_u = z_1\partial_1 + z_2\partial_2$ in terms of the Batyrev coordinates. Higher order operators are given in appendix C.2. The form of θ_u already leads to the conclusion that the m parameter defined in eq. (4.4.17) does not get any \hbar corrections like it was expected for trivial parameters. Computing the classical A-period as described in section 4.3.5.1 and using the operators to calculate quantum corrections gives the expression

$$a = \log(u) + 2(1+m)u + 3(1+4m+m^2)u^2 + \frac{20}{3}(1+9m+9m^2+m^3)u^3 + (2mu^2 + 20m(1+m)u^3)\hbar^2 + \mathcal{O}(\hbar^3, u^4) \quad (4.4.40a)$$

and the B-period is given by

$$a_D = -2\log(u)^2 - 2\log(m)\log(u) - 2\log(mu^2) \left(2u(1+m) + 3u^2(1+4m+m^2) + 2mu^2\hbar^2 \right) - 8u(1+m) - 2u^2(13+40m+13m^2) - \frac{1}{3}\hbar^2(1+2u(1+m) + 2u^2(3+32m+3m^2)) + \mathcal{O}(\hbar^3, u^3). \quad (4.4.40b)$$

Inverting the exponentiated A-period we find for the mirror map

$$u(Q_u) = Q_u - 2(1+m)Q_u^2 + 3Q_u^3(1+m^2) - 4Q_u^4(1+m+m^2+m^3) + (-2mQ_u^3 - 4m(1+m)Q_u^4)\hbar^2 + \mathcal{O}(\hbar^3, Q_u^5). \quad (4.4.41)$$

To integrate the special geometry relation we need the following relations

$$Q_u = Q_2, \quad m = \frac{Q_1}{Q_2}, \quad (4.4.42)$$

which can be checked by calculating the periods as solutions of the Picard-Fuchs equations. Then we find the instanton numbers given in the tables 4.1, 4.2, 4.3 and 4.4.

d_2	d_1	0	1	2	3	4	5
0			-2				
1		-2	-4	-6	-8	-10	-12
2			-6	-32	-110	-288	-644
3			-8	-110	-756	-3556	-13072
4			-10	-288	-3556	-27264	-153324
5			-12	-644	-13072	-153324	-1252040

Table 4.1: The instanton numbers for local \mathbb{F}_0 at order \hbar^0 .

4.4.2.3 Orbifold point

In this section we solve the problem at the orbifold point of the moduli space \mathcal{M} . This is very useful because it would be the point where we could compare our results to a matrix model

	d_1	0	1	2	3	4	5
d_2							
0			-1				
1		-1	-10	-35	-84	-165	-286
2			-35	-368	-2055	-7920	-24402
3			-84	-2055	-21570	-142674	-699048
4			-165	-7920	-142674	-1488064	-10871718
5			-286	-24402	-699048	-10871718	-113029140

Table 4.2: The instanton numbers for local \mathbb{F}_0 at order \hbar^2 .

	d_1	0	1	2	3	4	5
d_2							
0							
1			-6	-56	-252	-792	-2002
2			-56	-1352	-12892	-75016	-322924
3			-252	-12892	-219158	-2099720	-13953112
4			-792	-75016	-2099720	-30787744	-298075620
5			-2002	-322924	-13953112	-298075620	-4032155908

Table 4.3: The instanton numbers for local \mathbb{F}_0 at order \hbar^4 .

	d_1	0	1	2	3	4	5
d_2							
0							
1			-1	-36	-330	-1716	-6435
2			-36	-2412	-41594	-375052	-2288546
3			-330	-41594	-1209049	-17227788	-157648036
4			-1716	-375052	-17227788	-365040880	-4760491974
5			-6435	-2288546	-157648036	-4760491974	-85253551830

Table 4.4: The instanton numbers for local \mathbb{F}_0 at order \hbar^6 .

description of the refined topological string.

The coordinates around we want to expand at the orbifold point are given by [40]

$$x_1 = 1 - \frac{z_1}{z_2}, \quad x_2 = \frac{1}{\sqrt{z_2} \left(1 - \frac{z_1}{z_2}\right)}. \quad (4.4.43)$$

Due to the symmetry of local $\mathbb{P}^1 \times \mathbb{P}^1$ obtaining the quantum periods has not been very hard in the large radius case. Now we want to find the quantum periods, expanded in the coordinates at the orbifold point. The problem we are facing in this case is, that we do not know how to extract the relevant parts from the integrals over the quantum differential. Hence we have to pursue a different path in order to compute the quantum periods. In [95] certain operators have been derived which allow us to obtain the higher order corrections in \hbar via second order

differential operators, acting on the classical periods. We list the operators for the second and fourth order here

$$t_2 = -\frac{z_1 + z_2}{6}\Theta_u t + \frac{1 - 4z_1 - 4z_2}{12}\Theta_u^2 t \quad (4.4.44a)$$

$$\begin{aligned} t_4 = \frac{1}{360\Delta^2} \{ & 2[z_1^2(1 - 4z_1)^3 + z_2^2(1 - 4z_2)^3 + 4z_1z_2(8 - 37z_1 - 37z_2 - 328z_1^2 + 1528z_1z_2 \\ & - 328z_2^2 + 1392z_1^3 - 1376z_1^2z_2 - 1376z_1z_2^2 + 1392z_2^3)]\Theta_u t + [-z_1(1 - 4z_1)^4 - z_2(1 - 4z_2)^4 \\ & + 4z_1z_2(69 - 192z_1 - 192z_2 - 1712z_1^2 + 6880z_1z_2 - 1712z_2^2 + 5568z_1^3 - 5504z_1^2z_2 \\ & - 5504z_1z_2^2 + 5568z_2^3)]\Theta_u^2 t\}. \end{aligned} \quad (4.4.44b)$$

In the coordinates z_1, z_2 the logarithmic derivative Θ_u is given by

$$\Theta_u = u\partial_u = z_1\partial_{z_1} + z_2\partial_{z_2}. \quad (4.4.45)$$

We can transform this operator to the orbifold coordinates and act with it on the classical period. The expansion of classical periods in the orbifold coordinates can be computed via solving the Picard–Fuchs system. This has been done in [45] already so that we can build on the solutions already at hand.

Here we present the periods to zeroth order

$$\omega_0 = 1, \quad (4.4.46a)$$

$$s_1^{(0)} = -\log(1 - x_1) = t_1 - t_2 \quad (4.4.46b)$$

$$s_2^{(0)} = x_1x_2 + \frac{1}{4}x_1^2x_2 + \frac{9}{64}x_1^3x_2 + \mathcal{O}(x_i^4) \quad (4.4.46c)$$

$$F_{s_2}^{(0)} = \log(x_1)s_2 + x_1x_2 + \frac{3}{4}x_1^2x_2 + \frac{15}{32}x_1^3x_2 - \frac{1}{6}x_1x_2^3 + \mathcal{O}(x_i^4). \quad (4.4.46d)$$

Using (4.4.44a) and (4.4.44b) we are able to compute the periods at order two and four, respectively. As explained, we take the operators (4.4.44a) and (4.4.44b), corresponding to order two and four, respectively, change the coordinates via (4.4.43) and apply them to (4.4.46) to find

$$s_2^{(2)} = \frac{1}{64}x_1x_2 + \frac{1}{256}x_1^2x_2 + \frac{15}{8192}x_1^3x_2 + \frac{35}{32768}x_1^4x_2 + \mathcal{O}(x_i^5)$$

and

$$\begin{aligned} F_{s_2}^{(2)} = & -\frac{1}{8}x_2 + \frac{1}{6}x_2x_1 + \frac{3}{128}x_1x_2 + \frac{17}{1536}x_1^2x_2 + \frac{189}{32768}x_1^3x_2 + \frac{1387}{393216}x_1^4x_2 \\ & - \frac{5}{24}x_2^3 + \frac{1}{6}x_2^3x_1 + \frac{5}{128}x_1x_2^3 + \frac{5}{1536}x_1^2x_2^3 - \frac{7}{24}x_2^5 + \frac{1}{6}x_2^5x_1 \\ & + s_2^{(2)}\log(x_1) + \mathcal{O}(x_i^5) \end{aligned} \quad (4.4.47)$$

while $s_1^{(0)}$ will not get any quantum corrections at all.

The result we find be using special geometry is

$$\begin{aligned}
 F^{(1,0)} &= \frac{1}{24} (\log(S_1) + \log(S_2)) + \frac{1}{576} (S_1^2 + 30S_2S_1 + S_2^2) \\
 &\quad - \frac{1}{138\,240} (2S_1^4 - 255S_2S_1^3 + 1530S_2^2S_1^2 + S_1 \leftrightarrow S_2) \\
 &\quad + \frac{1}{34\,836\,480} (8S_1^6 + 945S_2S_1^5 - 43\,470S_2^2S_1^4 + 150\,570S_2^3S_1^3 + S_1 \leftrightarrow S_2) + \mathcal{O}(S^7)
 \end{aligned} \tag{4.4.48a}$$

$$\begin{aligned}
 F^{(2,0)} &= -\frac{7}{5760} \left(\frac{1}{S_1^2} + \frac{1}{S_2^2} \right) + \frac{1}{2\,438\,553\,600} (155S_1^2 - 16\,988\,774S_2S_1 + 155S_2^2) \\
 &\quad - \frac{1}{5\,573\,836\,800} (31S_1^4 + 13\,093\,484S_2S_1^3 - 27\,178\,854S_2^2S_1^2 + S_1 \leftrightarrow S_2) \\
 &\quad - \frac{1}{14\,714\,929\,152\,000} (4960S_1^6 + 3842\,949\,687S_2S_1^5 - 36\,703\,156\,395S_2^2S_1^4 \\
 &\quad\quad\quad + 82\,152\,486\,440S_2^3S_1^3 + S_1 \leftrightarrow S_2) + \mathcal{O}(S^7)
 \end{aligned} \tag{4.4.48b}$$

$$\begin{aligned}
 F^{(3,0)} &= -\frac{31}{161\,280} \left(\frac{1}{S_1^4} + \frac{1}{S_2^4} \right) - \frac{1}{1\,560\,674\,304\,000} (2667S_1^2 - 3\,669\,924\,266S_2S_1 + 2667S_2^2) \\
 &\quad + \frac{1}{1\,961\,990\,553\,600} (508S_1^4 + 4\,960\,681\,415S_2S_1^3 - 6\,516\,516\,390S_2^2S_1^2 + S_1 \leftrightarrow S_2) \\
 &\quad - \frac{1}{80\,343\,513\,169\,920\,000} (1\,930\,654S_1^6 - 6\,435\,720\,4136\,601S_2S_1^5 + 346\,657\,135\,824\,060S_2^2S_1^4 \\
 &\quad\quad\quad - 727\,232\,136\,215\,170S_2^3S_1^3 + S_1 \leftrightarrow S_2) + \mathcal{O}(S^7)
 \end{aligned} \tag{4.4.48c}$$

where the constants of integration have been fixed in a manner as to give the resolved Conifold if we send $S_1 \rightarrow 0$ or $S_2 \rightarrow 0$. The data before fixing the constant of integration can be found in appendix C.2.1.

The relation between the periods in this case and the 't Hooft parameters of the corresponding matrix model is, at least in the unrefined case, given by [45]

$$S_1 = \frac{1}{4}(s_1 + s_2), \quad S_2 = \frac{1}{4}(s_1 - s_2). \tag{4.4.49}$$

Hence the periods in terms of the 't Hooft parameters are given by

$$s_1 = 2(S_1 + S_2), \quad s_2 = 2(S_1 - S_2). \tag{4.4.50}$$

The case of $S_1 = 0$ or $S_2 = 0$ specializes to the resolved conifold at the orbifold point which can be easily computed. Using this result, we are able to fix the remaining constants and obtain the final result for the NS-limit of local $\mathbb{P}^1 \times \mathbb{P}^1$ at the orbifold point.

We have to send $\hbar \rightarrow 2i\hbar$ and introduce an overall factor of $1/8$ in order to compare the results to the Conifold computation.

This results seem to disagree with the results of [13], but they actually agree, except for the contribution coming from the constants of integration. However, due to the change (4.4.50) the

expressions change drastically. The raw data can be found in appendix C.2.1.

4.4.3 $\mathcal{O}(-3) \rightarrow \mathbb{P}^2$

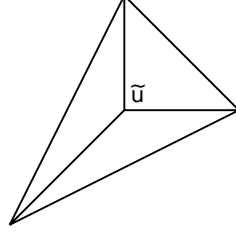


Figure 4.3: Toric diagram of local $\mathcal{O}(-3) \rightarrow \mathbb{P}^2$.

$$\begin{array}{c} D_u \\ D_1 \\ D_2 \\ D_3 \end{array} \left| \begin{array}{ccc} \nu_i & & l^{(1)} \\ 1 & 0 & 0 \\ 1 & 1 & 0 \\ 1 & 0 & 1 \\ 1 & -1 & -1 \end{array} \right| \begin{array}{c} -3 \\ 1 \\ 1 \\ 1 \end{array} . \quad (4.4.51)$$

The toric diagram of local \mathbb{P}^2 is given in fig. (4.3). By use of the toric data given in eq. (4.4.51) we find

$$z = \frac{1}{\tilde{u}^3}. \quad (4.4.52)$$

By defining $u = \frac{1}{\tilde{u}^3}$ we find for the quantum mirror curve

$$-1 + e^x + e^p + ue^{\hbar/2}e^{-x}e^{-p} = 0. \quad (4.4.53)$$

The corresponding Schrödinger equation reads

$$(-1 + e^x)\psi(x) + \psi(x + \hbar) + ue^{\hbar/2}e^{-x}\psi(x - \hbar) = 0. \quad (4.4.54)$$

Because we are not able to compute the full B-periods by only considering the patch given by this parameterization, we have to use a second one, given by

$$-1 + ue^{-x} + e^{-p} + e^{\hbar/2}e^xe^p = 0. \quad (4.4.55)$$

Therefore it is more convenient to use the operator approach in this case. In [95] operators have been derived which enable us to write higher order corrections to the periods in terms of the zero order period. For local \mathbb{P}^2 up to order four these are

$$\mathcal{D}_2 = \frac{\Theta_u^2}{8} \quad (4.4.56a)$$

$$\mathcal{D}_4 = \frac{2u(999u - 5)\Theta_u + 3u(2619u - 29)\Theta_u^2}{640\Delta^2} \quad (4.4.56b)$$

where $\Delta = 1 + 27u$. The data for the elliptic curve is

$$g_2 = 27u^4 (24u^3 + 1) \quad (4.4.57a)$$

$$g_3 = 27u^6 (216u^6 + 36u^3 + 1) \quad (4.4.57b)$$

and from this together with the operators the A -period

$$a = \log(u) - 2u^3 + 15u^6 - \frac{560u^9}{3} + \hbar^2 \left(-\frac{u^3}{4} + \frac{15u^6}{2} - 210u^9 \right) + \mathcal{O}(\hbar^4, u^{12}) \quad (4.4.58a)$$

and the B -period

$$a_D = -9 \left(\frac{1}{2} \log^2 u + \log(u)a - u^3 + \frac{47u^6}{4} - \frac{1486u^9}{9} \right) + \mathcal{O}(\hbar^2, u^{12}) \quad (4.4.58b)$$

follow. Having found these, we can easily integrate the special geometry relations to yield

$$\mathcal{W}^{(0)} = 3Q - \frac{45}{8}Q^2 + \frac{244}{9}Q^3 - \frac{12\,333}{64}Q^4 + \frac{211\,878}{125}Q^5 + \mathcal{O}(Q^6) \quad (4.4.59a)$$

$$\mathcal{W}^{(1)} = -\frac{7}{8}Q + \frac{129}{16}Q^2 - \frac{589}{6}Q^3 + \frac{43\,009}{32}Q^4 - \frac{392\,691}{20}Q^5 + \mathcal{O}(Q^6) \quad (4.4.59b)$$

$$\mathcal{W}^{(2)} = \frac{29Q}{640} - \frac{207Q^2}{64} + \frac{18447Q^3}{160} - \frac{526859Q^4}{160} + \frac{5385429Q^5}{64} + \mathcal{O}(Q^6). \quad (4.4.59c)$$

4.4.3.1 Orbifold point

The orbifold point is given by the change of coordinates $\psi = -\frac{1}{3u^{1/3}}$, which changes the logarithmic derivative of the large radius coordinate as

$$\Theta_u \rightarrow -\frac{1}{3}\psi\partial_\psi = -\frac{1}{3}\Theta_\psi. \quad (4.4.60)$$

According to [40] the classical part of the periods at this point can be written as

$$\Pi_{\text{orb}} = \begin{pmatrix} \sigma_D \\ \sigma \\ 1 \end{pmatrix} = \begin{pmatrix} -3\partial_\sigma F_0^{\text{orb}} \\ \sigma \\ 1 \end{pmatrix} = \begin{pmatrix} B_2 \\ B_1 \\ 1 \end{pmatrix} \quad (4.4.61)$$

where

$$B_k = (-1)^{\frac{k}{3}+k+1} \frac{(3\psi)^k}{k} \sum_{n=0}^{\infty} \frac{\left[\frac{k}{3}\right]_n^3}{\prod_{i=1}^3 \left[\frac{k+i}{3}\right]_n} \psi^{3n}. \quad (4.4.62)$$

Here $[a]_n = a(a+1)\dots(a+n+1)$ is the Pochhammer symbol. Knowing the operators (4.4.56b) and (4.4.62), computing the periods σ and σ_D to higher orders is very easy. We only have to change the coordinates of the operators to ψ and apply them to (4.4.62).

C.3.1 The quantum periods are defined by the expansion

$$t = \sigma = \sum_i \hbar^{2i} \sigma^{2i} \quad \text{and} \quad \sigma_D = \sum_i \hbar^{2i} \sigma_D^{2i}. \quad (4.4.63)$$

The first few orders can be found in (C.3.6) for the A -period and in (C.3.7) for the B -period. Inverting $t(\psi)$ and plugging it into a_D gives us

$$\sigma_D = \frac{\partial F_{\text{orb}}^{\text{NS}}}{\partial \sigma} \quad (4.4.64)$$

By integrating this with respect to σ , we finally find the free energies

$$F^{(0,0)} = c_0 + \frac{1}{18}t^3 - \frac{1}{19440}t^6 + \frac{1}{3265920}t^9 - \frac{1093}{349192166400}t^{12} + \frac{119401}{2859883842816000}t^{15} \quad (4.4.65a)$$

$$F^{(1,0)} = c_1 + \frac{1}{648}t^3 - \frac{1}{46656}t^6 + \frac{1319}{3174474240}t^9 - \frac{10453}{1142810726400}t^{12} + \frac{2662883}{12354698200965120}t^{15} \quad (4.4.65b)$$

$$F^{(2,0)} = c_2 + \frac{1}{6480}t^3 - \frac{79}{8398080}t^6 + \frac{29}{65318400}t^9 - \frac{423341}{22856214528000}t^{12} + \frac{1332163447}{1853204730144768000}t^{15}. \quad (4.4.65c)$$

Checking this against the results found in [101], we find an exact agreement up to the constants of integration.

4.4.3.2 Conifold point

In order to find the free energies at the conifold, we have to solve the Picard-Fuchs system at small Δ , which is defined in terms of the large radius variable by

$$u = \frac{\Delta - 1}{27}, \quad (4.4.66)$$

which changes the logarithmic derivative to

$$\theta_u \rightarrow \theta_\Delta = (\Delta - 1)\partial_\Delta. \quad (4.4.67)$$

The quantum corrections will be computed by making a coordinate transformation to Δ in (4.4.56b).

$$\Pi = \begin{pmatrix} at_c \\ 3at_{cD} \\ 1 \end{pmatrix}, \quad \text{where } a = -\frac{\sqrt{3}}{2\pi}. \quad (4.4.68)$$

The flat coordinates with quantum corrections are given in terms of Δ by equations (C.3.8) in appendix C.3.2. Plugging this into the B -periods given in (C.3.9) and integrating, we finally

arrive at the free energies

$$F^{(0,0)} = c_0 + \frac{a_0 t_c}{3} + t_c^2 \left(\frac{a_1}{6} + \frac{\log(t_c)}{6} - \frac{1}{12} \right) - \frac{t_c^3}{324} + \frac{t_c^4}{69984} + \frac{7t_c^5}{2361960} - \frac{529t_c^6}{1700611200} + \mathcal{O}(t_c^7) \quad (4.4.69a)$$

$$F^{(1,0)} = c_1 + \frac{\log(t_c)}{24} + \frac{7t_c}{432} - \frac{131t_c^2}{46656} - \frac{19t_c^3}{314928} + \frac{439t_c^4}{50388480} - \frac{1153t_c^5}{1530550080} + \mathcal{O}(t_c^6) \quad (4.4.69b)$$

$$F^{(2,0)} = -\frac{7}{1920t_c^2} + c_2 + \frac{1169t_c}{12597120} - \frac{7367t_c^2}{335923200} + \frac{16153t_c^3}{6122200320} + \frac{7729t_c^4}{881596846080} + \mathcal{O}(t_c^5) \quad (4.4.69c)$$

where

$$a_0 = -\frac{\pi}{3} - 1.678699904i = \frac{1}{i\sqrt{3}\Gamma\left(\frac{1}{3}\right)\Gamma\left(\frac{2}{3}\right)} G_{22}^{33} \left(\begin{matrix} \frac{1}{3} & \frac{2}{3} & 1 \\ 0 & 0 & 0 \end{matrix} \middle| -1 \right) \quad \text{and} \quad a_1 = \frac{3\log(3) + 1}{2\pi i}. \quad (4.4.70)$$

This again matches the results given in [101] up to misprints and constants of integration.

4.4.4 local \mathbb{F}_1

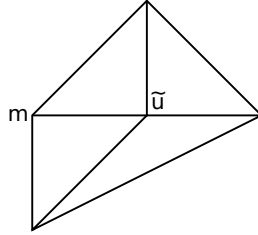


Figure 4.4: Toric diagram of local \mathbb{F}_1 .

$$\begin{array}{c} \nu_i \\ D_u \\ D_1 \\ D_2 \\ D_3 \\ D_4 \end{array} \left| \begin{array}{ccc} 1 & 0 & 0 \\ 1 & 1 & 0 \\ 1 & 0 & 1 \\ 1 & -1 & 0 \\ 1 & -1 & -1 \end{array} \right| \begin{array}{cc} l^{(1)} = l^{(f)} & l^{(2)} = l^{(b)} \\ -2 & -1 \\ 1 & 0 \\ 0 & 1 \\ 1 & -1 \\ 0 & 1 \end{array} \Bigg| \cdot \quad (4.4.71)$$

The toric data of eq. (4.4.71) together with the definition of the trivial m parameter in fig. (4.4) leads to the Batyrev coordinates

$$z_1 = \frac{m}{\tilde{u}^2}, \quad z_2 = \frac{1}{m\tilde{u}}. \quad (4.4.72)$$

We define $\tilde{u} = \frac{1}{u}$ and get for the quantum mirror curve

$$H(x, p) = -1 + e^x + mu^2 e^{-x} + e^p + e^{-\hbar/2} \frac{u}{m} e^x e^{-p}. \quad (4.4.73)$$

The coefficients of the classical Weierstrass normal form are

$$g_2(u, m) = 27u^4(1 - 8mu^2 + 24u^3 + 16m^2u^4), \quad (4.4.74a)$$

$$g_3(u, m) = 27u^6(1 - 12mu^2 + 36u^3 + 48m^2u^4 - 144mu^5 + 216u^6 - 64m^3u^6). \quad (4.4.74b)$$

4.4.4.1 Operator approach

The curve (4.4.73) has the following solution at zeroth order

$$S'_0(x) = \log \left(\frac{1}{2} e^{-x} \left(e^x - e^{2x} - z_1 - \sqrt{(-e^x + e^{2x} + z_1)^2 + 4e^{3x}z_2} \right) \right). \quad (4.4.75)$$

Further solutions can be found in appendix C.4.

By partially integrating we find for the first operator

$$\mathcal{D}_2 = \frac{mu^2(4m - 9u)}{6\delta} \Theta_u + \frac{4m - 3u - 16m^2u^2 + 36u^3m}{24\delta} \Theta_u^2, \quad (4.4.76)$$

with $\delta = (-8m + 9u)$. Higher order operators can as well be found in appendix C.4. Calculation of the nontrivial quantum periods leads to

$$a = \log(u) + mu^2 - 2u^3 - \frac{1}{4}u^3\hbar^2 + \mathcal{O}(\hbar^4, u^4), \quad (4.4.77a)$$

$$\begin{aligned} a_D = & -4 \log(u)^2 - \log(u) \log(m) - \log(u^8 m) \left(mu^2 - 2u^3 - \frac{1}{4}u^3\hbar^2 \right) + \frac{u}{m} + u^2 \left(\frac{1}{4m^2} - 4m \right) \\ & + 10u^3 + \frac{1}{9m^3}u^3 - \frac{1}{24}\hbar^2 \left(4 + \frac{u}{m} + u^2 \left(\frac{1}{m^2} + 8m \right) + u^3 \left(\frac{1}{m^3} - 62 \right) \right) + \mathcal{O}(\hbar^4, u^4). \end{aligned} \quad (4.4.77b)$$

With the nontrivial A-period we find for the mirror map

$$u(Q_u) = Q_u - mQ_u^3 + 2Q_u^4 + \frac{1}{4}Q_u^4\hbar^2 + \mathcal{O}(\hbar^4, Q_u^5). \quad (4.4.78)$$

The nontrivial coordinate Q_u and the trivial parameter m can be translated back to the usual description via two logarithmic solutions of the Picard-Fuchs equations. The connection is given by

$$Q_u = Q_1^{1/3} Q_2^{1/3}, \quad m = Q_1^{1/3} Q_2^{-2/3}. \quad (4.4.79)$$

These relations can be checked perturbatively. Using these relations after integrating the special geometry relation we find the instanton numbers in the Nekrasov–Shatashvili limit listed in the tables 4.5, 4.6, 4.7 and 4.8.

4.4.4.2 Difference equation

Another way to handle this problem would be to extract the relevant data directly from the integrals over the quantum differentials. For the A-periods this is quite straightforward and the non-logarithmic part is just given by the residues of the expansion around the large radius coordinates. The computation of the B-periods though is not as straightforward. We have to change the parameterization of the curve in order to find all contributions. Unfortunately we are not certain about the way to systematically find these parameterizations. The following

	d_1	0	1	2	3	4
d_2						
0			1			
1		-2	3			
2			5	-6		
3			7	-32	27	
4			9	-110	286	-192

Table 4.5: The instanton numbers for local \mathbb{F}_1 at order \hbar^0 .

	d_1	0	1	2	3	4
d_2						
0						
1		-1	4			
2			20	-35		
3			56	-368	396	
4			120	-2055	6732	-5392

Table 4.6: The instanton numbers for local \mathbb{F}_1 at order \hbar^2 .

	d_1	0	1	2	3	4
d_2						
0						
1			1			
2			21	-56		
3			126	-1352	1875	
4			462	-12892	55363	-53028

Table 4.7: The instanton numbers for local \mathbb{F}_1 at order \hbar^4 .

	d_1	0	1	2	3	4
d_2						
0						
1						
2			8	-36		
3			120	-2412	4344	
4			792	-41594	242264	-277430

Table 4.8: The instanton numbers for local \mathbb{F}_1 at order \hbar^6 .

curves yield all the parts needed for getting the correct B-period, at least for zeroth order in \hbar .

$$\begin{aligned}
 \mathcal{A} &: -1 + e^p + e^x + u^2 m e^{-x} - e^{\hbar/2} u^3 e^{-p-x} \\
 \mathcal{B} &: -1 + e^p + e^x + u^2 m e^{-p} - e^{\hbar/2} u^3 e^{-p-x} \\
 \mathcal{C} &: -1 + e^p + e^x + u^2 m e^{-x} - e^{-\hbar/2} \frac{u}{m} e^{-p+x}.
 \end{aligned} \tag{4.4.80}$$

The A-period is

$$a = \log(u) + mu^2 - \left(\sqrt{q} + \frac{1}{\sqrt{q}} \right) u^3 + \frac{3m^2 u^4}{2} + \mathcal{O}(u^5) \quad (4.4.81a)$$

while the B-period, after summing up the contributions from \mathcal{A} , \mathcal{B} and \mathcal{C} is given by

$$a_D = -\log(u) \log(mu^4) - \log(mu^8) \tilde{a} + \tilde{a}_D \quad (4.4.81b)$$

where

$$\begin{aligned} \tilde{a}_D = & \frac{\sqrt{q}u \log(q)}{m(q-1)} + \frac{u^2 (q - 4m^3(q+1)^2) \log(q)}{2m^2(q^2-1)} \\ & + \frac{u^3 (6m^3(2q^4 + 3q^3 + 5q^2 + 3q + 2) + q^2) \log(q)}{3m^3 \sqrt{q}(q^3-1)} + \mathcal{O}(u^4) \end{aligned} \quad (4.4.82)$$

which can be pieced together from the contributions of the different parameterizations like

$$\tilde{a}_D = -3I_{\mathcal{A}} - 4I_{\mathcal{B}} - I_{\mathcal{C}} \quad (4.4.83)$$

after symmetrization with respect to $\hbar \rightarrow -\hbar$, in order to get rid of the odd sector in \hbar .

By integrating the B-period with respect to Q_t we finally find the free energy

$$\mathcal{W} = \frac{((q+1)Q_1 - \sqrt{q}Q_2)}{1-q} + \frac{(q^2+1)Q_1^2 - qQ_2^2}{4(1-q^2)} - \frac{(4q^2+q+4)Q_1Q_2}{3(1-q)\sqrt{q}} + \mathcal{O}(Q_i^3). \quad (4.4.84)$$

4.4.5 $\mathcal{O}(-K_{\mathbb{F}_2}) \rightarrow \mathbb{F}_2$

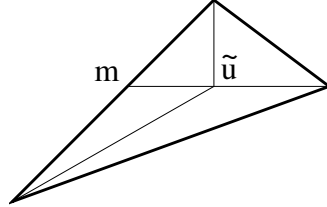


Figure 4.5: Toric diagram of $\mathcal{O}(-K_{\mathbb{F}_2}) \rightarrow \mathbb{F}_2$.

$$\begin{array}{c|ccc|cc} & \nu_i & & l^{(1)} = l^{(f)} & l^{(2)} = l^{(b)} & \\ \hline D_u & 1 & 0 & 0 & -2 & 0 \\ D_1 & 1 & 1 & 0 & 1 & 0 \\ D_2 & 1 & 0 & 1 & 0 & 1 \\ D_5 & 1 & -1 & 0 & 1 & -2 \\ D_6 & 1 & -2 & -1 & 0 & 1 \end{array} \quad (4.4.85)$$

This geometry is denoted in [96] as polyhedron 4. The toric diagram is depicted fig. (4.5). The toric data is given in eq. (4.4.85). With the toric data we find for the moduli

$$z_1 = \frac{m}{\tilde{u}^2}, \quad z_2 = \frac{1}{m^2}. \quad (4.4.86)$$

With the definition $\tilde{u}^2 = \frac{1}{u}$ we find that the elliptic mirror curve does not have any quantum corrections and looks like

$$H = 1 + e^x + e^p + mu e^{2x} + \frac{1}{m^2} e^{-p}. \quad (4.4.87)$$

The coefficients of the classical Weierstrass normal form are

$$g_2(u, m) = 27u^4 \left((1 - 4mu)^2 - 48u^2 \right), \quad (4.4.88a)$$

$$g_3(u, m) = -27u^6 \left(64m^3u^3 - 48m^2u^2 - 288mu^3 + 12mu + 72u^2 - 1 \right). \quad (4.4.88b)$$

The zeroth order solution to the resulting Schrödinger equation is

$$S'_0(x) = \log \left(\frac{1}{2} \left(-1 - e^x - e^{2x} mu - \sqrt{(1 + e^x + e^{2x} mu^2)^2 - \frac{4}{m^2}} \right) \right). \quad (4.4.89)$$

Some higher order WKB functions can be found in appendix C.5.

Partially integrating the WKB functions we find for operators mapping the zeroth order periods to higher periods

$$\mathcal{D}_2 = -\frac{1}{6}(mu)\Theta_u + \frac{1}{12}(1 - 4mu)\Theta_u^2, \quad (4.4.90a)$$

$$\begin{aligned} \mathcal{D}_4 = & \frac{u^2}{180\Delta^2} \left(-4m \left(3m^2 + 28 \right) u + m^2 - 64m \left(m^4 - 92m^2 + 352 \right) u^3 \right. \\ & \left. + 16 \left(3m^4 - 94m^2 + 552 \right) u^2 + 30 \right) \Theta_u \\ & + \frac{u}{360\Delta^2} \left(-96m \left(m^2 + 5 \right) u^2 + 4 \left(4m^2 + 61 \right) u - 256m \left(m^4 - 92m^2 + 352 \right) u^4 \right. \\ & \left. + 64 \left(4m^4 - 123m^2 + 652 \right) u^3 - m \right) \Theta_u^2. \end{aligned} \quad (4.4.90b)$$

where

$$\Delta = 16m^2u^2 - 8mu - 64u^2 + 1. \quad (4.4.91)$$

Higher order operators can as well be found in the appendix C.5.

This geometry has a particularly interesting property, namely that one can calculate more than one A-period by taking the residue at another point. This allows an additional check of the operators.

Proceeding with the calculation of the nontrivial periods leads to

$$a = \log(u) + mu^2 - 2mu^3 + \frac{1}{6}mu^2\hbar^2 - \frac{3}{2}mu^3\hbar^2 + \mathcal{O}(\hbar^4, u^4), \quad (4.4.92a)$$

$$\begin{aligned} a_D = & -\frac{5}{2}\log(u)^2 + \log(u) \left(-5mu^2 + 10mu^3 - \frac{5}{6}mu^2\hbar^2 + \frac{15}{2}mu^3\hbar^2 \right) + u + \frac{u^2}{4} - 4mu^2 + \frac{4}{9}u^3 \\ & + 9mu^3 + \frac{1}{3}m^3u^3 + \left(-\frac{5}{12} + \frac{u}{12} + \frac{u^2}{12} - \frac{4}{3}mu^2 + \frac{1}{3}u^3 + \frac{45}{4}mu^3 + \frac{1}{4}m^3u^3 \right) \hbar^2 + \mathcal{O}(\hbar^4, u^4). \end{aligned} \quad (4.4.92b)$$

After exponentiating the A-period we find for the mirror map

$$u(Q_u) = Q_u - mQ_u^3 - 3Q_u^5 + m^2Q_u^5 - \hbar^2Q_u^5 - \frac{1}{12}\hbar^4Q_u^5 + \mathcal{O}(\hbar^6, Q_u^6). \quad (4.4.93)$$

In the following we use the relation

$$\frac{1 + Q_2}{\sqrt{Q_2}} = \frac{1}{\sqrt{z_2}} = m, \quad (4.4.94)$$

which does not get any quantum corrections and is thus like a trivial period. Additionally we use $Q_u = Q_1^{1/2}Q_2^{1/4}$ to find after integrating the special geometry relation the instanton numbers listed in the tables 4.9, 4.10, 4.11 and 4.12.

Notice that we see at least a discrepancy in the contribution $\hat{n}_n^{0,1} = 1$ when comparing this to results from the (refined) topological vertex. Something along those lines has also been mentioned in [106].

	d_1	0	1	2	3	4
d_2						
0						
1			2	2		
2				4		
3				6	6	
4				8	32	8

Table 4.9: The instanton numbers for local \mathbb{F}_2 at order \hbar^0 .

	d_1	0	1	2	3	4
d_2						
0						
1			1	1		
2				10		
3				35	35	
4				84	368	84

Table 4.10: The instanton numbers for local \mathbb{F}_2 at order \hbar^2 .

	d_1	0	1	2	3	4
d_2						
0						
1						
2			6			
3			56	56		
4			252	1352	252	

Table 4.11: The instanton numbers for local \mathbb{F}_2 at order \hbar^4 .

	d_1	0	1	2	3	4
d_2						
0						
1						
2			1			
3			36	36		
4			330	2412	330	

Table 4.12: The instanton numbers for local \mathbb{F}_2 at order \hbar^6 .

4.4.6 $\mathcal{O}(-K_{\mathcal{B}_2}) \rightarrow \mathcal{B}_2$

The toric diagram of this geometry is given in fig. (4.6). Its toric data is given in eq. (4.4.95).

$$\begin{array}{c}
 \nu_i \\
 D_u \\
 D_1 \\
 D_2 \\
 D_3 \\
 D_4 \\
 D_5
 \end{array}
 \left|
 \begin{array}{ccc}
 1 & 0 & 0 \\
 1 & 1 & 0 \\
 1 & 1 & 1 \\
 1 & 0 & 1 \\
 1 & -1 & 0 \\
 1 & 0 & -1
 \end{array}
 \right|
 \begin{array}{ccc}
 l^{(1)} & l^{(2)} & l^{(3)} \\
 -1 & -1 & -1 \\
 -1 & 1 & 0 \\
 1 & -1 & 1 \\
 0 & 1 & -1 \\
 0 & 0 & 1 \\
 1 & 0 & 0
 \end{array}
 \right. . \tag{4.4.95}$$

With the toric data we find for the moduli

$$z_1 = \frac{1}{\tilde{u}m_2}, \quad z_2 = \frac{m_1m_2}{\tilde{u}}, \quad z_3 = \frac{1}{\tilde{u}m_1}. \tag{4.4.96}$$

For the quantum mirror curve for the \mathcal{B}_2 geometry we have with $\tilde{u} = \frac{1}{u}$

$$H = 1 + e^x + e^p + \frac{u}{m_2} e^{-\frac{\hbar}{2}+x-p} + um_1m_2 e^{-\frac{\hbar}{2}+p-x} + m_2u^2 e^{-x}. \tag{4.4.97}$$

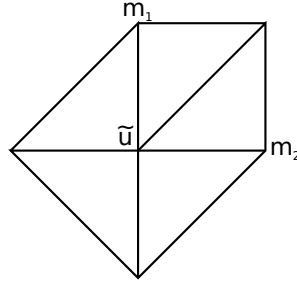


Figure 4.6: Toric diagram of $\mathcal{O}(-K_{\mathcal{B}_2}) \rightarrow \mathcal{B}_2$ with the assigned mass parameters and the modulus \tilde{u} .

The coefficients of the Weierstrass normal form are given by

$$g_2 = 27u^4 \left((16m_1^2 - 16m_2m_1 + 16m_2^2)u^4 + 24u^3 - (8m_1 + 8m_2)u^2 + 1 \right), \quad (4.4.98a)$$

$$g_3 = 27u^6 \left(1 - (12m_1 + 12m_2)u^2 + 36u^3 + (48m_1^2 + 24m_2m_1 + 48m_2^2)u^4 - (144m_1 + 144m_2)u^5 + (-64m_1^3 + 96m_2m_1^2 + 96m_2^2m_1 - 64m_2^3 + 216)u^6 \right). \quad (4.4.98b)$$

The zeroth order solution to the resulting Schrödinger equation is

$$S'_0(x) = \log \left(-\frac{e^x + e^{2x} + u^2m_2 + \sqrt{-4e^{2x}\frac{u}{m_2}(e^x + um_1m_2) + (e^x + e^{2x} + u^2m_2)^2}}{2(e^x + um_1m_2)} \right). \quad (4.4.99)$$

Due to an additional pole in the higher order WKB functions stemming from the non-quadratic term in the root this case and the following are considerably more complicated than the geometries \mathbb{F}_0 , \mathbb{F}_1 and \mathbb{F}_2 . Nonetheless one finds the operator

$$\begin{aligned} \mathcal{D}_2 = & -\frac{1}{6\delta} \left(u^2(m_2(4m_2 - 9u)u + 4m_1^3m_2u(m_2 + u) + m_1^2(-5m_2 + 4u + 4m_2^3u - 16m_2^2u^2) \right. \\ & \left. + m_1(-5m_2^2 + 20m_2u - 9u^2 + 4m_2^3u^2)) \right) \Theta_u \\ & + \frac{1}{24\delta} \left(-16m_1^3m_2u^3(m_2 + u) + u(-3u - 16m_2^2u^2 + 4m_2(1 + 9u^3)) + 4m_1^2u(6m_2u - 4u^2 \right. \\ & \left. - 4m_2^3u^2 + m_2^2(1 + 16u^3)) + m_1(24m_2^2u^2 - 16m_2^3u^4 - m_2(5 + 92u^3) + 4(u + 9u^4)) \right) \Theta_u^2, \end{aligned} \quad (4.4.100)$$

with $\delta = ((8m_2 - 9u)u + 4m_1^2m_2(2m_2 - u)u + m_1(-7m_2 + 8u - 4m_2^2u^2))$. Notice that this operator simplifies to the operator, that maps the classical periods of local \mathbb{F}_1 (section 4.4.4) to the second order, if we take the limit $m_1 \rightarrow 0$ or $m_2 \rightarrow 0$, as we would expect from (4.4.95). So we indeed find the correct amplitude when blowing down and passed this consistency check successfully.

Calculation of the nontrivial quantum periods leads to

$$a = \log(u) + m_1 u^2 + m_2 u^2 - 2u^3 - \frac{u^3}{4} \hbar^2 + \mathcal{O}(\hbar^4, u^4), \quad (4.4.101a)$$

$$\begin{aligned} a_D = & -\frac{7}{2} \log(u)^2 - \log(-m_1 m_2) \log(u) + \frac{u}{m_1} + \frac{u}{m_2} + m_1 m_2 u \\ & - \frac{1}{24} \left(5 + \frac{u}{m_1} + \frac{u}{m_2} + m_1 m_2 u \right) \hbar^2 + \mathcal{O}(\hbar^4, u^2). \end{aligned} \quad (4.4.101b)$$

Using this we find for the mirror map

$$u(Q_u) = Q_u - (m_1 + m_2) Q_u^3 + 2Q_u^4 + m_1^2 Q_u^5 - m_1 m_2 Q_u^5 + m_2^2 Q_u^5 + \left(\frac{1}{4} Q_u^4 - m_1 m_2 Q_u^5 \right) \hbar^2 + \mathcal{O}(\hbar^4, Q_u^6). \quad (4.4.102)$$

Since here we do not have any points sitting on an edge we can invert the relations between z and u, m_i and find for u, m_i in dependence of the coordinates Q_i

$$u = Q_1^{1/3} Q_2^{1/3} Q_3^{1/3}, \quad m_1 = Q_1^{1/3} Q_2^{1/3} Q_3^{-2/3}, \quad m_2 = Q_1^{-2/3} Q_2^{1/3} Q_3^{1/3}. \quad (4.4.103)$$

After integrating the special geometry relation and plugging this in we find the following free energy

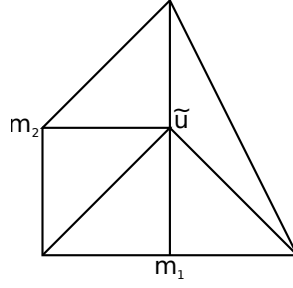
$$\begin{aligned} F^{(0,0)} = & (Q_1 + Q_2 + Q_3) + \left(\frac{Q_1^2}{8} - 2Q_1 Q_2 + \frac{Q_2^2}{8} - 2Q_2 Q_3 + \frac{Q_3^2}{8} \right) \\ & + \left(\frac{Q_1^3}{27} + \frac{Q_2^3}{27} + 3Q_1 Q_2 Q_3 + \frac{Q_3^3}{27} \right) + \left(\frac{Q_1^4}{64} - \frac{Q_1^2 Q_2^2}{4} + \frac{Q_2^4}{64} - 4Q_1 Q_2^2 Q_3 - \frac{Q_2^2 Q_3^2}{4} + \frac{Q_3^4}{64} \right) \\ & + \left(\frac{Q_1^5}{125} + \frac{Q_2^5}{125} + 5Q_1^2 Q_2^2 Q_3 + 5Q_1 Q_2^2 Q_3^2 + \frac{Q_3^5}{125} \right) + \mathcal{O}(Q^6), \end{aligned} \quad (4.4.104a)$$

$$\begin{aligned} F^{(1,0)} = & \left(-\frac{Q_1}{24} - \frac{Q_2}{24} - \frac{Q_3}{24} \right) + \left(-\frac{Q_1^2}{48} - \frac{Q_1 Q_2}{6} - \frac{Q_2^2}{48} - \frac{Q_2 Q_3}{6} - \frac{Q_3^2}{48} \right) \\ & + \left(-\frac{Q_1^3}{72} - \frac{Q_2^3}{72} + \frac{7Q_1 Q_2 Q_3}{8} - \frac{Q_3^3}{72} \right) + \left(-\frac{Q_1^4}{96} - \frac{Q_1^2 Q_2^2}{12} - \frac{Q_2^4}{96} - \frac{7Q_1 Q_2^2 Q_3}{3} - \frac{Q_2^2 Q_3^2}{12} - \frac{Q_3^4}{96} \right) \\ & + \left(-\frac{Q_1^5}{120} - \frac{Q_2^5}{120} + \frac{115Q_1^2 Q_2^2 Q_3}{24} + \frac{115Q_1 Q_2^2 Q_3^2}{24} - \frac{Q_3^5}{120} \right) + \mathcal{O}(Q^6). \end{aligned} \quad (4.4.104b)$$

4.4.7 local $\mathcal{B}_1(\mathbb{F}_2)$

$$\begin{array}{c|ccc|ccc} & \nu_i & & l^{(1)} & l^{(2)} & l^{(3)} \\ D_u & 1 & 0 & 0 & -1 & -1 & 0 \\ D_1 & 1 & 1 & -1 & 0 & 0 & 1 \\ D_2 & 1 & 0 & 1 & 1 & 0 & 0 \\ D_3 & 1 & -1 & 0 & -1 & 1 & 0 \\ D_4 & 1 & -1 & -1 & 1 & -1 & 1 \\ D_5 & 1 & 0 & -1 & 0 & 1 & -2 \end{array}. \quad (4.4.105)$$

The toric data of this geometry can be found in eq. (4.4.105) and the toric diagram with the


 Figure 4.7: Toric diagram of $\mathcal{B}_1(\mathbb{F}_2)$ with the assigned masses.

used mass assignment is given in fig. (4.7). The toric data leads to the coordinates

$$z_1 = \frac{1}{\tilde{u}m_2}, \quad z_2 = \frac{m_1m_2}{\tilde{u}}, \quad z_3 = \frac{1}{m_1^2}. \quad (4.4.106)$$

By defining $u = \frac{1}{\tilde{u}}$ we find for the quantum curve

$$H = 1 + e^x + e^p + m_1u^2e^{2p} + \frac{m_2}{m_1}ue^{-\frac{\hbar}{2}+p-x} + \frac{1}{m_1^2}e^{-x}. \quad (4.4.107)$$

The coefficients of the Weierstrass normal form of this curve are given by

$$g_2(u) = 27u^4(1 - 8m_1u^2 + 24m_2u^3 - 48u^4 + 16m_1^2u^4), \quad (4.4.108a)$$

$$g_3(u) = 27u^6(1 - 12m_1u^2 + 36m_2u^3 - 72u^4 + 48m_1^2u^4 - 144m_1m_2u^5 + 288m_1u^6 - 64m_1^3u^6 + 216m_2^2u^6). \quad (4.4.108b)$$

By solving the Schrödinger equation resulting from the quantum curve perturbatively in \hbar we find for the zeroth order WKB function which is equivalent to the classical differential

$$S'_0(x) = \log \left(\frac{-1 - e^{-x} \frac{m_2}{m_1} u - e^{-x} \sqrt{-4e^x m_1 u^2 (e^x + e^{2x} + \frac{1}{m_1^2}) + (e^x + \frac{m_2}{m_1} u)^2}}{2m_1 u^2} \right). \quad (4.4.109)$$

For the operator mapping the zeroth order periods to the second order periods we find

$$\begin{aligned} \mathcal{D}_2 = & \frac{u^2(4m_1^2m_2u(-m_2 + u) - 12m_2u(m_2 + 2u) - m_1(5m_2 + 4u + 9m_2^3u^2))}{6\delta} \Theta_u \\ & + \frac{1}{24\delta} \left(4u - 16m_1u^3 - 4m_2^2(-m_1u + 15u^3 + 4m_1^2u^3) + m_2^3(3u^2 - 36m_1u^4) \right. \\ & \left. + m_2(5 - 24m_1u^2 - 96u^4 + 16m_1^2u^4) \right) \Theta_u^2, \end{aligned} \quad (4.4.110)$$

with $\delta = (8u + 8m_1m_2^2u + 9m_2^3u^2 + m_2(7 + 4m_1u^2))$. The three logarithmic solutions of the Picard-Fuchs equations yield only one nontrivial period. This can be seen by combining them

in the following way

$$Q_u = Q_1^{\frac{1}{2}} Q_2^{\frac{1}{2}} Q_3^{\frac{1}{4}}, \quad (4.4.111)$$

$$m_1 = \frac{1 + Q_3}{\sqrt{Q_3}}, \quad (4.4.112)$$

$$m_2 = Q_1^{-\frac{1}{2}} Q_2^{\frac{1}{2}} Q_3^{\frac{1}{4}} \quad (4.4.113)$$

where m_1 is not just given by a simple linear combination of the periods. Using the operator we find for the nontrivial periods in the NS limit

$$\begin{aligned} a &= \log(u) + m_1 u^2 + \left(-2m_2 - \frac{m_2 \hbar^2}{4}\right) u^3 + \left(3 + \frac{3}{2} m_1^2 + \hbar^2\right) u^4 \\ &\quad + \left(-12m_1 m_2 - \frac{7}{2} m_1 m_2 \hbar^2\right) u^5 + \mathcal{O}(\hbar^4, u^6), \end{aligned} \quad (4.4.114a)$$

$$\begin{aligned} a_D &= -\frac{7}{2} \log(u)^2 - \log(-m_2) \log(u) - m_1 u^2 \log(-m_2 u^7) \\ &\quad + \frac{u}{m_2} + m_1 m_2 u - u^2 \left(4m_1 - \frac{1}{4m_2^2} + \frac{m_2^2}{2} - \frac{m_1^2 m_2^2}{4}\right) \\ &\quad - \frac{1}{12} \hbar^2 \left(5 + \frac{u}{m_2} + m_1 m_2 u + 8m_1 u^2 + \frac{u^2}{m_2^2} - 2m_2^2 u^2 + m_1^2 m_2^2 u^2\right) + \mathcal{O}(\hbar^4, u^3). \end{aligned} \quad (4.4.114b)$$

Exponentiating the nontrivial A-period we find for the mirror map

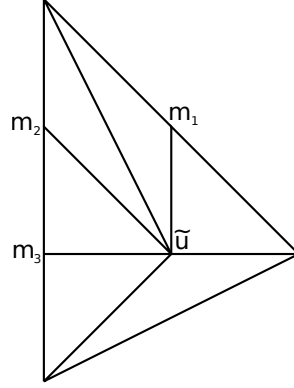
$$u(Q_u) = Q_u - m_1 Q_u^3 + (2m_2 + \frac{m_2}{4} \hbar^2) Q_u^4 + (-3 + m_1^2 - \hbar^2) Q_u^5 + 2m_1 m_2 \hbar^2 Q_u^6 + \mathcal{O}(\hbar^4, Q_u^7). \quad (4.4.115)$$

Plugging this into the B-period we can integrate the special geometry relation. After inserting the relations eq. (4.4.111) we get for the free energy

$$\begin{aligned} F^{(0,0)} &= (Q_1 + Q_2) + \left(\frac{Q_1^2}{8} - 2Q_1 Q_2 + \frac{Q_2^2}{8} + Q_2 Q_3\right) + \left(\frac{Q_1^3}{27} + \frac{Q_2^3}{27} - 2Q_1 Q_2 Q_3\right) \\ &\quad + \left(\frac{Q_1^4}{64} - \frac{Q_1^2 Q_2^2}{4} + \frac{Q_2^4}{64} + 3Q_1 Q_2^2 Q_3 + \frac{Q_2^2 Q_3^2}{8}\right) + \left(\frac{Q_1^5}{125} + \frac{Q_2^5}{125} - 4Q_1^2 Q_2^2 Q_3\right), \end{aligned} \quad (4.4.116a)$$

$$\begin{aligned} F^{(1,0)} &= \left(-\frac{Q_1}{24} - \frac{Q_2}{24}\right) + \left(-\frac{Q_1^2}{48} - \frac{Q_1 Q_2}{6} - \frac{Q_2^2}{48} - \frac{Q_2 Q_3}{24}\right) + \left(-\frac{Q_1^3}{72} - \frac{Q_2^3}{72} - \frac{Q_1 Q_2 Q_3}{6}\right) \\ &\quad + \left(-\frac{Q_1^4}{96} - \frac{Q_1^2 Q_2^2}{12} - \frac{Q_2^4}{96} + \frac{7}{8} Q_1 Q_2^2 Q_3 - \frac{Q_2^2 Q_3^2}{48}\right) + \left(-\frac{Q_1^5}{120} - \frac{Q_2^5}{120} - \frac{7}{3} Q_1^2 Q_2^2 Q_3\right). \end{aligned} \quad (4.4.116b)$$

As for local \mathbb{F}_2 (section 4.4.5), we see a discrepancy with the computations in the A -model concerning the instanton number $\hat{n}_n^{0,0,1} = 1$

4.4.8 A mass deformation of the local E_8 del PezzoFigure 4.8: Toric diagram of the mass deformed local E_8 de Pezzo with the assigned masses.

$$\begin{array}{c}
 \nu_i \\
 D_u \\
 D_1 \\
 D_2 \\
 D_3 \\
 D_4 \\
 D_5 \\
 D_6
 \end{array}
 \left| \begin{array}{ccc|cccc}
 1 & 0 & 0 & 0 & -1 & 0 & 0 \\
 1 & 1 & 0 & 1 & 0 & 0 & 0 \\
 1 & 0 & 1 & -2 & 1 & 0 & 0 \\
 1 & -1 & 2 & 1 & -1 & 1 & 0 \\
 1 & -1 & 1 & 0 & 1 & -2 & 1 \\
 1 & -1 & 0 & 0 & 0 & 1 & -2 \\
 1 & -1 & -1 & 0 & 0 & 0 & 1
 \end{array} \right. \cdot \quad (4.4.117)$$

This geometry is denoted in [96] as polyhedron 10. The diagram can be found in fig (4.8). The toric data is given in eq. (4.4.117). With the toric data we find for the coordinates

$$z_1 = \frac{1}{m_1^2}, \quad z_2 = \frac{m_1 m_2}{\tilde{u}}, \quad z_3 = \frac{m_3}{m_2^2}, \quad z_4 = \frac{m_2}{m_3^2}. \quad (4.4.118)$$

Defining $u = \frac{1}{\tilde{u}}$ we find for the quantum mirror curve in the u and m coordinates

$$H = 1 + e^x + e^p + m_3 u^2 e^{2p} - \frac{m_1 m_3}{m_2} u e^{\frac{\hbar}{2} + p + x} + \frac{m_3}{m_2^2} e^{2x} + \frac{m_2}{m_3^2} e^{-x}. \quad (4.4.119)$$

The coefficients of the classical Weierstrass normal form are

$$g_2(u, m_1, m_2, m_3) = 27u^4(1 - 8m_3u^2 + 24m_1u^3 - 48m_2u^4 + 16m_3^2u^4), \quad (4.4.120a)$$

$$g_3(u, m_1, m_2, m_3) = 27u^6(1 - 12m_3u^2 + 36m_1u^3 - 72m_2u^4 + 48m_3^2u^4 - 144m_1m_3u^5 - 864u^6 + 216m_1^2u^6 + 288m_2m_3u^6 - 64m_3^3u^6). \quad (4.4.120b)$$

The resulting Schrödinger equation can be solved perturbatively in \hbar and gives for the zeroth

order WKB function

$$S'_0(x) = \log \left(\frac{-1 + e^x z_2 z_3 - e^{-x} \sqrt{e^x (e^x (-1 + e^x z_2 z_3))^2 - 4 z_1 z_2^2 z_3 (e^x + e^{2x} + e^{3x} z_3 + z_4)}}{2 z_1 z_2^2 z_3} \right). \quad (4.4.121)$$

The second order WKB function can be calculated by use of the following operator up to exact terms out of the zeroth order

$$\begin{aligned} \mathcal{D}_2 = & \frac{1}{6\delta} \left(u^2 \left(4m_3^2 u^2 (m_2 m_1 u + m_1^2 - 6) + m_3 \left(-9m_1 (m_1^2 - 4) u^3 + 4m_2^2 u^2 - 5m_1 m_2 u + 6 \right) \right. \right. \\ & \left. \left. + 6u (2m_1 m_2 u - 3) (m_1 - 2m_2 u) \right) \Theta_u \right. \\ & + \frac{1}{24\delta} \left(4m_1 \left(4m_2 (m_3^2 - 6m_2) - 9 (m_1^2 - 4) m_3 \right) u^5 + 4 \left(4m_3 m_2^2 + 3 (5m_1^2 + 12) m_2 + \right. \right. \\ & \left. \left. + 4 (m_1^2 - 6) m_3^2 \right) u^4 + 3m_1 \left(m_1^2 - 8m_2 m_3 - 36 \right) u^3 \right. \\ & \left. - 4 \left(m_2^2 + (m_1^2 - 12) m_3 \right) u^2 + 5m_1 m_2 u - 6 \right) \Theta_u^2 \end{aligned} \quad (4.4.122)$$

where

$$\delta = m_1 \left(9m_1^2 + 4m_2 m_3 - 36 \right) u^3 - 8 \left(m_2^2 + (m_1^2 - 3) m_3 \right) u^2 + 7m_1 m_2 u - 6. \quad (4.4.123)$$

With this we find for the quantum corrected nontrivial periods

$$\begin{aligned} a = & \log(u) + m_3 u^2 - 2m_1 u^3 + 3m_2 u^4 + \frac{3m_3^2 u^4}{2} \\ & + \left(-\frac{5m_1 u^3}{4} + m_2 u^4 + \frac{1}{2} m_1^2 m_2 u^4 \right) \hbar^2 + \mathcal{O}(\hbar^4, u^5), \end{aligned} \quad (4.4.124a)$$

$$\begin{aligned} a_D = & -3 \log(u)^2 - 6m_3 u^2 \log(u) + m_1 m_2 u - \frac{m_2^2 u^2}{2} + \frac{1}{4} m_1^2 m_2^2 u^2 - 3m_3 u^2 - \frac{1}{2} m_1^2 m_3 u^2 \\ & + \left(-\frac{1}{4} + \frac{m_1 m_2 u}{8} + \frac{m_2^2 u^2}{12} - \frac{5}{72} m_1^2 m_2^2 u^2 - \frac{m_3 u^2}{2} + \frac{1}{12} m_1^2 m_3 u^2 \right) \hbar^2 + \mathcal{O}(\hbar^4, u^3). \end{aligned} \quad (4.4.124b)$$

This leads to the following mirror map after exponentiating the nontrivial A-period

$$\begin{aligned} u(Q_u) = & Q_u - m_3 Q_u^3 + 2m_1 Q_u^4 - 3m_2 Q_u^5 + m_3^2 Q_u^5 + \frac{1}{12} (15m_1 Q_u^4 - 12m_2 Q_u^5 \\ & - 6m_1^2 m_2 Q_u^5 - 12m_1 m_2^2 Q_u^6 + 7m_1^3 m_2^2 Q_u^6 + 72m_1 m_3 Q_u^6 - 12m_1^3 m_3 Q_u^6) \hbar^2 + \mathcal{O}(\hbar^4, Q_u^7). \end{aligned} \quad (4.4.125)$$

Now we can integrate the special geometry relation and plug in the following relations between

the mass parameters and the coordinates

$$m_1 = \frac{1 + Q_1}{\sqrt{Q_1}}, \quad (4.4.126a)$$

$$m_2 = \frac{1 + Q_3 + Q_3 Q_4}{Q_3^{2/3} Q_4^{1/3}}, \quad (4.4.126b)$$

$$m_3 = \frac{1 + Q_4 + Q_3 Q_4}{Q_3^{1/3} Q_4^{2/3}}. \quad (4.4.126c)$$

These relations do not get any quantum corrections as was expected since the mass parameters m_i are trivial parameters. Using additionally $Q_t = Q_1^{\frac{1}{2}} Q_2 Q_3^{\frac{2}{3}} Q_4^{\frac{1}{3}}$ we find for the refined free energies in the Nekrasov-Shatashvili limit

$$\begin{aligned} \mathcal{W}_0 = & \text{Li}_3^{(0,1,0,0)} + \text{Li}_3^{(0,1,1,0)} + \text{Li}_3^{(0,1,1,1)} + \text{Li}_3^{(1,1,0,0)} + \text{Li}_3^{(1,1,1,0)} + \text{Li}_3^{(1,1,1,1)} - 2 \text{Li}_3^{(1,2,1,0)} \\ & - 2 \text{Li}_3^{(1,2,1,1)} - 2 \text{Li}_3^{(1,2,2,1)} + 3 \text{Li}_3^{(1,3,2,1)} + 3 \text{Li}_3^{(2,3,2,1)} - 4 \text{Li}_3^{(2,4,2,1)} - 4 \text{Li}_3^{(2,4,3,1)} \\ & - 4 \text{Li}_3^{(2,4,3,2)} + 5 \text{Li}_3^{(2,5,3,1)} + 5 \text{Li}_3^{(2,5,3,2)} + 5 \text{Li}_3^{(3,5,3,1)} \end{aligned} \quad (4.4.127a)$$

$$\begin{aligned} -24\mathcal{W}_1 = & \text{Li}_1^{(0,1,0,0)} + \text{Li}_1^{(0,1,1,0)} + \text{Li}_1^{(0,1,1,1)} + \text{Li}_1^{(1,1,0,0)} + \text{Li}_1^{(1,1,1,0)} + \text{Li}_1^{(1,1,1,1)} + 4 \text{Li}_1^{(1,2,1,0)} \\ & + 4 \text{Li}_1^{(1,2,1,1)} + 4 \text{Li}_1^{(1,2,2,1)} - 21 \text{Li}_1^{(1,3,2,1)} - 21 \text{Li}_1^{(2,3,2,1)} + 56 \text{Li}_1^{(2,4,2,1)} + 56 \text{Li}_1^{(2,4,3,1)} \\ & + 56 \text{Li}_1^{(2,4,3,2)} - 115 \text{Li}_1^{(2,5,3,1)} - 115 \text{Li}_1^{(2,5,3,2)} - 115 \text{Li}_1^{(3,5,3,1)}. \end{aligned} \quad (4.4.127b)$$

Here we defined $\text{Li}_n^{(\beta)} = \text{Li}_n(Q^\beta)$.

4.5 Relation to the Fermi Gas

The Fermi Gas can be interpreted as the *spectral problem*

$$\int_{-\infty}^{\infty} \rho(x_1, x_2) \phi(x_2) dx_2 = e^{-E} \phi(x_1) \quad (4.5.1)$$

with the kernel

$$\rho(x_1, x_2) = \frac{1}{2\pi k} \frac{1}{(2 \cosh \frac{x_1}{2})^{1/2}} \frac{1}{(2 \cosh \frac{x_2}{2})^{1/2}} \frac{1}{(2 \cosh \frac{x_1 - x_2}{2k})}. \quad (4.5.2)$$

which corresponds to the Fermi gas for ABJM theory as it was explained in [99]. The spectral problem (4.5.1) can be written as a difference equation. In order to show this let us first consider the operator $\hat{\rho}$, defined in [48] by

$$\langle x | \hat{\rho} | x' \rangle = \rho(x, x'). \quad (4.5.3)$$

We can write this operator as

$$\hat{\rho} = e^{-\frac{1}{2}U(\hat{q})} e^{-T(\hat{p})} e^{-\frac{1}{2}U(\hat{q})}, \quad (4.5.4)$$

where \hat{q}, \hat{p} are canonically conjugate operators:

$$[\hat{q}, \hat{p}] = i\hbar. \quad (4.5.5)$$

We repeat that here U and T are given by

$$U(q) = \log \left(2 \cosh \frac{q}{2} \right), \quad T(p) = \log \left(2 \cosh \frac{p}{2} \right) \quad (4.5.6)$$

as defined in (3.2.87a). The spectral problem can now be written as

$$\hat{\rho}|\phi\rangle = e^{-E}|\phi\rangle. \quad (4.5.7)$$

If we define

$$|\psi\rangle = e^{\frac{1}{2}U(\hat{q})}|\phi\rangle, \quad (4.5.8)$$

we can derive the relation

$$e^{U(\hat{q})}e^{T(\hat{p})}|\psi\rangle = e^E|\psi\rangle. \quad (4.5.9)$$

The operator ρ in (4.5.4) can be used to define a quantum Hamiltonian by setting

$$\hat{\rho} = e^{-\hat{H}}, \quad (4.5.10)$$

which has the semiclassical limit

$$H_{\text{cl}}^{\text{FG}}(q, p) = T(p) + U(q). \quad (4.5.11)$$

We know that the mirror geometry of local $\mathbb{P}^1 \times \mathbb{P}^1$ is given by the equation

$$H^{\text{RS}}(z_1, z_2) = -1 + e^u + z_1 e^{-u} + e^v + z_2 e^{-v} = 0, \quad (4.5.12)$$

with $u, v \in \mathbb{C}$, which was analyzed in section 4.4.2.

If we make the change of variables

$$u = \frac{q+p}{2} - E, \quad v = \frac{q-p}{2} - E \quad (4.5.13)$$

and specialize the moduli to

$$z_1 = z_2 = z, \quad (4.5.14)$$

where we set

$$z = e^{-2E}, \quad (4.5.15)$$

we see that

$$H^{\text{RS}}(u, v; z, z) = 0 \Leftrightarrow H_{\text{cl}}^{\text{FG}}(q, p) = E. \quad (4.5.16)$$

This means that the quantum Hamiltonian of the Fermi gas of ABJM theory and the equation defining the Riemann surface of the B–model geometry which is the mirror of local $\mathbb{P}^1 \times \mathbb{P}^1$, considered in this chapter, are equivalent for this specialization.

This change of variables preserves the symplectic form up to an overall constant

$$du \wedge dv = -\frac{1}{2}dq \wedge dp. \quad (4.5.17)$$

In [48] the fact that the Hamiltonian of the Fermi gas can be considered as a Riemann surface

has been used to define period integrals after introducing the coordinates

$$Q = q, \quad P = p + q. \quad (4.5.18)$$

In the large E limit one finds the relation

$$n(E) \approx \frac{1}{2\pi\hbar} \oint_{\mathcal{A}} P dQ \approx 8E^2 \propto \log^2 z, \quad (4.5.19)$$

which starts with the square of a logarithm in z and corresponds therefore to the B-period in the quantum geometry considered in this chapter. The other relation is

$$\oint_{\mathcal{B}} P dQ = 8\pi i E + \mathcal{O}(e^{-cE}) \propto \log z \quad (4.5.20)$$

for some constant c , which corresponds to the A-periods in this chapter.

This relation is very interesting and it was analyzed for this case in [98] and [99]. The suggestion was that the instanton corrections in ABJM theory coming from the membrane instantons in the AdS/CFT duals are given by the refined topological string on local $\mathbb{P}^1 \times \mathbb{P}^1$ in the Nekrasov–Shatashvili limit. On the other hand, it is suggested that the non-perturbative sector of the Nekrasov–Shatashvili limit of the refined topological string has information about the unrefined topological string.

Conclusions and Outlook

5.1 Fermi gas

In this thesis we used the Fermi gas approach developed in [48] and we computed vevs of Wilson loop operators in the ABJM matrix model based on the localization computations conducted in [32]. The matrix model integral is rewritten as the partition function of an ideal Fermi gas in an exterior potential by means of the Cauchy trick. Using this picture we extracted the quantities of interest in a semiclassical expansion. Compared to the computation of the canonical partition function in [48], the computation of vevs of Wilson loop operators is more difficult, since a resummation of an infinite number of corrections in \hbar is necessary. Even though it is more complicated, we were able to show that such a resummation is possible and we have obtained expressions valid at all orders in the genus expansion and for strong 't Hooft coupling. These expressions are fully M-theoretic because they are valid for finite k and large N .

Let us first say something about the structure of (3.3.104) and (3.3.108). For any winding number n these expressions are *singular* if k is a divisor of $2n$. In case of

$$k = 1, 2 \tag{5.1.1}$$

the expression is singular for any n .

For these values of k , the semiclassical expression for the vev (3.2.35), which is simply an integral over phase space, is not convergent. This is reflected in the final expression through a pole in the csc function, from which we conclude that our expression is not valid for these values of k . The values $k = 1, 2$ are special, because they correspond to those values of the coupling constant which lead to the enhancement of supersymmetry from $\mathcal{N} = 6$ to $\mathcal{N} = 8$ [107, 24]. We found that the Fermi gas resums the genus expansion for k large, which means that $k = 2n$ sets the radius of convergence of this expansion, leading to the singularities described above in the resulting expression. Analyzing what happens at these special values would be very interesting.

From the expression (3.3.108) we can deduce that the *unnormalized* Wilson loop vev is given by the Fourier transform of an unnormalized disk amplitude at large radius,

$$\int d\mu e^{-\mu N} \Xi(\mu) \frac{e^{\frac{2n\mu}{k}}}{4 \sin \frac{2\pi n}{k}}, \tag{5.1.2}$$

where n is the multicovering degree. The Fourier transform (3.3.103) for the canonical partition function can be viewed [48] as the change of symplectic frame from the topological partition function at the large radius point to the partition function at the orbifold point [108]. The result (3.3.108) suggests that for the open sector, a similar structure should be valid. More precisely, the change of frame in the open sector is also implemented by a Fourier transform of the open string partition function.

Knowing this, we are able to identify the meaning of the csc in this formula. It is the all-genus bubbling factor for a disk in topological string theory. This was first found in [109] by using large N duality with Chern–Simons theory and derived in [110] with localization techniques. Here we have re-derived this factor by using the Sommerfeld expansion of the Fermi gas, i. e. the low temperature expansion. This bubbling factor resums the genus expansion, as in the Gopakumar–Vafa representation of the closed topological string free energy [11]. However, we see that this resummation leads to singularities when k is a divisor of $2n$, and this was already observed in the closed string sector in an attempt to resum worldsheet instantons in ABJM theory in the sense of Gopakumar–Vafa [111]. This means that the expression (3.3.108) has a natural interpretation as a generalization of the Fourier transform of [108] to the open sector. A better understanding of this structure would be very helpful and was analyzed in [112]. In general it would be worthwhile to develop more efficient techniques for computing topological open string amplitudes at higher genus.

The computation of Wilson loops via the Fermi gas approach can be generalized in many different ways. One interesting direction would be to look at the computation of Wilson loop operators in ABJM theory in higher representations. The Wilson loop operator for a representation with ℓ boxes is an ℓ -body operator in the Fermi gas. Let us consider for example a 1/6 BPS Wilson loop in the antisymmetric representation. We can write the corresponding matrix model operator as

$$\mathcal{O}_{\square} = \sum_{i < j} e^{\lambda_i + \lambda_j} = \frac{1}{2} \sum_{i \neq j} e^{\lambda_i + \lambda_j}, \quad (5.1.3)$$

which is a two-body operator. We then have, schematically,

$$\begin{aligned} \langle \mathcal{O}_{\square} \rangle^{\text{GC}} &= \frac{1}{2} \int d\lambda d\lambda' e^{\lambda + \lambda'} \rho_2^{\text{GC}}(\lambda, \lambda') \\ &= \frac{1}{2} \int d\lambda d\lambda' [n(\lambda, \lambda)n(\lambda', \lambda') - n(\lambda, \lambda')n(\lambda', \lambda)] e^{\lambda + \lambda'} \end{aligned} \quad (5.1.4)$$

which is a sum of *direct* (Hartree) and *exchange* (Fock) terms. The first term factorizes into the product of two one-body operator vevs, which we computed in this paper. However, we are left with the calculation of the exchange term. This also should be computable by using semiclassical techniques¹. So developing this formalism further to solve this problem would certainly be of interest.

Here we only considered Wilson loop operators in ABJM theory, but the Fermi gas formalism also works for more general $\mathcal{N} \geq 3$ CSM theories [48]. It would also be interesting to extend the work presented in this thesis for these theories. This is relevant especially because using the usual techniques for solving matrix models in the 't Hooft expansion makes it very difficult to obtain results. Using this formalism seems to be the simplest way to go beyond the large N limit. However, a detailed analysis will require computing quantum corrections to the Hamiltonian,

¹ See [113] for a closely related example

the Wigner–Kirkwood corrections, and finding an appropriate regularization of the resummed semiclassical expansion. We need to understand the regularization procedure developed in section 3.3 more thoroughly and extend it for more general theories. In ABJM theory we were able to successfully compare the results with the ’t Hooft expansion, but for more complicated $\mathcal{N} \geq 3$ theories we would need to understand this issue better.

The final result we obtained for the 1/2 BPS Wilson loops in terms of the Airy function (3.3.108) is an analytic result for finite $k \neq 1, 2$ and large N to all orders in $1/N$ up to exponentially suppressed contributions. Such an expression is very well suited for the type of numerical testing performed in [89]. Numerical calculations conducted in this paper provided verification of the analytic formulas proposed in [36, 43, 48]. Furthermore they helped in clarifying certain aspects of the analytic results (like for example the nature of the function $A(k)$ introduced in [48]). Such a numerical test would also be very useful in understanding what happens when $k = 1, 2$, where our formula displays a singular behavior.

5.2 Quantum Geometry of del Pezzo surfaces in the Nekrasov–Shatashvili limit

By quantizing the special geometry of local Calabi–Yau manifolds related to the del Pezzo surfaces we solved the topological string in the Nekrasov–Shatashvili limit for many new geometries. We confirmed the quantization approach in the large radius limit for $\mathbb{F}_0, \mathbb{F}_1, \mathbb{F}_2$, as well as for the blown up surfaces $\mathcal{B}_2(\mathbb{P}^2)$ and $\mathcal{B}_1(\mathbb{F}_2)$ and a mass deformed E_8 del Pezzo surface.

The mass deformation parameters m_i and the modular Coulomb branch parameter u , also called non-normalizable moduli and normalizable moduli are clearly distinguished in our approach. For the relevant genus one mirror curves the structure is encoded in a third order differential operator in the modular parameter with rational coefficients in the m_i determining the two classical periods $a(u, m_i)$ and $a_D(u, m_i)$. These two periods are the only objects that get quantum deformed. The quantum deformed periods are defined by applying one differential operator $\mathcal{D}^{(2)}(u, m_i; \hbar)$ to the classical periods. This operator is second order in the modular parameter with rational coefficients in the mass parameters, but so far we could only determine it perturbatively in \hbar . However given $\mathcal{D}^{(2)}(u, m_i; \hbar)$ to some order in \hbar we can immediately determine the quantum deformation perturbatively at any point in the (u, m_i) space. With this information we can predict and in some cases check the orbifold and conifold expansions for the quantum deformed free energy.

We only considered the closed sector though and it would be very interesting to see whether the wavefunctions which solve the Schrödinger equations also compute correct open amplitudes or if they are only useful for deriving quantum deformed meromorphic differentials which are evaluated over closed contours.

The way the quantum special geometry was derived, somewhat suggested that we take the zeroth order contributions to the periods and deform them by a parameter \hbar . Considering that the Picard–Fuchs operators annihilate the zeroth order contributions, maybe also a Picard–Fuchs operator, that annihilates the quantum deformed periods exists.

We also used the difference equation ansatz to derive the free energies of local \mathbb{F}_0 and local \mathbb{F}_1 at large radius. For the conifold and orbifold point however, we were not able to extract the necessary data to solve the problem in this way. This computation would lead to an expression exact in \hbar , which is an expression we do not yet have for the topological string B–model.

One problem we encountered are certain missing instanton numbers corresponding to Kähler

parameters, related to non-normalizable divisors. These are not captured by the Picard–Fuchs system, like e. g. in the case of the resolved conifold. We still were able to apply our methods by making use of [105], where it was noted, that we can find the generating series for the B-cycle via the Frobenius method.

The Schrödinger equation for brane-wavefunctions in the full refined topological string depends on multiple times, which are the Kähler parameters. Having our results in mind, it would certainly be important to carefully distinguish between normalizable and non-normalizable moduli when analyzing this problem in full generality.

Matrix Models

A.1 Schwinger Dyson

Here we will provide some details concerning the computation of vevs in hermitian matrix models. We want to compute correlators for the matrix model given by the integral

$$\int \frac{d^N \lambda}{(2\pi)^N} \prod_{i \neq j} (\lambda_i - \lambda_j) \exp \left(-\frac{1}{2g_s} \sum_i \text{Tr} V(\lambda_i) \right). \quad (\text{A.1.1})$$

We start with the expression with the inserted total derivative

$$\sum_k \int \frac{d^N \lambda}{(2\pi)^N} \frac{\partial}{\partial \lambda_k} \left(\lambda_k^{p+1} \prod_{i \neq j} (\lambda_i - \lambda_j) \exp \left(-\frac{1}{2g_s} \sum_i V(\lambda_i) \right) \right) = 0 \quad (\text{A.1.2})$$

and compute the correlator. The derivative acting on the Vandermonde determinant leads to

$$\frac{\partial}{\partial \lambda_k} \prod_{i \neq j} (\lambda_i - \lambda_j) = \sum_{i \neq k} \left(\frac{1}{\lambda_k - \lambda_i} - \frac{1}{\lambda_i - \lambda_k} \right) \quad (\text{A.1.3})$$

therefore

$$\sum_k \lambda_k^{p+1} \frac{\partial}{\partial \lambda_k} \prod_{i \neq j} (\lambda_i - \lambda_j) = \sum_{i \neq k} \frac{\lambda_k^{p+1} - \lambda_i^{p+1}}{\lambda_k - \lambda_i} = \sum_{i \neq k} \sum_{j=0}^p \lambda_i^j \lambda_k^{p-j} = \sum_{i,k} \sum_{j=0}^p \lambda_i^j \lambda_k^{p-j} - (p+1) \sum_k \lambda_k^p. \quad (\text{A.1.4})$$

The derivative on the potential gives

$$- \sum_k \lambda_k^{p+1} \frac{1}{2g_s} V'(\lambda_k). \quad (\text{A.1.5})$$

Therefore, putting everything together, we find

$$\sum_{j=0}^p \left\langle \text{Tr} M^j \text{Tr} M^{p-j} \right\rangle = \frac{1}{2g_s} \text{Tr} M^{p+1} V'(M) \quad (\text{A.1.6})$$

A.1.1 Correlators of the β -ensemble

A more general case is the β -ensemble, which we also used in 4.3.2. The matrix integral is given by

$$\int d\lambda^N |\Delta(\lambda)|^{2\beta} e^{-\frac{\beta}{2g_s} \sum_{i=1}^N \lambda_i^2}. \quad (\text{A.1.7})$$

The Schwinger–Dyson approach yields in the most general case

$$\begin{aligned} & - (p+1)(1-\beta^{-1}) \left\langle \left(\prod_{i=1}^l \text{tr } M^{q_i} \right) \text{tr } M^p \right\rangle + \beta^{-1} \sum_{j=1}^l q_j \left\langle \left(\prod_{i \neq j}^l \text{tr } M^{q_i} \right) \text{tr } M^{p+q_j} \right\rangle \\ & + \sum_{j=0}^p \left\langle \left(\prod_{i=1}^l \text{tr } M^{q_i} \right) \text{tr } M^j \text{tr } M^{p-j} \right\rangle = \frac{1}{2g_s} \left\langle \left(\prod_{i=1}^l \text{tr } M^{q_i} \right) \text{tr}(M^{p+1} V') \right\rangle. \end{aligned} \quad (\text{A.1.8})$$

Using this result we give a few selected correlators in the Gaussian β -ensemble

$$\langle \text{tr } M^2 \rangle = g_s (-\gamma N + N^2) \quad (\text{A.1.9a})$$

$$\langle (\text{tr } M)^2 \rangle = g_s \beta^{-1} N \quad (\text{A.1.9b})$$

$$\langle \text{tr } M^4 \rangle = g_s (-3\gamma \langle \text{tr } M^2 \rangle + 2N \langle \text{tr } M^2 \rangle + \langle (\text{tr } M)^2 \rangle) \quad (\text{A.1.9c})$$

$$\langle \text{tr } M \text{tr } M^3 \rangle = g_s (-2\gamma \langle (\text{tr } M)^2 \rangle + 2N \langle (\text{tr } M)^2 \rangle + \beta^{-1} \langle \text{tr } M^2 \rangle) \quad (\text{A.1.9d})$$

$$\langle \text{tr } M^2 (\text{tr } M)^2 \rangle = g_s (-\gamma N \langle (\text{tr } M)^2 \rangle + 2\beta^{-1} \langle (\text{tr } M)^2 \rangle + N^2 \langle (\text{tr } M)^2 \rangle), \quad (\text{A.1.9e})$$

where $\gamma = 1 - \beta^{-1}$.

Fermi Gas

B.1 1/6 BPS Wilson loops at arbitrary winding number

In this appendix, we present the details of the matrix model computation which led to (2.3.96). Our starting point is the integral (2.3.95). This integral can be explicitly evaluated in terms of elliptic functions [114]

$$\mathcal{I}_n = \frac{1}{2}(-b)^n \frac{2\sqrt{ab}}{1+ab} \sum_{j=0}^n \left(-\frac{a+b}{b}\right)^j \binom{n}{j} V_j, \quad (\text{B.1.1})$$

where the functions V_j are defined recursively, in terms of elliptic integrals, as follows

$$\begin{aligned} V_0 &= K(k), \\ V_1 &= \Pi(\alpha^2, k), \\ V_2 &= \frac{1}{2(\alpha^2 - 1)(k^2 - \alpha^2)} \left[\alpha^2 E(k) + (k^2 - \alpha^2)K(k) + (2\alpha^2 k^2 + 2\alpha^2 - \alpha^4 - 3k^2)\Pi(\alpha^2, k) \right], \\ V_3 &= \frac{1}{2(m+2)(1-\alpha^2)(k^2-\alpha^2)} \left[(2m+1)k^2 V_m + (2m+1)(\alpha^2 k^2 + \alpha^2 - 3k^2)V_{m+1} \right. \\ &\quad \left. + (2m+3)(\alpha^4 - 2\alpha^2 k^2 - 2\alpha^2 + 3k^2)V_{m+2} \right]. \end{aligned} \quad (\text{B.1.2})$$

In the above expressions, the moduli of the elliptic functions are defined by

$$k^2 = \frac{(a^2 - 1)(b^2 - 1)}{(1 + ab)^2}, \quad \alpha^2 = \frac{1 - a^2}{1 + ab}. \quad (\text{B.1.3})$$

To understand the strong coupling behavior of the integral (2.3.95), we need to expand the above functions in the large κ regime. First, we notice that

$$\begin{aligned} V_0 &\approx 2 \log \kappa, \\ V_1 &\approx \frac{\kappa}{16} (\pi - 6i \log \kappa), \\ V_2 &\approx \frac{\kappa^2}{32} \left(1 - \frac{i\pi}{2} - 3 \log \kappa \right), \end{aligned} \quad (\text{B.1.4})$$

and the recursion relation becomes, at large κ ,

$$V_{3+m} \approx \frac{1+m}{16(2+m)} \kappa^2 V_{m+1} - \frac{i(3+2m)}{4(2+m)} \kappa V_{m+2} . \quad (\text{B.1.5})$$

We can easily find the solution to the above recursion relation. We have

$$V_j \approx \left(\frac{\kappa}{4i}\right)^j \left(\frac{H_{j-1}}{2} + \frac{i\pi}{4} + \frac{3}{2} \log \kappa\right), \quad j \geq 1. \quad (\text{B.1.6})$$

Using the above solution (B.1.6), we then compute the integral (2.3.95) in regime of large κ

$$\mathcal{I}_n \approx i^n \kappa^{n-1} \left(\sum_{j=1}^n \left(-\frac{H_{j-1}}{2} + \frac{i\pi}{4} + \frac{3}{2} \log \kappa \right) (-1)^j \binom{n}{j} + 2 \log \kappa \right). \quad (\text{B.1.7})$$

In order to perform the sum on the harmonic numbers in the above expression, we use the following integral representation of harmonic numbers

$$H_{j-1} = \int_0^1 \frac{1-x^{j-1}}{1-x} dx . \quad (\text{B.1.8})$$

Using the above representation, we then obtain

$$\sum_{j=1}^n (-1)^j \binom{n}{j} H_{j-1} = \int_0^1 \frac{dx}{x} \left(1 - (1-x)^{n-1} \right) = H_{n-1} . \quad (\text{B.1.9})$$

The sum on the rest of the terms in (B.1.7) is easy to perform

$$\sum_{j=1}^n (-1)^j \binom{n}{j} \left(\frac{i\pi}{4} + \frac{3}{2} \log \kappa \right) + 2 \log \kappa = -\frac{i\pi}{4} + \frac{1}{2} \log \kappa . \quad (\text{B.1.10})$$

Putting things together, we therefore conclude

$$\mathcal{I}_n \approx i^n \kappa^{n-1} \left(-\frac{H_{n-1}}{2} - \frac{i\pi}{4} + \frac{1}{2} \log \kappa \right), \quad (\text{B.1.11})$$

which is the sought-for result (2.3.96).

B.2 Results at $g = 3$ and $g = 4$

It is evident from (3.3.104) that extracting higher genus contributions to the expectation values of the ABJM Wilson loops is more efficient than for instance the topological recursion in the matrix model approach. To demonstrate this, we summarize the result of the 't Hooft expansion for $g = 3$ and $g = 4$ in this appendix. It is not necessary to find the expansions in terms of κ , as there exists no matrix model computation we can use for comparison yet. It will be sufficient to directly expand the Airy functions in (3.3.104) in terms of the 't Hooft coupling at strong coupling regime.

For $g = 3$, we obtain

$$\begin{aligned}
 \langle W_n^{1/6} \rangle_{g=3} &= -\frac{i^{n+1}\lambda}{(2\pi)^5} \left(\frac{62\pi^5 n^5}{945\sqrt{2\lambda}} - \left(\frac{\pi^4 n^4 (62nH_n + 147n - 323)}{1890} + \frac{31i\pi^5 n^5}{1890} + \frac{31i\pi^6 n^6}{22680} \right) \frac{1}{\lambda} \right. \\
 &\quad + \left(\frac{\pi^3 n^3 (3n+1)(14nH_n + 15n - 65)}{540} + \frac{7i\pi^4 n^4 (3n+1)}{540} \right. \\
 &\quad \left. \left. + \frac{\pi^5 n^5 (62nH_n + 147n - 385)}{45360} + \frac{31i\pi^6 n^6}{45360} + \frac{31\pi^7 n^7}{1088640} \right) \frac{1}{\lambda\sqrt{2\lambda}} + \mathcal{O}(\lambda^{-2}) \right) e^{\pi n\sqrt{2\lambda}}, \tag{B.2.1}
 \end{aligned}$$

while the $g = 4$ contribution is given by

$$\begin{aligned}
 \langle W_n^{1/6} \rangle_{g=4} &= \frac{i^{n+1}}{(2\pi)^7} \left(\frac{127\pi^7 n^7}{4725\sqrt{2\lambda}} - \left(\frac{\pi^6 n^6 (381nH_n + 930n - 2738)}{28350} + \frac{127i\pi^7 n^7}{18900} + \frac{127\pi^8 n^8}{226800} \right) \frac{1}{\lambda} \right. \\
 &\quad + \left(\frac{\pi^5 n^5 (3n+1)(124nH_n + 147n - 819)}{11340} + \frac{31i\pi^6 n^6 (3n+1)}{5670} \right. \\
 &\quad \left. \left. + \frac{\pi^7 n^7 (381nH_n + 930n - 3119)}{680400} + \frac{127i\pi^8 n^8}{453600} + \frac{127\pi^9 n^9}{10886400} \right) \frac{1}{\lambda\sqrt{2\lambda}} + \mathcal{O}(\lambda^{-2}) \right) e^{\pi n\sqrt{2\lambda}}. \tag{B.2.2}
 \end{aligned}$$

Applying (2.3.49), we can immediately find the result for the 1/2 BPS Wilson loop correlator at $g = 3$ and $g = 4$.

Quantum Geometry

C.1 Eisenstein series

The divisor function σ_x is defined by

$$\sigma_x(n) = \sum_{d|n} d^x \quad (\text{C.1.1})$$

and the Eisenstein series E_4 and E_6 are defined by

$$E_4(\tau) = 1 + 240 \sum_{n=1}^{\infty} \sigma_3(n) q^n \quad (\text{C.1.2a})$$

$$E_6(\tau) = 1 - 504 \sum_{n=1}^{\infty} \sigma_5(n) q^n \quad (\text{C.1.2b})$$

in terms of it. The parameter q is defined by

$$q = e^{2\pi i \tau} \quad (\text{C.1.3})$$

C.2 local \mathbb{F}_0

The higher order operators are

$$\mathcal{D}_2 = \frac{1}{6}(-u - mu)\Theta_u + \frac{1}{12}(1 - 4u - 4mu)\Theta_u^2, \quad (\text{C.2.1})$$

$$\begin{aligned} \mathcal{D}_4 = & -\frac{1}{180\Delta^2} u^2 (64m^5 u^3 + (-1 + 4u)^3 - 48m^4 u^2 (1 + 116u) + 4m^3 u (3 + 328u + 1376u^2) \\ & - 4m(8 - 37u - 328u^2 + 1392u^3) + m^2(-1 + 148u - 6112u^2 + 5504u^3)) \Theta_u \\ & - \frac{1}{360\Delta^2} u((1 - 4u)^4 + 256m^5 u^4 - 256m^4 u^3 (1 + 87u) + 32m^3 u^2 (3 + 214u + 688u^2) \\ & - m(1 - 4u)^2 (-1 + 268u + 1392u^2) + 16m^2 u (-1 + 48u - 1720u^2 + 1376u^3)) \Theta_u^2, \end{aligned} \quad (\text{C.2.2})$$

with $\Delta = (1 - 8(1 + m)u + 16(-1 + m)^2u^2)$. And some higher WKB functions are

$$S'_0(x) = \log \left(\frac{1}{2} e^{-x} (e^x - e^{2x} - z_1 + \sqrt{(-e^x + e^{2x} + z_1)^2 - 4e^{2x}z_2}) \right), \quad (\text{C.2.3a})$$

$$S'_1(x) = \frac{e^{3x} - e^{4x} - e^x z_1 + z_1^2}{2(-2e^{3x} + e^{4x} - 2e^x z_1 + z_1^2 + e^{2x}(1 + 2z_1 - 4z_2))}, \quad (\text{C.2.3b})$$

$$\begin{aligned} S'_2(x) = & -\frac{1}{12((-e^x + e^{2x} + z_1)^2 - 4e^{2x}z_2)(5/2)} e^x (e^{8x} + z_1^4 - e^x z_1^3 (3 + 4z_1 - 22z_2) \\ & + e^{6x} (3 + 16z_1 - 18z_2) + e^{2x} z_1^2 (3 + 16z_1 - 18z_2) + e^{7x} (-3 - 4z_1 + 22z_2) \\ & + 2e^{4x} z_1 (5 + 15z_1 + 34z_2) - e^{5x} (1 + 12z_1^2 + 4z_2 - 32z_2^2 + z_1(21 + 38z_2)) \\ & - e^{3x} z_1 (1 + 12z_1^2 + 4z_2 - 32z_2^2 + z_1(21 + 38z_2))). \end{aligned} \quad (\text{C.2.3c})$$

C.2.1 Orbifold point

Here we present the raw data of the computation at the orbifold point in terms of periods s_t and s_m without having fixed the constants of integration. Also neither the shift in \hbar nor the normalization have been carried out.

$$\begin{aligned} \tilde{F}^{(0,0)} = & c_0(s_m) + f_0^6 + \frac{\log s_m s_t^2}{2} + \frac{s_t^2}{2} + \frac{s_t^4}{1152} - \frac{1}{384} s_m^2 s_t^2 - \frac{31 s_m^2 s_t^4}{1474560} \\ & + \frac{73 s_m^4 s_t^2}{2949120} + \frac{283 s_t^6}{44236800} + \mathcal{O}(s_i^7) \end{aligned} \quad (\text{C.2.4a})$$

$$\begin{aligned} \tilde{F}^{(1,0)} = & c_1(s_m) + f_1^6 + \frac{7}{1152} s_2^2 - \frac{253}{1474560} s_1^2 s_2^2 + \frac{511}{4423680} s_2^4 \\ & + \frac{2959}{594542592} s_1^4 s_2^2 - \frac{1103}{148635648} s_1^2 s_2^4 + \frac{29923}{8918138880} s_2^6 + \mathcal{O}(s_i^7) \end{aligned} \quad (\text{C.2.4b})$$

$$\begin{aligned} \tilde{F}^{(2,0)} = & c_2(s_m) + f_2^6 + \frac{9631}{44236800} s_2^2 - \frac{8089}{424673280} s_1^2 s_2^2 + \frac{1489}{79626240} s_2^4 + \\ & + \frac{9712951}{8697308774400} s_1^4 s_2^2 - \frac{10152757}{4348654387200} s_1^2 s_2^4 + \frac{5466903857}{260919263232000} s_2^6 + \mathcal{O}(s_i^7) \end{aligned} \quad (\text{C.2.4c})$$

$$\begin{aligned} \tilde{F}^{(3,0)} = & c_3(s_m) + f_3^6 + \frac{1146853 s_t^2}{62426972160} + \frac{373588141 s_t^4}{91321742131200} - \frac{98735143 s_m^2 s_t^2}{30440580710400} \\ & - \frac{170286827 s_m^2 s_t^4}{200907832688640} + \frac{1031514229 s_m^4 s_t^2}{3214525323018240} + \frac{28374740293 s_t^6}{48217879845273600} + \mathcal{O}(s_i^7) \end{aligned} \quad (\text{C.2.4d})$$

where

$$f_0^n = - \sum_{i=1}^n \frac{1}{4i(2i^2 + 3i + 1)} \frac{s_f^{2i+2}}{s_m^{2i}} \quad (\text{C.2.5a})$$

$$f_1^n = \sum_{i=1}^n \frac{1}{12i} \frac{s_f^{2i}}{s_m^{2i}} \quad (\text{C.2.5b})$$

$$f_2^n = - \sum_{i=1}^n \frac{7(2i + 1)}{360} \frac{s_f^{2i}}{s_m^{2i+2}} \quad (\text{C.2.5c})$$

$$f_3^n = \sum_{i=1}^n \frac{31(4i^3 + 12i^2 + 11i + 3)}{7560} \frac{s_f^{2i}}{s_m^{2n+4}}. \quad (\text{C.2.5d})$$

There are some additional terms of order zero in s_f/s_m , which are suppressed if we go to higher orders in the expansion, hence we dropped them here.

C.3 $\mathcal{O}(-3) \rightarrow \mathbb{P}^2$

The A-periods:

$$a^{(0)} = \log(u) - 2u^3 + 15u^6 - \frac{560u^9}{3} + \frac{5775u^{12}}{2} + \mathcal{O}(u^{15}) \quad (\text{C.3.1})$$

$$a^{(2)} = -\frac{u^3}{4} + \frac{15u^6}{2} - 210u^9 + 5775u^{12} + \mathcal{O}(u^{15}) \quad (\text{C.3.2})$$

$$a^{(4)} = -\frac{u^3}{192} + \frac{13u^6}{8} - \frac{987u^9}{8} + 6545u^{12} + \mathcal{O}(u^{15}) \quad (\text{C.3.3})$$

The mirror map:

$$u|_{\hbar^0} = Q_t + 2Q_t^4 - Q_t^7 + 20Q_t^{10} + \mathcal{O}(Q_t^{13}) \quad (\text{C.3.4a})$$

$$u|_{\hbar^2} = \frac{Q_t^4}{4} - 4Q_t^7 + \frac{145Q_t^{10}}{2} + \mathcal{O}(Q_t^{13}) \quad (\text{C.3.4b})$$

$$u|_{\hbar^4} = +\frac{Q_t^4}{192} - \frac{4Q_t^7}{3} + \frac{7549Q_t^{10}}{96} + \mathcal{O}(Q_t^{13}) \quad (\text{C.3.4c})$$

The B-periods:

$$a_D^{(0)} = 9u^3 - \frac{423u^6}{4} + 1486u^9 - \frac{389415u^{12}}{16} + \mathcal{O}(u^{13}) \quad (\text{C.3.5a})$$

$$a_D^{(2)} = -\frac{1}{8} + \frac{21u^3}{8} - \frac{603u^6}{8} + \frac{8367u^9}{4} - \frac{458715u^{12}}{8} + \mathcal{O}(u^{13}) \quad (\text{C.3.5b})$$

$$a_D^{(4)} = \frac{87u^3}{640} - \frac{3633u^6}{160} + \frac{485649u^9}{320} - \frac{607657u^{12}}{8} + \mathcal{O}(u^{13}) \quad (\text{C.3.5c})$$

C.3.1 Orbifold point

The periods σ are given by

$$(-1)^{2/3}\sigma^{(0)} = -3\psi - \frac{1}{8}\psi^4 - \frac{4}{105}\psi^7 - \frac{49}{2700}\psi^{10} - \frac{245}{23166}\psi^{13} + \mathcal{O}(\psi^{16}) \quad (\text{C.3.6a})$$

$$(-1)^{2/3}\sigma^{(2)} = -\frac{1}{24}\psi - \frac{1}{36}\psi^4 - \frac{7}{270}\psi^7 - \frac{49}{1944}\psi^{10} - \frac{3185}{128304}\psi^{13} + \mathcal{O}(\psi^{16}) \quad (\text{C.3.6b})$$

$$(-1)^{2/3}\sigma^{(4)} = -\frac{23}{17280}\psi - \frac{11}{1620}\psi^4 - \frac{637}{38880}\psi^7 - \frac{2107}{69984}\psi^{10} - \frac{886067}{18475776}\psi^{13} + \mathcal{O}(\psi^{16}), \quad (\text{C.3.6c})$$

while the dual periods are given by

$$(-1)^{1/3}\sigma_D^{(0)} = -\frac{3}{2}\psi^2 - \frac{1}{5}\psi^5 - \frac{25}{336}\psi^8 - \frac{80}{2079}\psi^{11} - \frac{1210}{51597}\psi^{14} + \mathcal{O}(\psi^{17}) \quad (\text{C.3.7a})$$

$$(-1)^{1/3}\sigma_D^{(2)} = -\frac{1}{12}\psi^2 - \frac{5}{72}\psi^5 - \frac{25}{378}\psi^8 - \frac{110}{1701}\psi^{11} - \frac{605}{9477}\psi^{14} + \mathcal{O}(\psi^{17}) \quad (\text{C.3.7b})$$

$$(-1)^{1/3}\sigma_D^{(4)} = -\frac{1}{144}\psi^2 - \frac{85}{3456}\psi^5 - \frac{10}{189}\psi^8 - \frac{3751}{40824}\psi^{11} - \frac{16093}{113724}\psi^{14} + \mathcal{O}(\psi^{17}). \quad (\text{C.3.7c})$$

C.3.2 Conifold point

$$t^{(0)} = \Delta + \frac{11\Delta^2}{18} + \frac{109\Delta^3}{243} + \frac{9389\Delta^4}{26244} + \frac{88351\Delta^5}{295245} + \mathcal{O}(\Delta^6) \quad (\text{C.3.8a})$$

$$t^{(2)} = \frac{1}{36} + \frac{\Delta}{324} + \frac{5\Delta^2}{4374} + \frac{35\Delta^3}{59049} + \frac{385\Delta^4}{1062882} + \frac{7007\Delta^5}{28697814} + \mathcal{O}(\Delta^6) \quad (\text{C.3.8b})$$

$$t^{(4)} = \frac{19}{139968} - \frac{91\Delta}{1259712} - \frac{89\Delta^2}{2834352} - \frac{3521\Delta^3}{229582512} - \frac{34265\Delta^4}{4132485216} - \frac{179179\Delta^5}{37192366944} + \mathcal{O}(\Delta^6). \quad (\text{C.3.8c})$$

The first corrections to the dual period are

$$t_c^{(0)}{}_D = a_0 + a_1 t_c^{(0)} - \frac{1}{2\pi i} \left(t_c^{(0)} \log(\Delta) + \frac{7\Delta^2}{12} + \frac{877\Delta^3}{1458} + \frac{176015\Delta^4}{314928} + \frac{9065753\Delta^5}{17714700} + \mathcal{O}(\Delta^6) \right) \quad (\text{C.3.9a})$$

$$t_c^{(2)}{}_D = a_1 t_c^{(2)} - \frac{1}{2\pi i} \left(t_c^{(2)} \log(\Delta) + \frac{1}{8\Delta} + \frac{\Delta}{108} + \frac{211\Delta^2}{52488} + \frac{3139\Delta^3}{1417176} + \frac{35663\Delta^4}{25509168} + \mathcal{O}(\Delta^5) \right) \quad (\text{C.3.9b})$$

$$t_c^{(4)}{}_D = a_1 t_c^{(4)} - \frac{1}{2\pi i} \left(t_c^{(4)} \log(\Delta) + \frac{7}{320\Delta^3} - \frac{251}{5760\Delta^2} + \frac{247}{10368\Delta} - \frac{691}{419904} - \frac{941\Delta}{3779136} + \mathcal{O}(\Delta^2) \right) \quad (\text{C.3.9c})$$

In these expressions we use

$$a_0 = -\frac{\pi}{3} - 1.678699904i = \frac{1}{i\sqrt{3}\Gamma\left(\frac{1}{3}\right)\Gamma\left(\frac{2}{3}\right)} G_{22}^{333} \left(\begin{matrix} \frac{1}{3} & \frac{2}{3} & 1 \\ 0 & 0 & 0 \end{matrix} \middle| -1 \right) \quad \text{and} \quad a_1 = \frac{3\log(3) + 1}{2\pi i}. \quad (\text{C.3.10})$$

C.4 local \mathbb{F}_1

The higher order operators are

$$\mathcal{D}_2 = \frac{mu^2(4m-9u)}{6(-8m+9u)}\Theta_u + \frac{4m-3u-16m^2u^2+36u^3m}{24(8m-9u)}\Theta_u^2, \quad (\text{C.4.1a})$$

$$\begin{aligned} \mathcal{D}_4 = & -\frac{1}{2880(8m-9u)(m-u-8m^2u^2+36mu^3-27u^4+16m^3u^4)^2}u^3(27u^3(-5+999u^3) \\ & + 1536m^7u^5(-2+121u^3) + 768m^6(u^3+209u^6) + 2m^3(53-23148u^3+8856u^6) \\ & - 2m^2u(163-49113u^3+52488u^6) + 16m^4u^2(457+8802u^3+58806u^6) \\ & + 4096m^8u^7 - 64m^5(u+1292u^4+12582u^7) + m(453u^2-81972u^5+87480u^8))\Theta_u \\ & - \frac{1}{5760(8m-9u)(m-u-8m^2u^2+36mu^3-27u^4+16m^3u^4)^2}u(8192m^8u^9 \\ & + 1024m^7u^7(-8+363u^3) + 768m^6u^5(4+401u^3) + 27u^5(-29+2619u^3) \\ & - 36m^3u^2(-15+4060u^3+1416u^6) - 128m^5u^3(4+1673u^3+12168u^6) \\ & + m^2(7-1780u^3+289260u^6-136080u^9) + mu(7+2796u^3-222264u^6+174960u^9) \\ & + 32m^4(u+819u^4+12114u^7+58806u^{10}))\Theta_u^2 \end{aligned} \quad (\text{C.4.1b})$$

$$S'_0(x) = \log\left(\frac{1}{2}e^{-x}\left(e^x - e^{2x} - z_1 - \sqrt{(-e^x + e^{2x} + z_1)^2 + 4e^{3x}z_2}\right)\right), \quad (\text{C.4.2a})$$

$$S'_1(x) = -\frac{e^x z_1 + e^{3x}(2z_2 - 1) + e^{4x} - z_1^2}{2((e^x(e^x - 1) + z_1)^2 + 4e^{3x}z_2)}, \quad (\text{C.4.2b})$$

$$\begin{aligned} S'_2(x) = & -\frac{5(e^x + e^{2x} - 3z_1)^2(e^x(e^x - 1) + z_1)^3}{32((-e^x + e^{2x} + z_1)^2 + 4e^{3x}z_2)^{5/2}} \\ & + \frac{(e^x(e^x - 1) + z_1)(-6e^x(3e^x + 23)z_1 + e^{2x}(e^x(19e^x + 14) + 19) + 171z_1^2)}{96((-e^x + e^{2x} + z_1)^2 + 4e^{3x}z_2)^{3/2}} \\ & - \frac{e^x(e^x - 1) + 9z_1}{24\sqrt{(-e^x + e^{2x} + z_1)^2 + 4e^{3x}z_2}}. \end{aligned} \quad (\text{C.4.2c})$$

C.5 local \mathbb{F}_2

Some higher WKB functions are

$$S'_0(x) = \log \left(\frac{1}{2} \left(-1 - e^x - e^{2x}mu - \sqrt{(1 + e^x + e^{2x}mu^2)^2 - \frac{4}{m^2}} \right) \right) \quad (\text{C.5.1a})$$

$$S'_1(x) = -\frac{e^x m^2 (1 + 3e^{2x}mu^2 + 2e^{3x}m^2u^4 + e^x(1 + 2mu^2))}{2(-4 + m^2(1 + e^x + e^{2x}mu^2)^2)} \quad (\text{C.5.1b})$$

$$\begin{aligned} S'_2(x) = & \frac{1}{12(-4 + m^2(1 + e^x + e^{2x}mu^2)^2)^{5/2}} e^x m^5 \left(1 - \frac{32}{m^4} + \frac{4}{m^2} + e^{8x}m^4u^8 \right. \\ & + e^{7x}m^3u^6(3 + 4mu^2) + e^{6x}m^2u^4(3 + 16mu^2) + 2e^{4x}u^2(5m - 86u^2 + 15m^2u^2) \\ & + e^{2x} \left(3 - \frac{22}{m^2} + \frac{16(-4 + m^2)u^2}{m} \right) + e^x \left(3 - \frac{18}{m^2} + \frac{4(-32 + 4m^2 + m^4)u^2}{m^3} \right) \\ & \left. + e^{5x}mu^2(1 + 21mu^2 - 88u^4 + 12m^2u^4) + e^{3x} \left(1 + \left(21 - \frac{106}{m^2} \right) mu^2 + 12(-6 + m^2)u^4 \right) \right). \end{aligned} \quad (\text{C.5.1c})$$

Additional operators are

$$\mathcal{D}_2 = -\frac{1}{6}(mu)\Theta_u + \frac{1}{12}(1 - 4mu)\Theta_u^2, \quad (\text{C.5.2a})$$

$$\begin{aligned} \mathcal{D}_4 = & \frac{u^2}{180\Delta^2} \left(-4m(3m^2 + 28)u + m^2 - 64m(m^4 - 92m^2 + 352)u^3 \right. \\ & \left. + 16(3m^4 - 94m^2 + 552)u^2 + 30 \right) \Theta_u \\ & + \frac{u}{360\Delta^2} \left(-96m(m^2 + 5)u^2 + 4(4m^2 + 61)u - 256m(m^4 - 92m^2 + 352)u^4 \right. \\ & \left. + 64(4m^4 - 123m^2 + 652)u^3 - m \right) \Theta_u^2 \end{aligned} \quad (\text{C.5.2b})$$

$$\begin{aligned}
\mathcal{D}_6 = & \frac{1}{7560\Delta^4} u^4 \left(45056m^8u^6 - 32768m^9u^7 - 2048m^7u^5(12 + 4883u^2) \right. \\
& + 1280m^6u^4(5 + 5168u^2) + 128m^5u^3(-5 + 542u^2 + 9792u^4) \\
& - 16m^4u^2(3 + 66744u^2 + 8158976u^4) \\
& - 32mu(-32 + 58757u^2 + 8863616u^4 + 40161280u^6) \\
& + 8m^3u(2 + 40573u^2 + 8116224u^4 + 59797504u^6) \\
& + 6(7 + 39032u^2 + 7728128u^4 + 123830272u^6) \\
& \left. + m^2(-1 - 36328u^2 - 4319232u^4 + 227704832u^6) \right) \Theta_u \\
& + \frac{1}{15120\Delta^4} u \left(212992m^8u^7 - 131072m^9u^8 - 4096m^7u^6(35 + 9766u^2) \right. \\
& + 1024m^6u^5(49 + 29990u^2) + 256m^5u^4(-35 - 5364u^2 + 19584u^4) \\
& - 64m^4u^3(-7 + 81220u^2 + 8528768u^4) \\
& + 16m^3u^2(7 + 120530u^2 + 19097600u^4 + 119595008u^6) \\
& + 4m^2u(-5 - 65394u^2 - 6316032u^4 + 221945856u^6) \\
& + 4u(119 + 398200u^2 + 59192320u^4 + 790593536u^6) \\
& \left. + m(1 + 9320u^2 - 10643584u^4 - 1288617984u^6 - 5140643840u^8) \right) \Theta_u^2, \\
& \tag{C.5.2c}
\end{aligned}$$

with $\Delta = (1 - 8mu - 64u^2 + 16m^2u^2)$.

Bibliography

- [1] A. Belavin et al. “Pseudoparticle solutions of the Yang-Mills equations.”
In: *Physics Letters B* 59 (Oct. 1975), pp. 85–87.
DOI: 10.1016/0370-2693(75)90163-X.
- [2] G. 't Hooft. “How instantons solve the U(1) problem.”
In: *Physics Reports* 142.6 (1986), pp. 357–387. ISSN: 0370-1573.
DOI: [http://dx.doi.org/10.1016/0370-1573\(86\)90117-1](http://dx.doi.org/10.1016/0370-1573(86)90117-1).
- [3] S. Weinberg. *The Quantum Theory of Fields*.
The Quantum Theory of Fields 3 Volume Hardback Set Bd. 2.
Cambridge University Press, 1996.
- [4] N. Seiberg and E. Witten. “Electric - magnetic duality, monopole condensation, and confinement in N=2 supersymmetric Yang-Mills theory.”
In: *Nucl.Phys.* B426 (1994), pp. 19–52. DOI: 10.1016/0550-3213(94)90124-4.
arXiv:[hep-th/9407087](https://arxiv.org/abs/hep-th/9407087) [[hep-th](#)].
- [5] N. Seiberg and E. Witten.
“Monopoles, duality and chiral symmetry breaking in N=2 supersymmetric QCD.”
In: *Nucl.Phys.* B431 (1994), pp. 484–550. DOI: 10.1016/0550-3213(94)90214-3.
arXiv:[hep-th/9408099](https://arxiv.org/abs/hep-th/9408099) [[hep-th](#)].
- [6] S. H. Katz, A. Klemm, and C. Vafa.
“Geometric engineering of quantum field theories.”
In: *Nucl.Phys.* B497 (1997), pp. 173–195. DOI: 10.1016/S0550-3213(97)00282-4.
arXiv:[hep-th/9609239](https://arxiv.org/abs/hep-th/9609239) [[hep-th](#)].
- [7] S. Katz, P. Mayr, and C. Vafa.
“Mirror symmetry and exact solution of 4-D N=2 gauge theories: 1.”
In: *Adv.Theor.Math.Phys.* 1 (1998), pp. 53–114. arXiv:[hep-th/9706110](https://arxiv.org/abs/hep-th/9706110) [[hep-th](#)].
- [8] R. Dijkgraaf and C. Vafa. “On geometry and matrix models.”
In: *Nucl.Phys.* B644 (2002), pp. 21–39. DOI: 10.1016/S0550-3213(02)00764-2.
arXiv:[hep-th/0207106](https://arxiv.org/abs/hep-th/0207106) [[hep-th](#)].
- [9] R. Dijkgraaf and C. Vafa.
“Matrix models, topological strings, and supersymmetric gauge theories.”
In: *Nucl.Phys.* B644 (2002), pp. 3–20. DOI: 10.1016/S0550-3213(02)00766-6.
arXiv:[hep-th/0206255](https://arxiv.org/abs/hep-th/0206255) [[hep-th](#)].
- [10] N. A. Nekrasov. “Seiberg-Witten prepotential from instanton counting.”
In: *Adv.Theor.Math.Phys.* 7 (2004), pp. 831–864. DOI: 10.4310/ATMP.2003.v7.n5.a4.
arXiv:[hep-th/0206161](https://arxiv.org/abs/hep-th/0206161) [[hep-th](#)].

- [11] R. Gopakumar and C. Vafa. “M theory and topological strings. 2.” In: (1998). arXiv:hep-th/9812127 [hep-th].
- [12] S. H. Katz, A. Klemm, and C. Vafa. “M theory, topological strings and spinning black holes.” In: *Adv.Theor.Math.Phys.* 3 (1999), pp. 1445–1537. arXiv:hep-th/9910181 [hep-th].
- [13] J. Choi, S. Katz, and A. Klemm. “The refined BPS index from stable pair invariants.” In: (2012). arXiv:1210.4403 [hep-th].
- [14] A. Iqbal, C. Kozcaz, and C. Vafa. “The Refined topological vertex.” In: *JHEP* 0910 (2009), p. 069. DOI: 10.1088/1126-6708/2009/10/069. arXiv:hep-th/0701156 [hep-th].
- [15] M.-x. Huang and A. Klemm. “Direct integration for general Ω backgrounds.” In: *Adv.Theor.Math.Phys.* 16.3 (2012), pp. 805–849. DOI: 10.4310/ATMP.2012.v16.n3.a2. arXiv:1009.1126 [hep-th].
- [16] D. Krefl and J. Walcher. “Extended Holomorphic Anomaly in Gauge Theory.” In: *Lett.Math.Phys.* 95 (2011), pp. 67–88. DOI: 10.1007/s11005-010-0432-2. arXiv:1007.0263 [hep-th].
- [17] D. Krefl and J. Walcher. “Shift versus Extension in Refined Partition Functions.” In: (2010). arXiv:1010.2635 [hep-th].
- [18] M. Aganagic et al. “Topological strings and integrable hierarchies.” In: *Commun.Math.Phys.* 261 (2006), pp. 451–516. DOI: 10.1007/s00220-005-1448-9. arXiv:hep-th/0312085 [hep-th].
- [19] M. Aganagic et al. “Quantum Geometry of Refined Topological Strings.” In: *JHEP* 1211 (2012), p. 019. DOI: 10.1007/JHEP11(2012)019. arXiv:1105.0630 [hep-th].
- [20] N. A. Nekrasov and S. L. Shatashvili. “Quantization of Integrable Systems and Four Dimensional Gauge Theories.” In: (2009). arXiv:0908.4052 [hep-th].
- [21] R. Dijkgraaf. “Les Houches lectures on fields, strings and duality.” In: (1997). arXiv:hep-th/9703136 [hep-th].
- [22] E. Witten. “String theory dynamics in various dimensions.” In: *Nucl.Phys.* B443 (1995), pp. 85–126. DOI: 10.1016/0550-3213(95)00158-0. arXiv:hep-th/9503124 [hep-th].
- [23] A. Gustavsson. “Algebraic structures on parallel M2-branes.” In: *Nucl.Phys.* B811 (2009), pp. 66–76. DOI: 10.1016/j.nuclphysb.2008.11.014. arXiv:0709.1260 [hep-th].
- [24] O. Aharony et al. “N=6 superconformal Chern-Simons-matter theories, M2-branes and their gravity duals.” In: *JHEP* 0810 (2008), p. 091. DOI: 10.1088/1126-6708/2008/10/091. arXiv:0806.1218 [hep-th].
- [25] J. M. Maldacena. “The Large N limit of superconformal field theories and supergravity.” In: *Adv.Theor.Math.Phys.* 2 (1998), pp. 231–252. arXiv:hep-th/9711200 [hep-th].

-
- [26] G. 't Hooft. “Dimensional reduction in quantum gravity.” In: (1993). arXiv:gr-qc/9310026 [gr-qc].
- [27] L. Susskind. “The World as a hologram.” In: *J.Math.Phys.* 36 (1995), pp. 6377–6396. DOI: 10.1063/1.531249. arXiv:hep-th/9409089 [hep-th].
- [28] Y. Imamura and K. Kimura.
“On the moduli space of elliptic Maxwell-Chern-Simons theories.”
In: *Prog.Theor.Phys.* 120 (2008), pp. 509–523. DOI: 10.1143/PTP.120.509. arXiv:0806.3727 [hep-th].
- [29] D. L. Jafferis and A. Tomasiello. “A Simple class of N=3 gauge/gravity duals.”
In: *JHEP* 0810 (2008), p. 101. DOI: 10.1088/1126-6708/2008/10/101. arXiv:0808.0864 [hep-th].
- [30] C. P. Herzog et al. “Multi-Matrix Models and Tri-Sasaki Einstein Spaces.”
In: *Phys.Rev.* D83 (2011), p. 046001. DOI: 10.1103/PhysRevD.83.046001. arXiv:1011.5487 [hep-th].
- [31] V. Pestun.
“Localization of gauge theory on a four-sphere and supersymmetric Wilson loops.”
In: *Commun.Math.Phys.* 313 (2012), pp. 71–129. DOI: 10.1007/s00220-012-1485-0. arXiv:0712.2824 [hep-th].
- [32] A. Kapustin, B. Willett, and I. Yaakov. “Exact Results for Wilson Loops in Superconformal Chern-Simons Theories with Matter.” In: *JHEP* 1003 (2010), p. 089. DOI: 10.1007/JHEP03(2010)089. arXiv:0909.4559 [hep-th].
- [33] N. Drukker and D. Trancanelli.
“A Supermatrix model for N=6 super Chern-Simons-matter theory.”
In: *JHEP* 1002 (2010), p. 058. DOI: 10.1007/JHEP02(2010)058. arXiv:0912.3006 [hep-th].
- [34] N. Drukker, J. Plefka, and D. Young. “Wilson loops in 3-dimensional N=6 supersymmetric Chern-Simons Theory and their string theory duals.”
In: *JHEP* 0811 (2008), p. 019. DOI: 10.1088/1126-6708/2008/11/019. arXiv:0809.2787 [hep-th].
- [35] N. Drukker, M. Marino, and P. Putrov. “Nonperturbative aspects of ABJM theory.”
In: *JHEP* 1111 (2011), p. 141. DOI: 10.1007/JHEP11(2011)141. arXiv:1103.4844 [hep-th].
- [36] N. Drukker, M. Marino, and P. Putrov.
“From weak to strong coupling in ABJM theory.”
In: *Commun.Math.Phys.* 306 (2011), pp. 511–563. DOI: 10.1007/s00220-011-1253-6. arXiv:1007.3837 [hep-th].
- [37] M. Bershadsky et al.
“Kodaira-Spencer theory of gravity and exact results for quantum string amplitudes.”
In: *Commun.Math.Phys.* 165 (1994), pp. 311–428. DOI: 10.1007/BF02099774. arXiv:hep-th/9309140 [hep-th].
- [38] B. Eynard, M. Marino, and N. Orantin. “Holomorphic anomaly and matrix models.”
In: *JHEP* 0706 (2007), p. 058. DOI: 10.1088/1126-6708/2007/06/058. arXiv:hep-th/0702110 [HEP-TH].

- [39] M.-x. Huang and A. Klemm. “Holomorphic Anomaly in Gauge Theories and Matrix Models.” In: *JHEP* 0709 (2007), p. 054. DOI: 10.1088/1126-6708/2007/09/054. arXiv:hep-th/0605195 [hep-th].
- [40] B. Haghighat, A. Klemm, and M. Rauch. “Integrability of the holomorphic anomaly equations.” In: *JHEP* 0810 (2008), p. 097. DOI: 10.1088/1126-6708/2008/10/097. arXiv:0809.1674 [hep-th].
- [41] M. Marino and P. Putrov. “Exact Results in ABJM Theory from Topological Strings.” In: *JHEP* 1006 (2010), p. 011. DOI: 10.1007/JHEP06(2010)011. arXiv:0912.3074 [hep-th].
- [42] I. R. Klebanov and A. A. Tseytlin. “Entropy of near extremal black p-branes.” In: *Nucl.Phys.* B475 (1996), pp. 164–178. DOI: 10.1016/0550-3213(96)00295-7. arXiv:hep-th/9604089 [hep-th].
- [43] H. Fuji, S. Hirano, and S. Moriyama. “Summing Up All Genus Free Energy of ABJM Matrix Model.” In: *JHEP* 1108 (2011), p. 001. DOI: 10.1007/JHEP08(2011)001. arXiv:1106.4631 [hep-th].
- [44] M. Marino. “Chern-Simons theory, matrix integrals, and perturbative three manifold invariants.” In: *Commun.Math.Phys.* 253 (2004), pp. 25–49. DOI: 10.1007/s00220-004-1194-4. arXiv:hep-th/0207096 [hep-th].
- [45] M. Aganagic et al. “Matrix model as a mirror of Chern-Simons theory.” In: *JHEP* 0402 (2004), p. 010. DOI: 10.1088/1126-6708/2004/02/010. arXiv:hep-th/0211098 [hep-th].
- [46] M. Tierz. “Soft matrix models and Chern-Simons partition functions.” In: *Mod.Phys.Lett.* A19 (2004), pp. 1365–1378. DOI: 10.1142/S0217732304014100. arXiv:hep-th/0212128 [hep-th].
- [47] N. Halmagyi and V. Yasnov. “The Spectral curve of the lens space matrix model.” In: *JHEP* 0911 (2009), p. 104. DOI: 10.1088/1126-6708/2009/11/104. arXiv:hep-th/0311117 [hep-th].
- [48] M. Marino and P. Putrov. “ABJM theory as a Fermi gas.” In: *J.Stat.Mech.* 1203 (2012), P03001. DOI: 10.1088/1742-5468/2012/03/P03001. arXiv:1110.4066 [hep-th].
- [49] A. Strominger. “Special geometry.” In: *Communications in Mathematical Physics* 133.1 (1990), pp. 163–180.
- [50] A. Ceresole, R. D’Auria, and S. Ferrara. “On the geometry of moduli space of vacua in N=2 supersymmetric Yang-Mills theory.” In: *Phys.Lett.* B339 (1994), pp. 71–76. DOI: 10.1016/0370-2693(94)91134-7. arXiv:hep-th/9408036 [hep-th].
- [51] M. Marino. “Les Houches lectures on matrix models and topological strings.” In: (2004). arXiv:hep-th/0410165 [hep-th].
- [52] M. Marino. “Chern-Simons theory, matrix models, and topological strings.” In: *Int.Ser.Monogr.Phys.* 131 (2005), pp. 1–197.

-
- [53] B. Eynard.
“Topological expansion for the 1-Hermitian matrix model correlation functions.”
In: *JHEP* 0411 (2004), p. 031. DOI: 10.1088/1126-6708/2004/11/031.
arXiv:hep-th/0407261 [hep-th].
- [54] B. Eynard and N. Orantin. “Invariants of algebraic curves and topological expansion.”
In: *Commun.Num.Theor.Phys.* 1 (2007), pp. 347–452.
DOI: 10.4310/CNTP.2007.v1.n2.a4. arXiv:math-ph/0702045 [math-ph].
- [55] G. ’t Hooft. “A Planar Diagram Theory for Strong Interactions.”
In: *Nucl.Phys.* B72 (1974), p. 461. DOI: 10.1016/0550-3213(74)90154-0.
- [56] D. Kreff and J. Walcher. “ABCD of Beta Ensembles and Topological Strings.”
In: *JHEP* 1211 (2012), p. 111. DOI: 10.1007/JHEP11(2012)111.
arXiv:1207.1438 [hep-th].
- [57] E. Brézin et al. “Planar diagrams.”
In: *Communications in Mathematical Physics* 59.1 (1978), pp. 35–51.
- [58] L. Chekhov and B. Eynard.
“Hermitean matrix model free energy: Feynman graph technique for all genera.”
In: *JHEP* 0603 (2006), p. 014. DOI: 10.1088/1126-6708/2006/03/014.
arXiv:hep-th/0504116 [hep-th].
- [59] L. Chekhov et al. “Complex geometry of matrix models.”
In: *Proc.Steklov Inst.Math.* 251 (2005), pp. 254–292. arXiv:hep-th/0506075 [hep-th].
- [60] J. Ambjorn et al. “Matrix model calculations beyond the spherical limit.”
In: *Nucl.Phys.* B404 (1993), pp. 127–172. DOI: 10.1016/0550-3213(93)90476-6.
arXiv:hep-th/9302014 [hep-th].
- [61] G. Akemann.
“Higher genus correlators for the Hermitian matrix model with multiple cuts.”
In: *Nucl.Phys.* B482 (1996), pp. 403–430. DOI: 10.1016/S0550-3213(96)00542-1.
arXiv:hep-th/9606004 [hep-th].
- [62] A. Klemm, M. Marino, and S. Theisen.
“Gravitational corrections in supersymmetric gauge theory and matrix models.”
In: *JHEP* 0303 (2003), p. 051. DOI: 10.1088/1126-6708/2003/03/051.
arXiv:hep-th/0211216 [hep-th].
- [63] E. Cremmer, B. Julia, and J. Scherk. “Supergravity Theory in Eleven-Dimensions.”
In: *Phys.Lett.* B76 (1978), pp. 409–412. DOI: 10.1016/0370-2693(78)90894-8.
- [64] J. H. Schwarz. “Superconformal Chern-Simons theories.”
In: *JHEP* 0411 (2004), p. 078. DOI: 10.1088/1126-6708/2004/11/078.
arXiv:hep-th/0411077 [hep-th].
- [65] J. Bagger and N. Lambert. “Modeling Multiple M2’s.”
In: *Phys.Rev.* D75 (2007), p. 045020. DOI: 10.1103/PhysRevD.75.045020.
arXiv:hep-th/0611108 [hep-th].
- [66] J. Bagger and N. Lambert.
“Gauge symmetry and supersymmetry of multiple M2-branes.”
In: *Phys.Rev.* D77 (2008), p. 065008. DOI: 10.1103/PhysRevD.77.065008.
arXiv:0711.0955 [hep-th].

- [67] J. Bagger and N. Lambert. “Comments on multiple M2-branes.”
In: *JHEP* 0802 (2008), p. 105. DOI: 10.1088/1126-6708/2008/02/105.
arXiv:0712.3738 [hep-th].
- [68] K. Hori et al. *Mirror symmetry*. 2003.
- [69] O. Aharony et al. “The Hagedorn - deconfinement phase transition in weakly coupled large N gauge theories.” In: *Adv.Theor.Math.Phys.* 8 (2004), pp. 603–696.
DOI: 10.4310/ATMP.2004.v8.n4.a1. arXiv:hep-th/0310285 [hep-th].
- [70] S.-J. Rey, T. Suyama, and S. Yamaguchi. “Wilson Loops in Superconformal Chern-Simons Theory and Fundamental Strings in Anti-de Sitter Supergravity Dual.”
In: *JHEP* 0903 (2009), p. 127. DOI: 10.1088/1126-6708/2009/03/127.
arXiv:0809.3786 [hep-th].
- [71] M. Lee and S. Lee. “1/2-BPS Wilson Loops and Vortices in ABJM Model.”
In: *JHEP* 1009 (2010), p. 004. DOI: 10.1007/JHEP09(2010)004.
arXiv:1006.5589 [hep-th].
- [72] I. Bars. “Supergroups and Their Representations.”
In: *Lectures Appl.Math.* 21 (1983), p. 17.
- [73] O. Aharony, O. Bergman, and D. L. Jafferis. “Fractional M2-branes.”
In: *JHEP* 0811 (2008), p. 043. DOI: 10.1088/1126-6708/2008/11/043.
arXiv:0807.4924 [hep-th].
- [74] A. Klemm and E. Zaslow. “Local mirror symmetry at higher genus.” In: (1999).
arXiv:hep-th/9906046 [hep-th].
- [75] A. Brini and A. Tanzini.
“Exact results for topological strings on resolved $Y^{**p,q}$ singularities.”
In: *Commun.Math.Phys.* 289 (2009), pp. 205–252. DOI: 10.1007/s00220-009-0814-4.
arXiv:0804.2598 [hep-th].
- [76] B. Chen and J.-B. Wu.
“Supersymmetric Wilson Loops in N=6 Super Chern-Simons-matter theory.”
In: *Nucl.Phys.* B825 (2010), pp. 38–51. DOI: 10.1016/j.nuclphysb.2009.09.015.
arXiv:0809.2863 [hep-th].
- [77] L. Ballentine. *Quantum Mechanics: A Modern Development*. World Scientific, 1998.
- [78] C. Zachos, D. Fairlie, and T. Curtright.
Quantum Mechanics in Phase Space: An Overview with Selected Papers.
World Scientific series in 20th century physics. World Scientific, 2005.
- [79] T. L. Curtright and C. K. Zachos. “Quantum Mechanics in Phase Space.”
In: *Asia Pac.Phys.Newsllett.* 1 (2012), pp. 37–46. DOI: 10.1142/S2251158X12000069.
arXiv:1104.5269 [physics.hist-ph].
- [80] M. Hillery et al. “Distribution functions in physics: Fundamentals.”
In: *Physics Reports* 106 (Apr. 1984), pp. 121–167.
DOI: 10.1016/0370-1573(84)90160-1.
- [81] R. Feynman. *Statistical Mechanics: A Set Of Lectures*. Advanced book classics.
Westview Press, 1998. ISBN: 9780813346106.

-
- [82] R. Ziff, G. Uhlenbeck, and M. Kac. “The ideal Bose-Einstein gas, revisited.”
In: *Physics Reports* 32 (Sept. 1977), pp. 169–248.
DOI: 10.1016/0370-1573(77)90052-7.
- [83] H. Hara. “Behavior of Reduced Density Matrices of the Ideal Fermi Gas.”
In: *Progress of Theoretical Physics* 43 (Mar. 1970), pp. 647–659.
DOI: 10.1143/PTP.43.647.
- [84] W. Krauth. *Statistical Mechanics: Algorithms and Computations*.
Oxford Master Series in Physics. Oxford University Press, UK, 2006.
ISBN: 9780198515357.
- [85] M. Chevallier and W. Krauth. “Off-diagonal long-range order, cycle probabilities, and condensate fraction in the ideal Bose gas.”
In: *Phys. Rev. E* 76 (5 Nov. 2007), p. 051109. DOI: 10.1103/PhysRevE.76.051109.
- [86] B. Grammaticos and A. Voros. “Semiclassical Approximations for Nuclear Hamiltonians. 1. Spin Independent Potentials.” In: *Annals Phys.* 123 (1979), p. 359.
DOI: 10.1016/0003-4916(79)90343-9.
- [87] Y. Imamura and K. Kimura.
“On the moduli space of elliptic Maxwell-Chern-Simons theories.”
In: *Prog.Theor.Phys.* 120 (2008), pp. 509–523. DOI: 10.1143/PTP.120.509.
arXiv:0806.3727 [hep-th].
- [88] D. L. Jafferis and A. Tomasiello. “A Simple class of N=3 gauge/gravity duals.”
In: *JHEP* 0810 (2008), p. 101. DOI: 10.1088/1126-6708/2008/10/101.
arXiv:0808.0864 [hep-th].
- [89] M. Hanada et al. “Numerical studies of the ABJM theory for arbitrary N at arbitrary coupling constant.” In: *JHEP* 1205 (2012), p. 121. DOI: 10.1007/JHEP05(2012)121.
arXiv:1202.5300 [hep-th].
- [90] T. Curtright, T. Uematsu, and C. K. Zachos. “Generating all Wigner functions.”
In: *J.Math.Phys.* 42 (2001), p. 2396. DOI: 10.1063/1.1366327.
arXiv:hep-th/0011137 [hep-th].
- [91] A. Voros. “Asymptotic \hbar -expansions of stationary quantum states.”
In: *Ann. Inst. H. Poincaré Sect. A (N.S.)* 26 no. 4 (1977), pp. 343–403.
- [92] N. Drukker and D. J. Gross.
“An Exact prediction of N=4 SUSYM theory for string theory.”
In: *J.Math.Phys.* 42 (2001), pp. 2896–2914. DOI: 10.1063/1.1372177.
arXiv:hep-th/0010274 [hep-th].
- [93] R. Dijkgraaf and C. Vafa.
“Toda Theories, Matrix Models, Topological Strings, and N=2 Gauge Systems.”
In: (2009). arXiv:0909.2453 [hep-th].
- [94] A. Mironov and A. Morozov.
“Nekrasov Functions and Exact Bohr-Zommerfeld Integrals.”
In: *JHEP* 1004 (2010), p. 040. DOI: 10.1007/JHEP04(2010)040.
arXiv:0910.5670 [hep-th].

- [95] M.-x. Huang.
“On Gauge Theory and Topological String in Nekrasov-Shatashvili Limit.”
In: *JHEP* 1206 (2012), p. 152. DOI: 10.1007/JHEP06(2012)152.
arXiv:1205.3652 [hep-th].
- [96] M.-X. Huang, A. Klemm, and M. Poretschkin.
“Refined stable pair invariants for E-, M- and $[p, q]$ -strings.”
In: *JHEP* 1311 (2013), p. 112. DOI: 10.1007/JHEP11(2013)112.
arXiv:1308.0619 [hep-th].
- [97] R. Dijkgraaf, C. Vafa, and E. Verlinde. “M-theory and a topological string duality.”
In: (2006). arXiv:hep-th/0602087 [hep-th].
- [98] Y. Hatsuda et al. “Non-perturbative effects and the refined topological string.”
In: (2013). arXiv:1306.1734 [hep-th].
- [99] J. Kallen and M. Marino. “Instanton effects and quantum spectral curves.” In: (2013).
arXiv:1308.6485 [hep-th].
- [100] D. Krefl. “Non-Perturbative Quantum Geometry.” In: (2013).
arXiv:1311.0584 [hep-th].
- [101] M.-x. Huang, A.-K. Kashani-Poor, and A. Klemm.
“The Ω deformed B-model for rigid $\mathcal{N} = 2$ theories.”
In: *Annales Henri Poincaré* 14 (2013), pp. 425–497.
DOI: 10.1007/s00023-012-0192-x. arXiv:1109.5728 [hep-th].
- [102] F. Klein and R. Fricke.
Vorlesungen Ueber Die Theorie Der Elliptischen Modulfunktionen. Vol. Bd. 1.
Teubner, Stuttgart, 1966.
- [103] A. Brandhuber and S. Stieberger. “Periods, coupling constants and modular functions
in N=2 SU(2) SYM with massive matter.”
In: *Int.J.Mod.Phys. A* 13 (1998), pp. 1329–1344. DOI: 10.1142/S0217751X98000627.
arXiv:hep-th/9609130 [hep-th].
- [104] C. Vafa. “Supersymmetric Partition Functions and a String Theory in 4 Dimensions.”
In: (2012). arXiv:1209.2425 [hep-th].
- [105] B. Forbes and M. Jinzenji.
“Extending the Picard-Fuchs system of local mirror symmetry.”
In: *J.Math.Phys.* 46 (2005), p. 082302. DOI: 10.1063/1.1996441.
arXiv:hep-th/0503098 [hep-th].
- [106] T. Chiang et al. “Local mirror symmetry: Calculations and interpretations.”
In: *Adv.Theor.Math.Phys.* 3 (1999), pp. 495–565. arXiv:hep-th/9903053 [hep-th].
- [107] E. Halyo. “Supergravity on AdS(5/4) x Hopf fibrations and conformal field theories.”
In: *Mod.Phys.Lett. A* 15 (2000), pp. 397–406. DOI: 10.1016/S0217-7323(00)00038-4.
arXiv:hep-th/9803193 [hep-th].
- [108] M. Aganagic, V. Bouchard, and A. Klemm.
“Topological Strings and (Almost) Modular Forms.”
In: *Commun.Math.Phys.* 277 (2008), pp. 771–819. DOI: 10.1007/s00220-007-0383-3.
arXiv:hep-th/0607100 [hep-th].

-
- [109] H. Ooguri and C. Vafa. “Knot invariants and topological strings.”
In: *Nucl.Phys.* B577 (2000), pp. 419–438. DOI: 10.1016/S0550-3213(00)00118-8.
arXiv:hep-th/9912123 [hep-th].
- [110] S. Katz and C.-C. M. Liu. “Enumerative geometry of stable maps with Lagrangian
boundary conditions and multiple covers of the disc.” English.
In: *Adv. Theor. Math. Phys.* 5.1 (2001), pp. 1–49.
- [111] M. Marino and P. Putrov. “unpublished.”
- [112] A. Grassi, J. Kallen, and M. Marino. “The topological open string wavefunction.”
In: (2013). arXiv:1304.6097 [hep-th].
- [113] M. Marino and P. Putrov.
“Interacting fermions and N=2 Chern-Simons-matter theories.”
In: *JHEP* 1311 (2013), p. 199. DOI: 10.1007/JHEP11(2013)199.
arXiv:1206.6346 [hep-th].
- [114] P. Byrd and M. Friedman. *Handbook of elliptic integrals for engineers and scientists.*
Grundlehren der mathematischen Wissenschaften. Springer-Verlag, 1971.

List of Figures

2.1	This figure depicts two cubic vertices. On the left-hand side a genus zero diagram is depicted, while the diagram shown on the right-hand side is of genus one. . . .	11
2.2	A gauge quiver describing the field content of ABJM theory.	20
2.3	The cycles in the ABJM geometry in the x -plane. The non-vanishing residua of the forms at $x = \infty$	30
3.1	Necklace quiver	47
3.2	The regions in the Fermi surface.	50
4.1	local \mathcal{B}_2 . In the first column we denote the divisors and in the fourth column the moduli and parameters associated with them.	86
4.2	Polyhedron 2 depicting the toric geometry \mathbb{F}_0	89
4.3	Toric diagram of local $\mathcal{O}(-3) \rightarrow \mathbb{P}^2$	97
4.4	Toric diagram of local \mathbb{F}_1	100
4.5	Toric diagram of $\mathcal{O}(-K_{\mathbb{F}_2}) \rightarrow \mathbb{F}_2$	103
4.6	Toric diagram of $\mathcal{O}(-K_{\mathcal{B}_2}) \rightarrow \mathcal{B}_2$ with the assigned mass parameters and the modulus \tilde{u}	107
4.7	Toric diagram of $\mathcal{B}_1(\mathbb{F}_2)$ with the assigned masses.	109
4.8	Toric diagram of the mass deformed local E_8 de Pezzo with the assigned masses.	111

List of Tables

2.1	Number of terms involved in the recursive definition of $W_{g,h}$.	19
4.1	The instanton numbers for local \mathbb{F}_0 at order \hbar^0 .	93
4.2	The instanton numbers for local \mathbb{F}_0 at order \hbar^2 .	94
4.3	The instanton numbers for local \mathbb{F}_0 at order \hbar^4 .	94
4.4	The instanton numbers for local \mathbb{F}_0 at order \hbar^6 .	94
4.5	The instanton numbers for local \mathbb{F}_1 at order \hbar^0 .	102
4.6	The instanton numbers for local \mathbb{F}_1 at order \hbar^2 .	102
4.7	The instanton numbers for local \mathbb{F}_1 at order \hbar^4 .	102
4.8	The instanton numbers for local \mathbb{F}_1 at order \hbar^6 .	102
4.9	The instanton numbers for local \mathbb{F}_2 at order \hbar^0 .	105
4.10	The instanton numbers for local \mathbb{F}_2 at order \hbar^2 .	105
4.11	The instanton numbers for local \mathbb{F}_2 at order \hbar^4 .	106
4.12	The instanton numbers for local \mathbb{F}_2 at order \hbar^6 .	106

Acronyms

ABJM Aharony–Bergman–Jafferis–Maldacena. 3, 4, 6, 20, 22, 25–33, 37, 38, 46, 47, 49, 51–53, 65–67, 113–115, 117–119, 124, 145

BCH Baker–Campbell–Hausdorff. 54–56

BLG Bagger–Lambert–Gustavsson. 3

BPS Bogomol’nyi–Prasad–Sommerfield. 1–4, 26, 27, 31–33, 35, 38, 53, 54, 61, 65–68, 77, 125

CSM Chern Simons matter. 3–5, 19, 20, 22, 25, 37, 38, 52, 118

SYM supersymmetric Yang–Mills. 3, 22, 68

vev vacuum expectation value. 4, 6, 22, 23, 25–28, 32–35, 37, 38, 40–43, 45, 49, 53, 54, 61, 65, 66, 68, 117, 118, 121

WKB Wentzel–Kramers–Brillouin. 4, 5, 74, 76, 82, 84, 87, 107, 128